ELECTRONICALLY TUNED 23 GHZ

GUNN OSCILLATORS

FOR A MICROWAVE DATALINK

by

L.Kratzenstein

A dissertation submitted to the Faculty of Engineering, University of Cape Town in fulfilment for the Degree of Master of Science in Electrical and Electronic Engineering.

Cape Town, 1988.

Declaration

I declare that this dissertation is my own unaided work. It is being submitted for the degree of Masters of Science in Engineering, at the University of Cape Town. It has not been submitted before for any degree or examination at any other university.

Signed by candidate Signature Removed

Signature of Candidate

30th day of September 1988

Abstract

A market has been identified for 23 GHz, short-haul, low-capacity, digital radio. The dissertation presents the development of the varactor controlled Gunn oscillators that constitute the crystal locked microwave sources of the radio. An accurate description of a design procedure for Gunn oscillators at 23 GHz is presented. With reference to advanced modulation methods which require constant modulation indices, a method of linearising the voltage/frequency characteristic of the varactor controlled Gunn oscillator is described, which allows direct modulation of the source at 23 GHz. Due to the wide operating temperature of the radio a technique to temperature compensate the oscillator is presented. The dissertation ends with an investigation how the semiconductor device's spread affects the oscillator characteristics and an evaluation of the noise performance of the Gunn oscillator.

Acknowledgements

The author wishes to express his gratitude to his supervisor Professor B.J. Downing for his supervision and his constructive criticism during the course of this work.

The support and the assistance of the following people is also acknowleged:

I. Robertson, Project Manager, and the Directors of Plessey South Africa for providing the facilities and finances to carry out the research, without which this dissertation would have been impossible.

Table of Contents

List of Figures

List of Tables

CHAPTER 1

1. INTRODUCTION TO DIGITAL MICROWAVE COMMUNICATIONS

1.1 Introduction

The ever-increasing demand in the amount of telephone traffic and the introduction of new services such as facsimile, digitised television and high speed data transmission increased the burden of the existing, already overloaded communication links. Until the mid 1970's most microwave communication links were analog, employing frequency-division multiplex (FDM) techniques. Digital microwave systems did not present themselves as alternatives to analog systems, because they had less efficient radio-frequency bandwidth utilisation and were higher in cost.

However, the introduction of time division multiplexing (TDM) which became feasible, costwise, with the mass production of high-speed, digital integrated circuitry led to the revival of digital microwave systems.

Digital communication does not only provide a more cost-effective solution to the increasing demand for communication links, but it also has other important advantages.

1) The transmission performance of analog microwave systems is very dependent on the length of the communication path due to the accumulation of noise and the degradation of the signal-to-noise ratio when large numbers of repeaters are deployed. The use of regenerative repeaters in digital communication links makes the system almost independent of distance as noise cannot accumulate.

2) Frequency congestion problems in the lower frequency bands (below 10 GHz) require that other, higher frequencies are being used. Radio systems operating in these high-frequency bands necessitate the application of more repeaters and therefore there is no choice but to employ digital communication techniques.

3) Interfacing digital radio to other existing digital systems like digital fiber optics, digital satellite and digital cable systems is easier than interfacing with analog radio systems.

4) One of the most important features of digital communication is that many advanced modulation techniques can be used, while analog modulation techniques are constrained to simple FM and AM modulation. As spectral efficiency is of considerable concern in congested frequency bands, modulation techniques to bandlimit the transmission are important.

1.2 Digital Modulation Techniques

The choice of the modulation technique is a trade-off between complexity and therefore cost of the system and the bandwidth efficiency of the transmitted signal. The system spectral efficiency can be expressed in terms of the transmitted bits per second per hertz bandwidth (b/s/Hz). This also means that the higher the transmitted data rate is the more bandwidth efficient the modulation technique has to be.

There are the basic systems which are frequency-shift keying (FSK), phase-shift keying (PSK) and pulse-amplitude modulation (PAM). An ideal Nyquist channel would transmit a binary signal with PAM modulation with an efficiency of 2 b/s/Hz [1]. Practical systems do not meet the characteristics of an ideal Nyquist channel and therefore spectral efficiencies are lower than 2 b/s/Hz. FSK and PSK have even lower spectral efficiencies (less than 1 b/s/Hz).

The more advanced modulation methods use the technique of transmitting symbols which carry more than one bit of information. This is done by multiple level modulation (M-ary modulation) and by combining different modulation techniques. Typical modulation methods of this type would be 8-level pulse amplitude modulation (theoretical 6 b/s/Hz), 4-level phase shift keying or quadrature phase shift keying (QPSK) which is widely used in practical systems (theoretical 2 b/s/Hz) or 16-level quadrature amplitude modulation (QAM) a combination of PAM and PSK (theoretical 4 b/s/Hz). Another advanced modulation technique, minimum

shift keying or MSK, is a special form of FSK which also realises more efficient bandwidth utilisation. The problem with many of these advanced modulation methods is however that they require constant modulation indices otherwise their performance regarding the bit error rate of the digital link will be degraded.

1.3 Microwave Datalink Configurations and Requirements

There are three basic types of communication configurations that can be considered: a) simplex communication, in which communication in only one direction is possible, b) half duplex communication, where communication in either direction is possible but not at the same time and, c) full duplex communication which permits communication in both directions independent from each other. For most applications like digitised voice traffic, full duplex communication is necessary and therefore any digital communication must support this configuration unless it is otherwise required.

In the same way that standardised hierarchies were established in analog FDM transmission systems, digital transmission networks required that digital hierarchies be established. Hierarchies are necessary to standardise the transmission bit rates, interface specifications and signal coding formats. Unfortunately there are currently two hierarchies widely accepted. One was introduced by Bell Telephone Laboratories and is based on a transmission rate of 1,544 Mbit/s or 24 digitised voice channels and forms the

basic building block of the North American hierarchy. The other is based on 2,048 Mbit/s or 30 digitised voice channels and is the fundamental building block for the European hierarchy. Other digital transmission rates in the latter hierarchy are 8,448 Mbit/s, 34,368 Mbit/s and 139,264 Mbit/s.

The CCIR identifies seven frequency bands with corresponding channel bandwidths below 15 GHz. These frequency bands are at 2, 4, 6, 7, 8, 11 and 13 GHz. Because of the frequent simultaneous use of digital and analog systems in these frequency bands, stringent regulations are necessary. More recently the frequency bands at 18, 23 and 50 GHz have become feasible for digital communication as lower frequency bands became too congested. Due to the reduction of range with increasing frequency these high frequency transmitters are predominantly used for short-haul communications, while lower transmit frequencies are mainly used for long-haul communications.

1.4 The 23 GHz Datalink System

A marketplace for short-haul microwave digital datalinks operating at a data rate of 2,048 or 8,448 Mbits/sec was identified. They are to be used in congested urban areas for rapidly deployable digital communication links. Their main function is to provide short-range communication links from long-haul high capacity microwave bearers. It has been decided to use the frequency band from 21.2 GHz to 23.6 GHz, which is reserved by the CCIR and FCC for private fixed link

communication. The under-utilisation of that frequency band is caused by the peak absorption of microwaves at those frequencies due to the water vapor in the atmosphere (Fig.1). The minimum range of the datalink is required to be 10km under worst case conditions (as defined by the British Department of Trade and Industry).

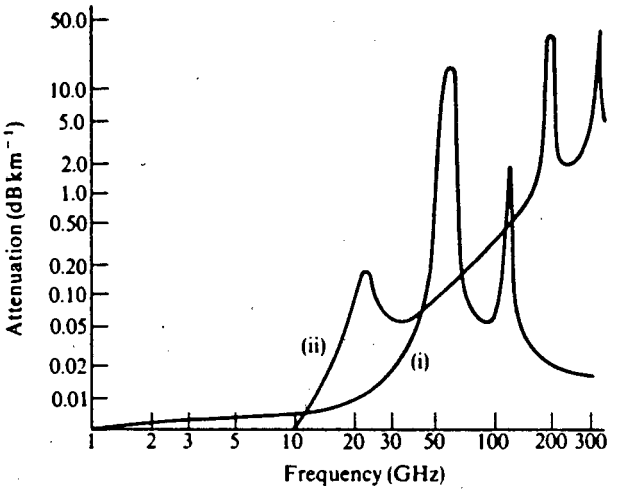

Fig.1 Atmospheric Attenuation due to i) Oxygen and ii) Watervapour.

The system (Fig.2) requires two electronically tunable Gunn oscillators. One oscillator is being used as the local oscillator and the other is being used as the transmit oscillator. This requirement was the motivation for this dissertation.

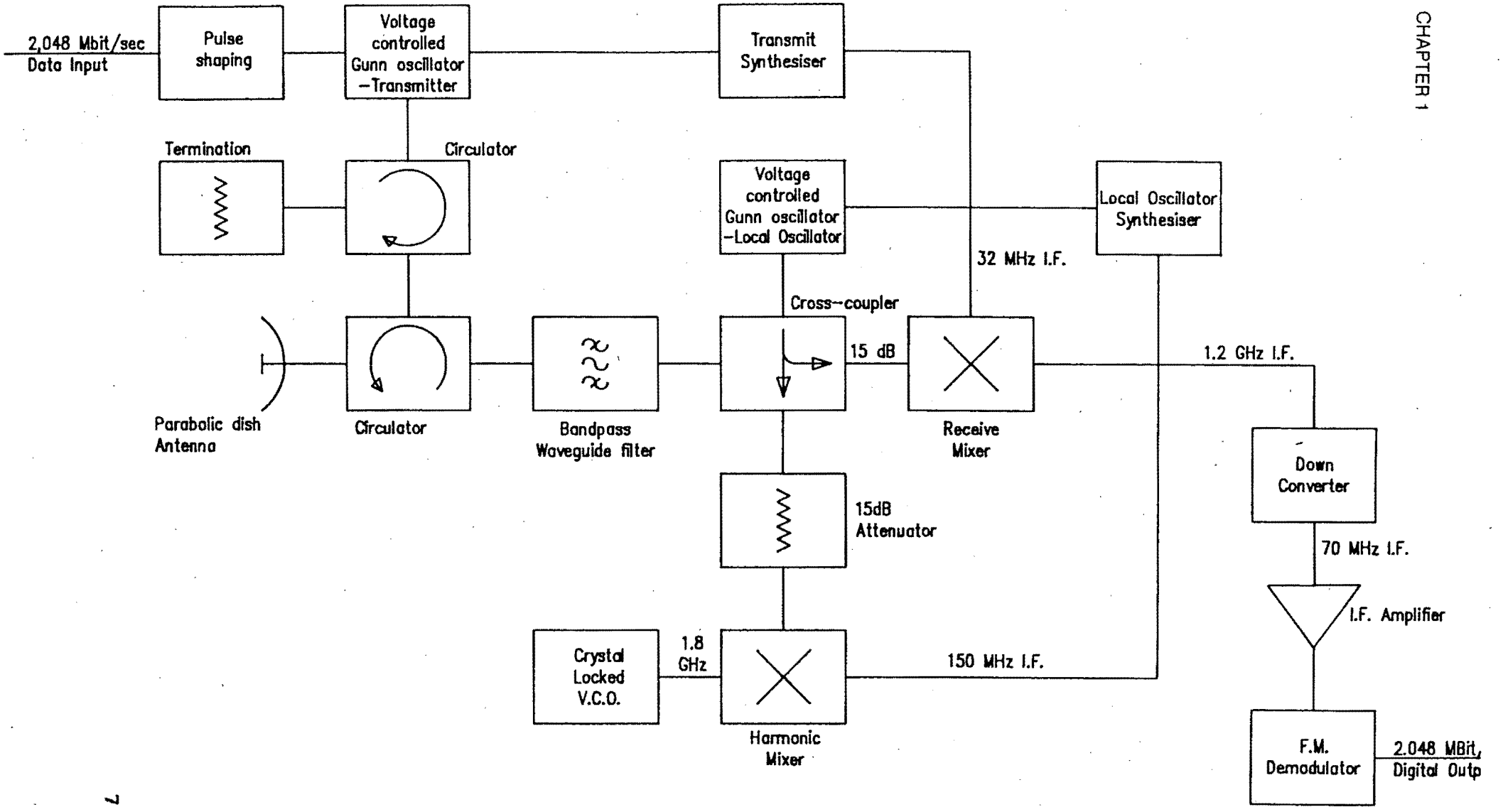

Fig. 2 The basic Microwave Digital Data Link functional Block Diagram.

1.5 Specification Motivation

As the radio unit will be pole mounted it will be exposed to the environment. In European conditions it therefore has to operate over a temperature range from -30°C to +55°C.

The Gunn oscillators are to be crystal locked and therefore the tuning range had to be large enough to cover the channel bandwidth as well as to cope with the temperature drift.

The modulation system was chosen to be simple baseband frequency shift keying (FSK) due to cost factors. This modulation scheme needs to have a constant modulation index to meet the specifications of the authorities as well as to improve the noise performance of the system. The choice of this frequency modulation scheme required therefore a high tuning linearity of the transmit voltage controlled oscillator. The prime design object regarding the electronic tuning range was therefore to linearise the characteristic.

As bit error rates are main performance criteria of the datalink and are affected by noise performance and stability, the oscillators have to be low noise. The noise specifications and the range specifications (10 km under worst case conditions) therefore also determine the required transmit power of +16 dBm the unit has to maintain over the temperature and the tuning range.

Not only have the above specifications to be met but as the datalink is being produced by the thousands the repeatability of the performance of all subsystems have to be high regardless of device spread and other factors.

The above criteria therefore determine the constraints regarding tuning range, output power, temperature range, linearity, low noise (and stability) and repeatability of the design of the voltage controlled Gunn oscillators (Fig.2) that are required.

1.6 Dissertation Organisation

The dissertation will firstly review the Gunn effect and Gunn oscillators. In the third chapter the two design concepts and the test results are being presented. The linearisation of the Gunn oscillator and the importance of a linear electronic tuning characteristic with special reference to the bandwidth efficient modulation method MSK is discussed in chapter four. The fifth chapter discusses the temperature effects on the oscillators as well as the test results of the temperature compensation. The effect of device spread is investigated in chapter six. The dissertation is concluded with a brief discussion of the noise performance of the Gunn oscillator.

CHAPTER 2

2. REVIEW OF THE GUNN-EFFECT

2.1 Introduction

Gunn-effect devices (or Gunn diodes) are named after J.B.Gunn, who, in 1963, whilst studying the properties of thin specimens of Gallium Arsenide (GaAs) and Indium Phosphide (InP) under high electric stress, discovered periodic fluctuations in the current passed by both materials when the applied electric field exceeded a certain critical value [2]. The mechanism responsible for this effect has since been shown to be that predicted earlier independently by Ridley and Watkins [3] and by Hilsum [4]. The principle involved is to excite electrons in a light-mass, high-mobility subband of the conduction band with an electric field so that the electrons can transfer to a heavy-mass, low-mobility, higher-energy subband when they have a high enough energy. This leads to a negative differential resistivity and the formation of travelling domains of high electric field within the semiconductor.

The above theory has been further verified by the observation that the critical field is reduced as the energy gap between the valleys is reduced by applying pressure or by alloying with Gallium Phosphide [5]. Gunn demonstrated the existence of travelling domains by using an

elaborate capacitive probe to measure the electric field distribution within a specimen of n-type GaAs [6].

2.2 The Gunn Effect

2.2.1 The Negative Resistance Effect

The Gunn effect is dependent on a certain range in the electron-velocity/electric-field characteristic to have negative differential mobility, as indicated in Fig.3 for n-type GaAs. The origin of this negative differential mobility (and therefore negative resistance) may be understood by reference to the conduction band structure for this material, illustrated in Fig.4. The central valley at wave vector k=0 contains electrons of effective mass ratio 0.067 and a mobility of about $7500cm^2/Vs$. There are also satellite valleys in which the effective mass ratio is 0.35 and the mobility around $150cm^2/Vs$. The minimum of these satellite valleys is at 0.36eV above the minimum of the central valley.

Applying an increasing electric field across GaAs has the effect of increasing the energy and the momentum of the electrons in the central valley. When the field is high enough for electrons to gain an energy of 0.36eV they may remain in the central valley, but most of them will transfer to a satellite valley in which the electron mobility is low and the electron mass is high. As a result, the electron mobility falls (the electrons slow down) by a factor of

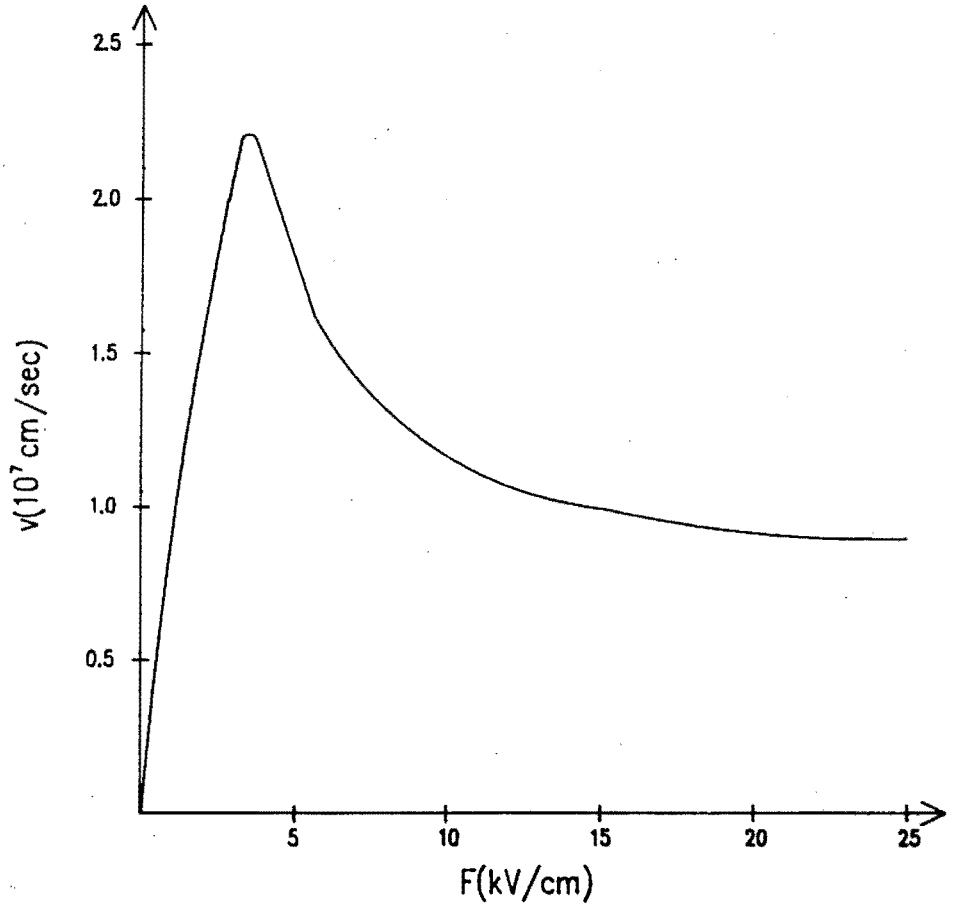

Fig. 3 The Average Electron Velocity in Gallium Arsenide as a Function of Applied Electric Field.

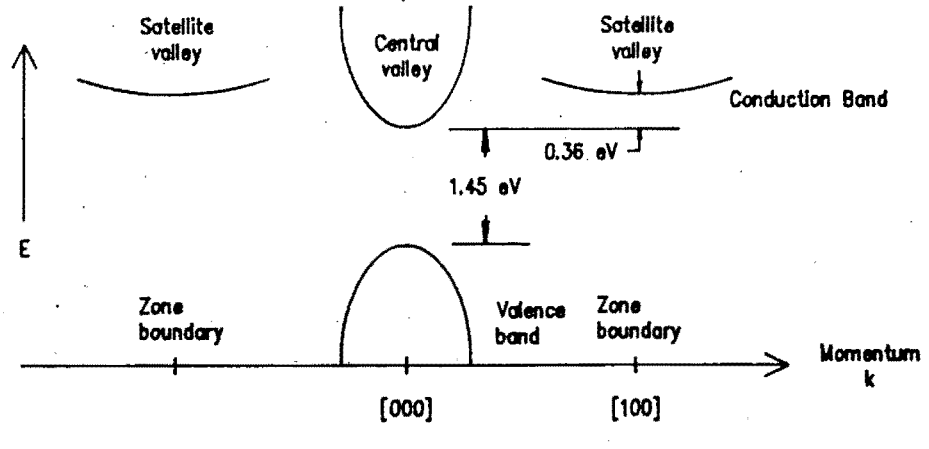

Fig. 4 The Band Structure of GaAs.

about 50 times, which accounts for the region of negative differential mobility as shown in Fig.3.

The required properties of materials for Gunn-effect devices are therefore that a low-mobility satellite valley should exist at an energy level difference W above a high-mobility central valley. The value of W must be large enough to prevent the thermal excitation of electrons from the valence to the conduction band but small enough to prevent field excitation between these bands occurring before the electron transfer mechanism becomes fully effective. Also the inter-valley transfer of electrons must set in rapidly with increasing field because the current decrease due to electron transfer into the satellite valleys must be stronger than the current increase due to the velocity increase of those electrons that remain in the central valley. This results in an overall current drop as shown in Fig.5 and the crystal exhibits a bulk negative differential conductivity.

Compound semiconductors that have been shown to meet these requirements include GaAs, InP, CdTe, ZnSe, $GaAs_xP_{1-x}$ and InAs (under pressure).

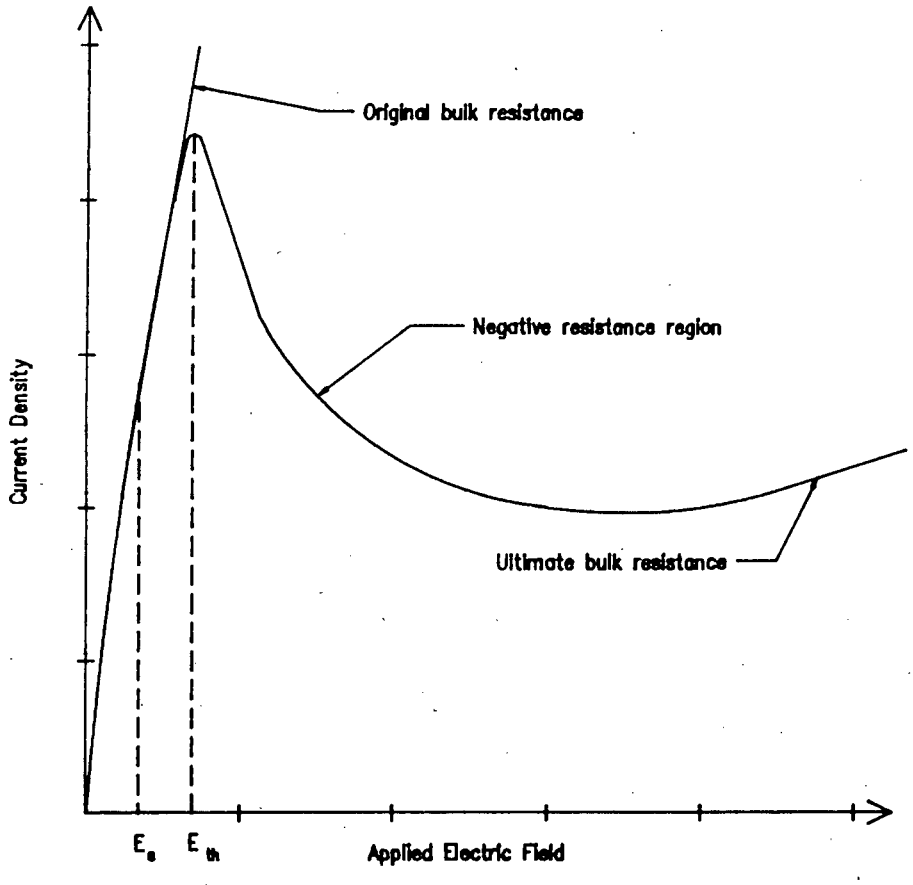

Fig. 5 The I/V Characteristic of GaAs.

2.2.2 The Formation of Domains

As the applied electric field to the bulk semiconductor is increased above the critical level E_{th} (3.6kV/cm for short specimens) the electrons that are excited into the satellite valleys (Fig.4) will increase their mass with a consequent reduction in drift velocity.

Initially an accumulation layer of negative charge is formed due to a random fluctuation of carrier density at some nucleation center near the cathode end of the specimen. The exact mechanism that controls the random fluctuation is not fully understood yet. There will be an increase of the field locally and because it is a region of negative slope mobility this will lead to a reduction of electron velocity. This develops into an accumulation of electrons which is followed by a layer of positive charge due to electron depletion. The dipole layer that is formed drifts through the semiconductor material as a unit structure with the saturation velocity of electrons in the material (10^7cm/s for GaAs). This is a travelling domain which becomes extinguished at the anode after which the whole process is immediately repeated. Since the formation of the domain reduces the field outside it, only one domain forms at a time. Shoji [7] derived an equation of motion for the domain using a resistive probe.

This mode of operation is the Gunn mode or transit-time mode. Assuming that the dielectric relaxation time and the transition time of the electrons between the central and satellite valley is short, the frequency of operation is determined by the saturation velocity of electrons in GaAs (10^7cm/s) and the length of the specimen. Although some electronic tuning is possible by varying the applied electric field, this mode is not useful as its current waveform (Fig.6) is rich in harmonics and has poor frequency stability.

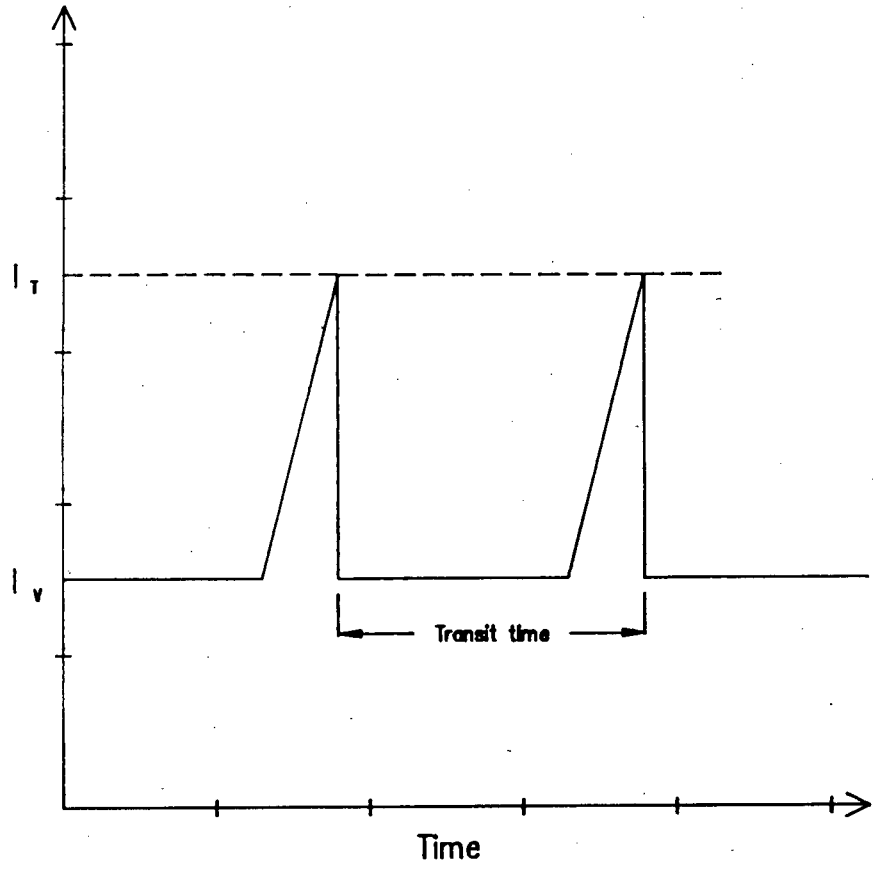

Fig. 6 Current Waveform for Domain Transit Mode.

If at any stage the external electric field drops below a value E_S (Fig.5), the sustaining field, the domain collapses before it reaches the anode.

2.2.3 Sinusoidal Modes of Operation

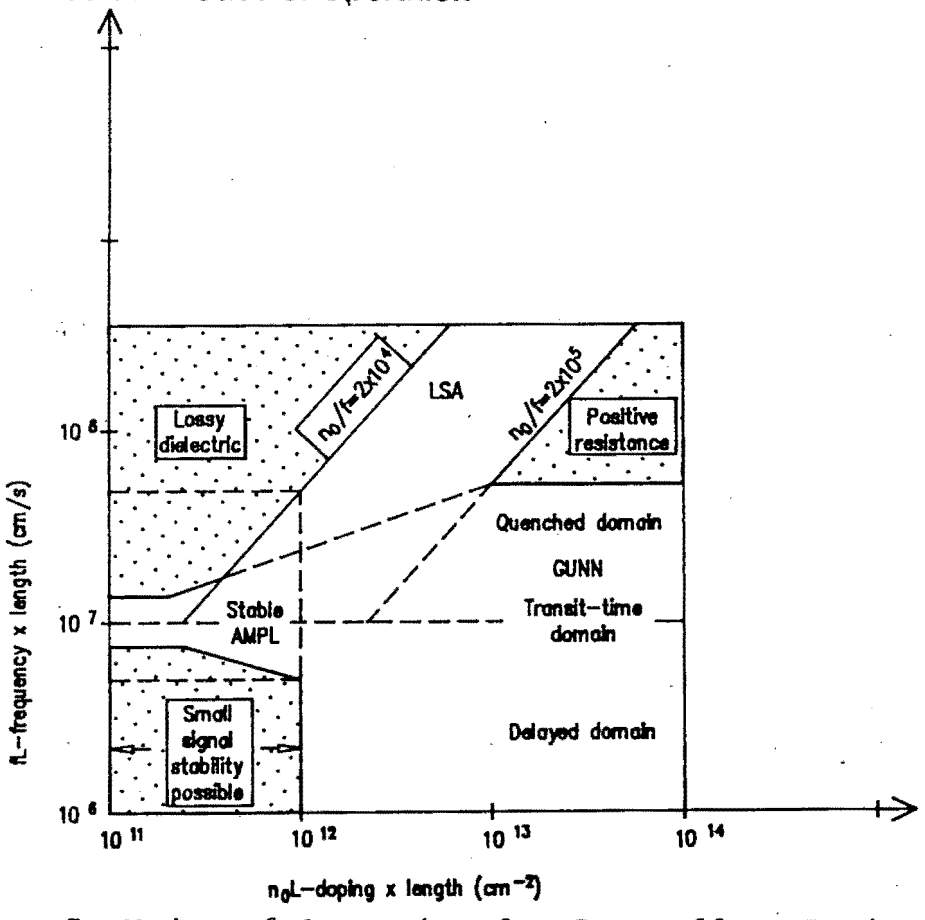

Fig. 7 Modes of Operation for Gunn-effect Devices.

Connecting an external circuit to the Gunn-effect device, a number of sinusoidal modes of operation are possible. The mode of operation is determined by the device parameters and the external circuit. In particular the following parameters are important.

- doping density
- specimen length

- frequency of operation
- circuit Q-factor and loading

Copeland [8] proposed four basic modes of operation of uniformly doped bulk diodes with low resistance contacts as shown in Fig.7.

2.2.3.1 Domain Mode

This mode of operation, described by Robson and Mahrous [9], is relatively stable and easy to tune and most commercially available devices operate in this mode. Kino and Kuru [10] show that theoretical efficiencies of up to 28% for square current and voltage waveforms are possible in this mode. Carroll and Giblin [11] built a low-frequency analog to simulate the Gunn-effect oscillator and produced under different circuit conditions numerous modes of oscillation.

For a product of doping and length (n_0L) of greater than $10^{12}/cm^2$ there are three important modes.

a) Transit-time domain mode

If the oscillation period of the Gunn device and the external circuit is equal to the transit time ($t_t = L_{eff}/v_{dom}$; where L_{eff} = the effective length that the domain travels and v_{dom} = is the domain velocity) the mode is said to be transit-time domain mode (Fig.8)

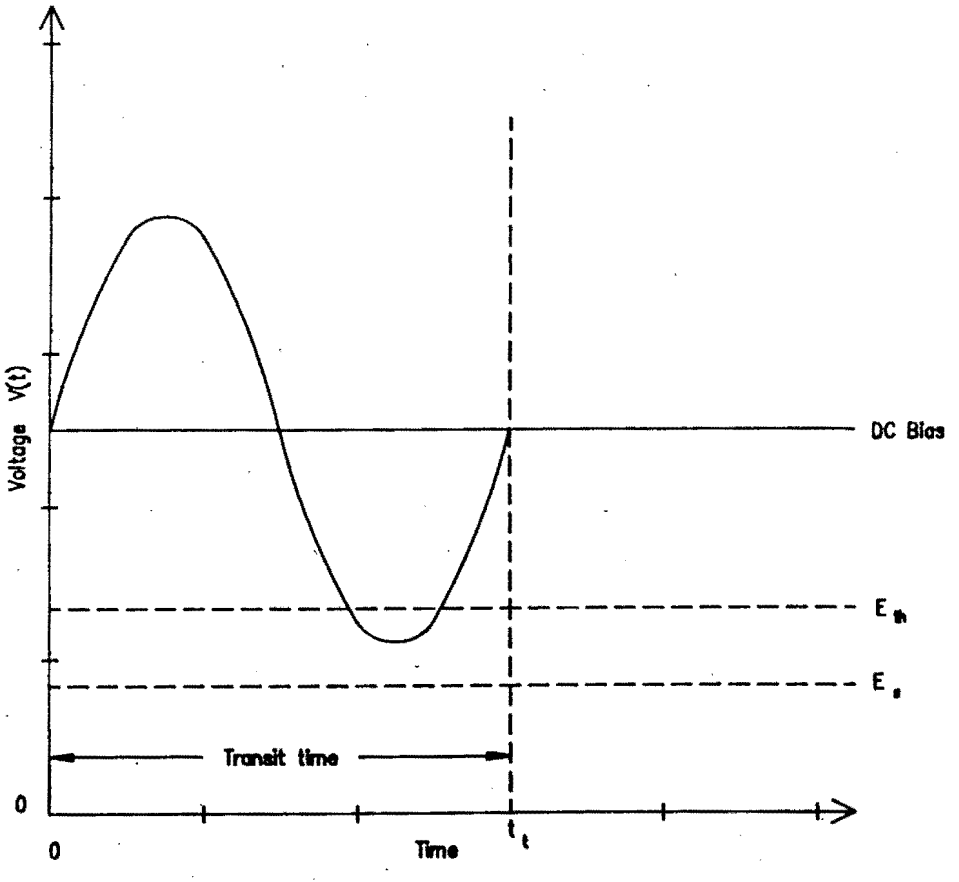

Fig. 8 Transit Time Mode.

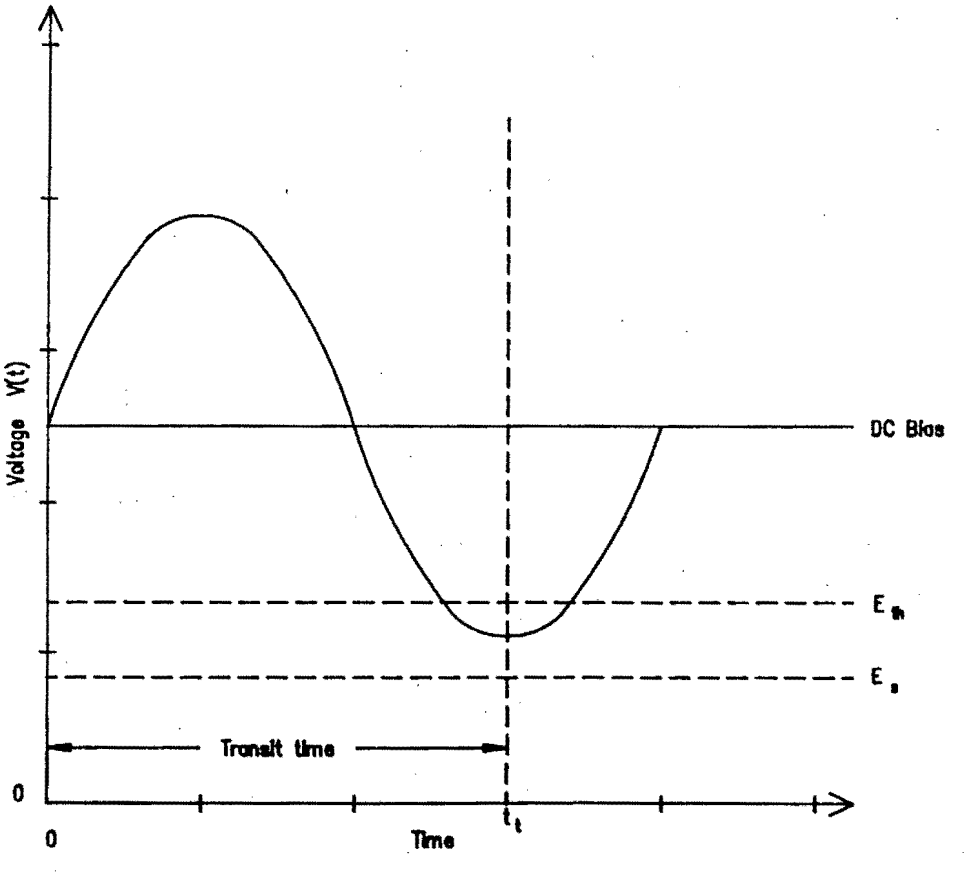

Fig. 9 Delayed Domain Mode.

It is important to note that the energy relaxation time of the electrons in the conductance band of GaAs set the upper frequency limit of oscillation. The calculations that have been made previously assume that the energy relaxation time is very much less than the transit time of the domain. It has been found [12] that the energy relaxation time for electron transfer from the central valley to the satellite valley is $\tau = 2.0 \times 10^{-14}$ sec and from the satellite valley to the central valley it is $\tau = 5.0 \times 10^{-13}$ sec. The longer of the two relaxation times sets the upper frequency limit which is calculated as

$$f = 1/(2\pi\tau) \approx 150 \text{ GHz}$$

Gunn-effect devices of up to frequencies of 80 GHz have been manufactured to date.

b) Delayed domain mode

If the period of oscillation of the Gunn device and the external circuit is such that the electric field falls below the threshold to prevent the formation of another domain till the field rises above the threshold again the circuit operates in the delayed domain mode (Fig.9). In this case the period of oscillation is longer than the transit-time (t_t). Tuning is possible in this mode over an octave with oscillation periods t_0 of $t_t < t_0 < 2t_t$. Robson and

Mahrous [9] predicted an octave tuning bandwidth for this mode. Most practical circuits operate in this mode.

c) Quenched domain mode

If the external electric field drops below the sustaining field E_s the domain collapses before it reaches the anode (Fig.10). Only when the field rises above the threshold again, a new domain is formed at the cathode and the process is repeated. The frequency of the resonant circuit is several times the transit-time frequency.

2.2.3.2 Limited-Space-Charge Accumulation Mode

For the product n_0L larger than $10^{12}/cm^2$ and if the ratio of doping n_0 to frequency f is within $2x10^5$ to $2x10^4 s/cm$ (Fig.7) and when the frequency of operation is high enough the domains do not have sufficient time to build up. The domains are therefore kept in the negative conductance state during a large fraction of the voltage cycle (Fig.11). This mode thus consists of a uniformly doped semiconductor without any internal space charges. The device appears therefore as a negative resistance.

2.2.3.3 Other Modes

There is also the stable amplification mode (for $n_0L < 10^{12}/cm^2$) in which the device will exhibit amplification at

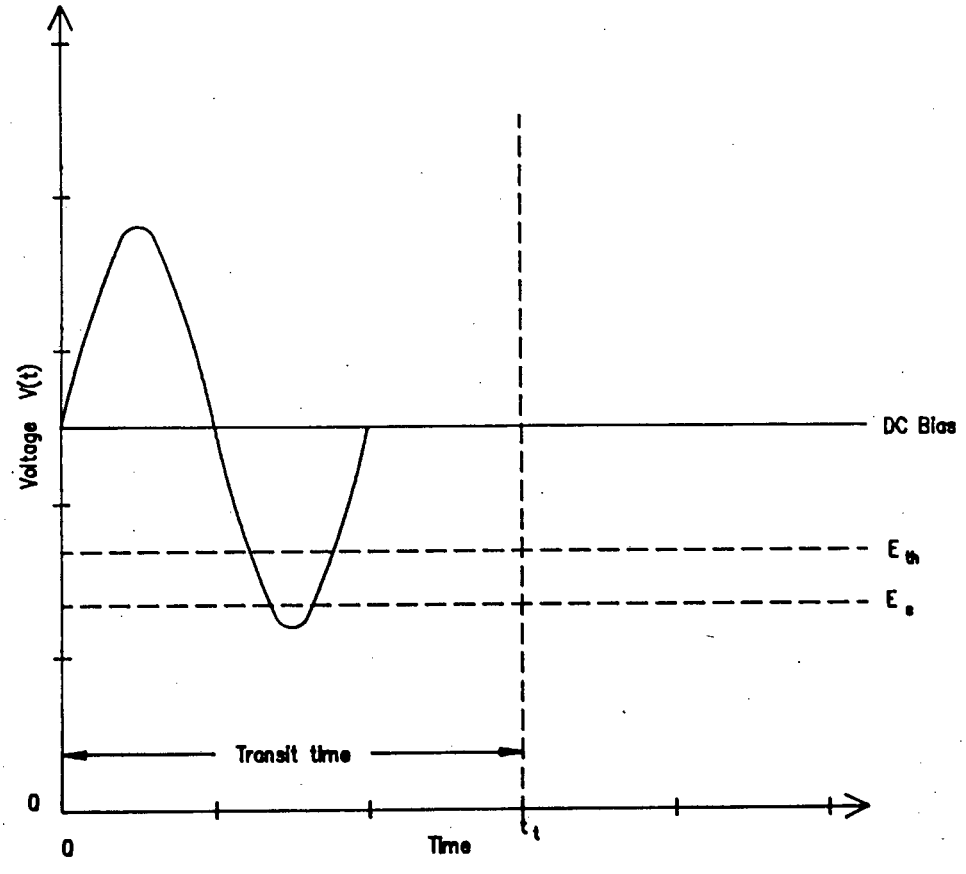

Fig. 10 Quenched Domain Mode.

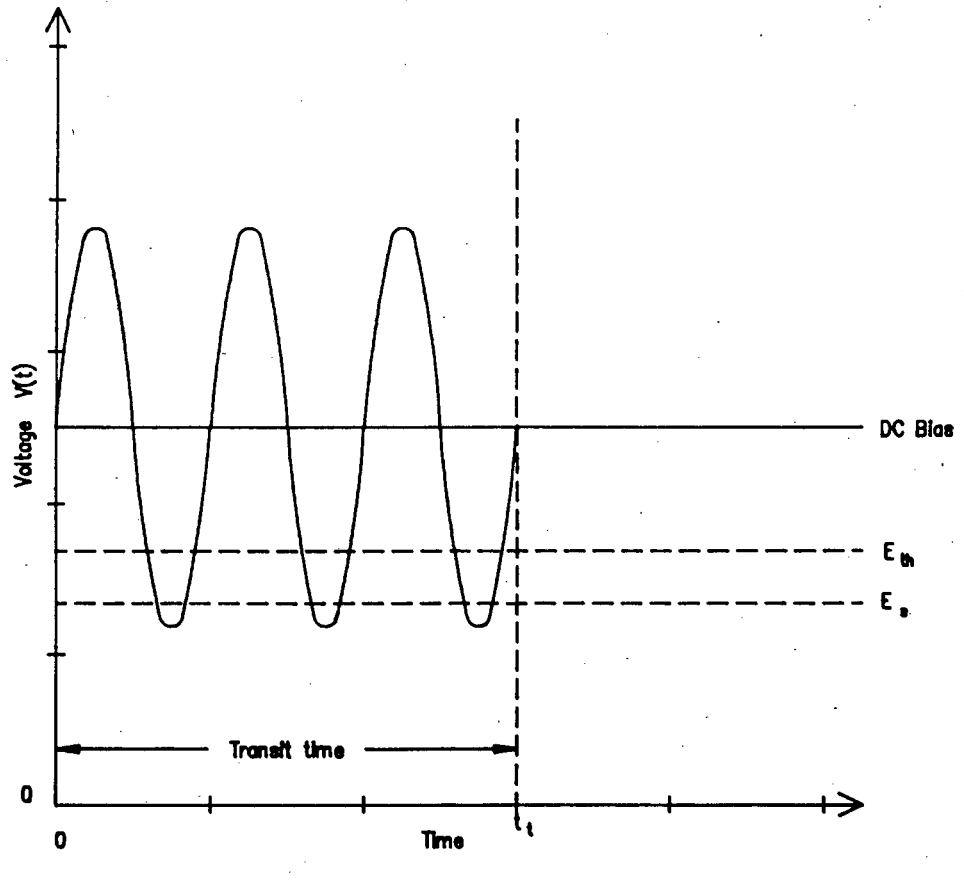

Fig. 11 LSA Mode.

the transit-time frequency rather than oscillation. In this case the negative resistance is utilised without domain formation.

Another mode is the bias circuit oscillation mode which can be caused by the sudden drop in current when the Gunn device is biased beyond its threshold. Oscillations of this nature are unwanted and range from a few hundred hertz to hundreds of megahertz.

2.3 The Varactor Diode

The variable capacitance diode or varactor is a P-N junction or Schottky barrier diode which is used for its voltage dependent reactive properties. Reverse biasing the diode produces a depletion layer at the junction which depth varies with the applied voltage. The depletion layer capacitance varies accordingly and therefore produces the required variable reactance. As the variable capacitance is the functional element of the device, all other properties of the diode are minimised and in particular the loss elements of the diode have been reduced.

By specifying the doping profile, the characteristic of the voltage dependent reactance can be varied to suit the application. There are three basic types of variable capacitance diodes. The abrupt junction varactor, the graded junction varactor which has got a more level slope of voltage versus capacitance and the hyper-abrupt junction

varactor which has the steepest characteristic. A typical characteristic is shown in Fig.12 [13].

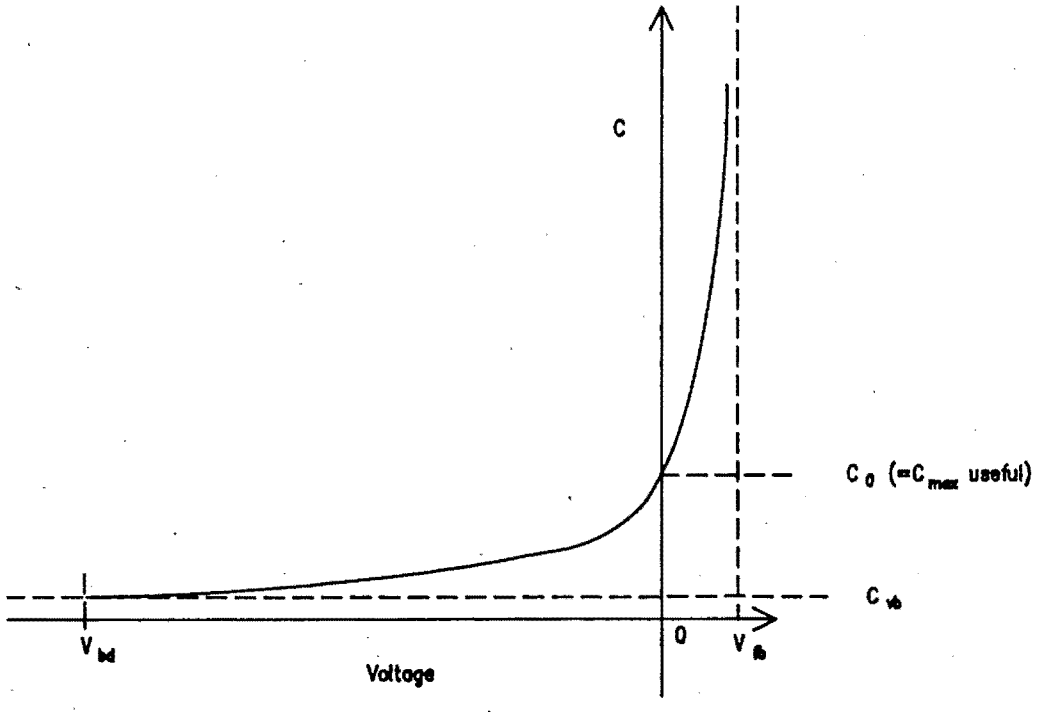

Fig. 12 Voltage/Capacitance Characteristic of a typical Varactor Diode.

2.4 The Electronically tuned Gunn Oscillator

Several ways of electronic tuning of Gunn Oscillators have been reported. Although the implementation of the different oscillator and tuning methods varies with the physical

constraints of the technology, the advantages and disadvantages of each tuning method remains the same.

The simplest method would be to vary the bias voltage of the Gunn-effect device (Fig.13) . The problem with this method is that not only the frequency variation would be different from device to device, but also the output power would vary considerably (Fig.14) [14]. This results in unwanted AM modulation.

Zieger [15] showed electronic tuning ranges of up to 1200 MHz at X-Band are possible by variation of the permeability of a ferrite filled cavity. Electronic tuning using YIG-spheres have been reported [16,17] but despite wide and linear tuning ranges their use is limited to low modulation frequencies due to the use of large magnetic coils.

The most well understood method of electronic tuning of Gunn oscillators is with the use of varactor diodes. The advantages of varactor controlled tuning are that the varactors can a) be modulated with high frequencies, b) they are small enough to be mounted in a microwave package and c) they have extremely low power consumption. Their disadvantages however are that they have a low Q at microwave frequencies, the capacitance-voltage characteristic is highly nonlinear (Fig.12) and they have limited peak power handling capacity.

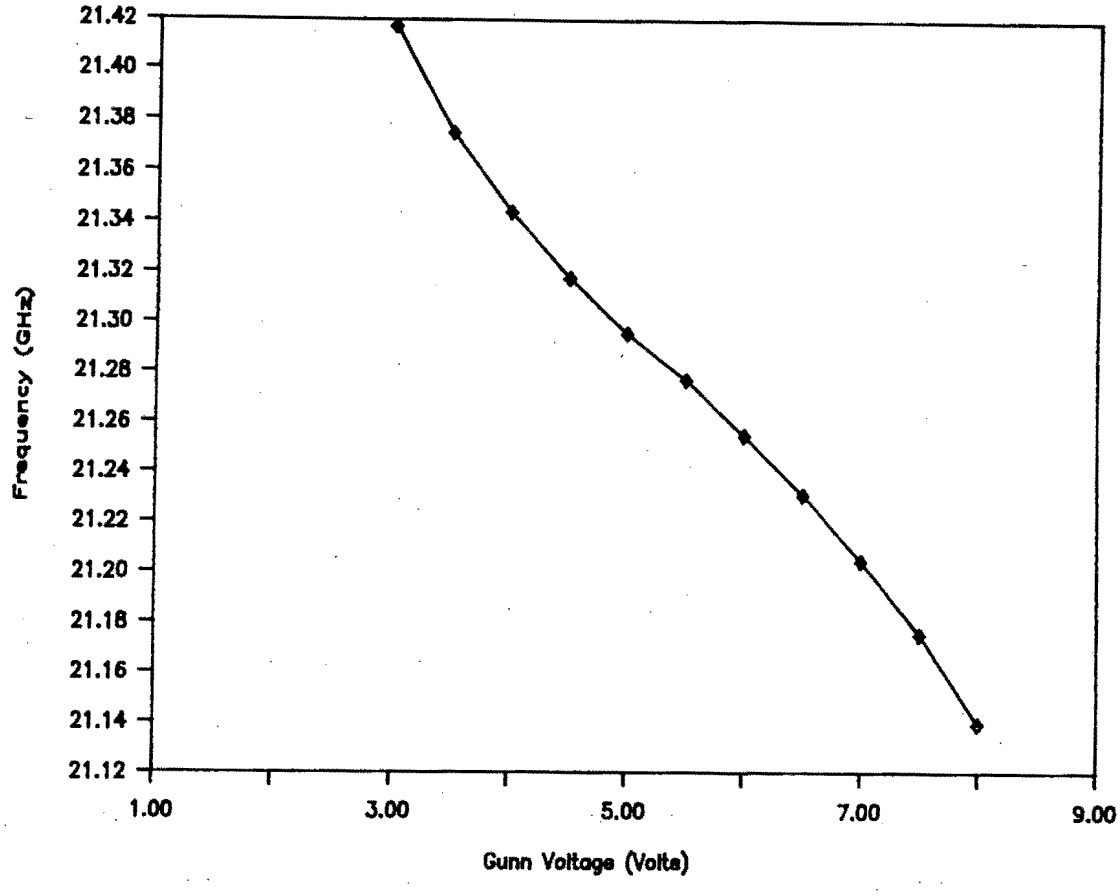

Fig. 13 Frequency Variation of Gunn Oscillator versus Bias Voltage.

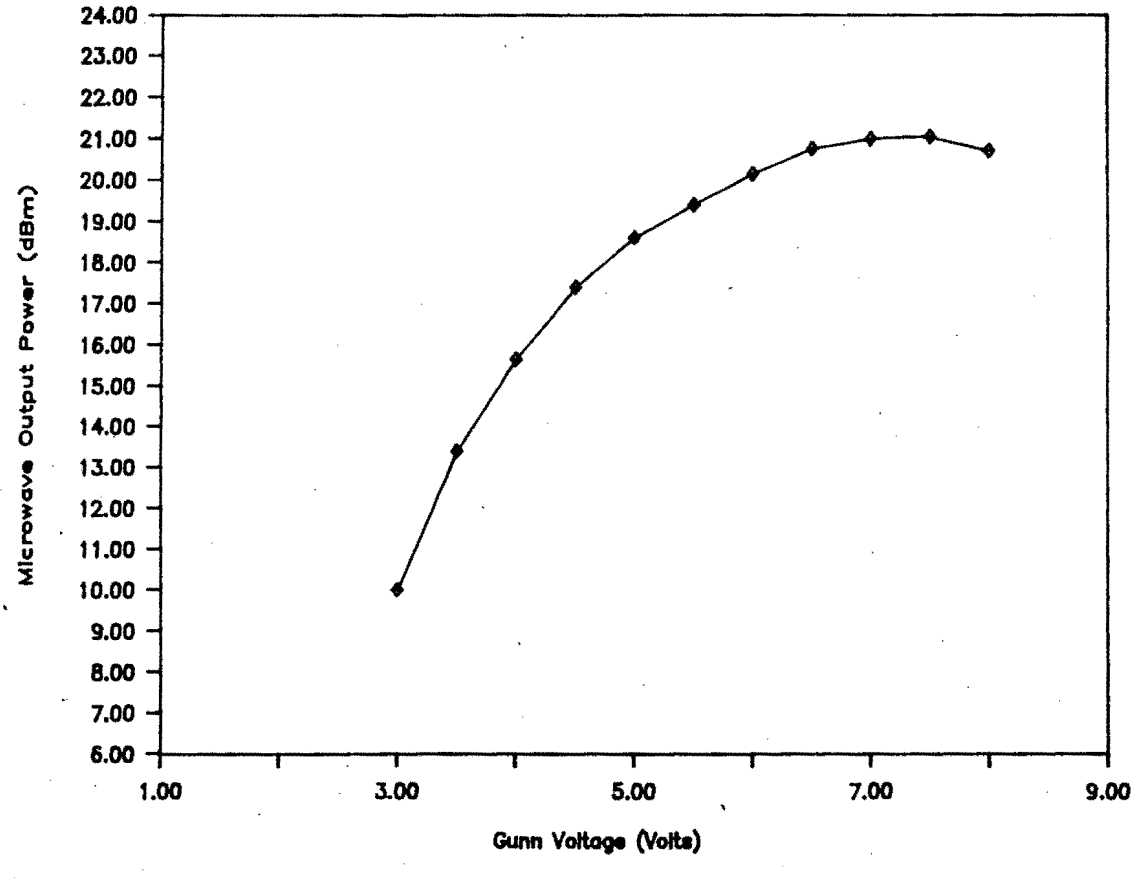

Fig. 14 Power Variation of Gunn Oscillator versus Bias Voltage.

2.4.1 Theoretical Limitations of Varactor tuned Oscillators

The tuning bandwidth of a varactor tuned Gunn oscillator is determined by the following factors.

a) Variation of capacitance of the varactor.

b) Parasitic elements of the package.

c) Coupling between Gunn diode and varactor.

d) Loaded Q-factor.

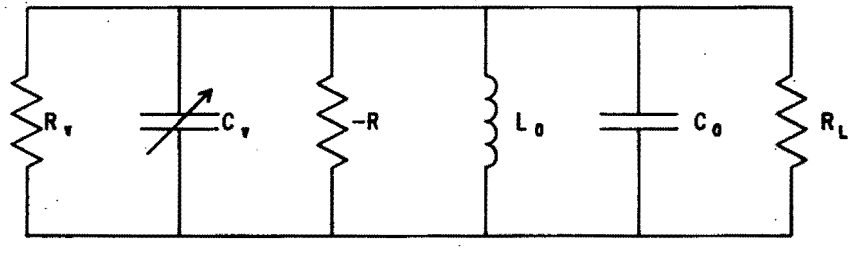

Fig. 15 Approximate Equivalent Circuit of a Varactor-tuned Negative Resistance Oscillator.

A very simplified equivalent circuit diagram [18] of a varactor tuned negative resistance oscillator (like the Gunn

oscillator) is shown in Fig.15. In practice the varactor, the load and the negative resistance element are coupled together by transformers. The circuit parameters therefore refer to the transformed quantities. The varactor is for simplicity represented by a parallel combination of a resistance (R_v) and a capacitance (C_v). All parasitics are assumed to be included in the main resonator consisting of L_0 and C_0.

If C_{v0} is the varactor capacitance at zero bias and C_{vb} varactor capacitance at breakdown voltage then the frequency of oscillation of the circuit ranges from

$$f_1 = [L_0(C_0+C_{v0})]^{-(1/2)}/2\pi$$
$$f_2 = [L_0(C_0+C_{vb})]^{-(1/2)}/2\pi$$

Assuming the difference between C_{v0} and C_{vb} is small compared to the total capacitance (C_0+C_{v0}) the tuning range referenced to f_1 can be expressed as follows:

$$\delta f/f_1 \approx (1/2)[(C_{v0} - C_{vb})/(C_0 + C_{v0})] \quad .... (1)$$

If P_{rv} is the reactive power and P_v the power dissipated in the varactor and P_{rc} the reactive power and P_c the power dissipated in the rest of the circuit the following relation hold.

$$\text{Varactor } Q = Q_v = P_{rv}/P_v = 1/(2\pi f R_v C_{v0}) \quad .... (2)$$

$$\text{Loaded } Q = Q_l = (P_{rv} + P_{rc})/(P_v + P_c) \quad .... (3)$$

As voltages across all elements of the circuit are

the same, the following relation holds:

$$C_{v0}/(C_{v0} + C_0) = P_{rv}/(P_{rv} + P_{rc}) \quad \ldots\ (4)$$

Combining (2), (3) and (4) the following relation is obtained:

$$C_{v0}/(C_{v0} + C_0) = Q_v P_v/Q_l(P_v + P_c) \quad \ldots\ (5)$$

Combining (1) and (5) the equation is obtained:

$$\delta f/f_l = -(C_{v0} - C_{vb})Q_v P_v/[2C_0 Q_l(P_v + P_c)] \quad \ldots\ (6)$$

From equation (6) a number of characteristics regarding the varactor controlled tuning of Gunn oscillators can be obtained.

The factor $C_{v0} - C_{vb}$ is determined by the varactor and it can be seen that the larger the capacitance range of the varactor is the larger is the tuning range of the oscillator.

The Q-factor of the varactor, Q_v, is at microwave frequencies very low. Using the equation (2) for the varactor Q and the data from the specification sheet in Appendix A (pg.144) for the varactor diode it can be calculated that the varactor Q drops from 5500 at 1 MHz to a Q less than 1 at 23 GHz. The varactor Q thus influences the tuning range of the oscillator to a large extent [19], the higher the Q-factor of the varactor the larger the electronic bandwidth.

The power dissipated in the varactor P_v is in direct relation on how well the varactor is coupled into the

microwave circuit. A varactor that is strongly coupled into the microwave circuit will have a high P_v and therefore wider electronic bandwidths are possible with such an arrangement [20].

As the factor C_0 takes the parasitic elements into account it can be seen from the equation that if the parasitic elements have got large values the tuning range will be reduced.

If the loaded Q-factor Q_l of the circuit is high the tuning range of the oscillator will be small. The total dissipated power of the oscillator $P_v + P_c$ is determined by the active device.

2.4.2 Practical Gunn Oscillators

There are several types of circuit techniques that have been used to make Gunn oscillators.

Aitchison and Newton [21] used unencapsulated Gunn and varactor diodes and associated circuitry using lumped elements, fabricated utilising thin-film technology. A tuning range of 1 GHz at X-band and an output power of 10mW have been achieved. The problem with this implementation is that for elements to be considered as lumped they must be very small. Elements are in general being considered to be lumped at microwave frequencies if their physical size is less than 1/10 (l = wavelength) [22]. At 23 GHz those

elements would have to be not larger than 0.13 mm. The other problem with this implementation is that it cannot be mechanically tuned.

Lee and Hodgart [23] achieved an electronic tuning range of 1 GHz at J-band with a through line cavity. The oscillator was mechanically tunable over 3 GHz and had a Q-factor of approximately 35. Low stability and poor FM noise performance is the result of the low Q-factor.

Coaxial cavities have been reported to have electronic tuning ranges up to 1.1 GHz at X-band by Smith and Crane [24]. This was achieved by coupling the varactor and the Gunn diode very tightly and by using a low Q cavity.

Waveguide cavities have higher Q-factors than all the other oscillator implementations, resulting in better noise performance and stability. They can be easily mechanically tuned over octave bandwidths. Using reduced height waveguide Downing and Myers [25] achieved an electronic tuning range of 1.95 GHz at X-band. This was only possible because the waveguide cavity had a very low Q-factor. They also reported [26] a varactor-tuned Gunn oscillator having an electronic bandwidth of 1.18 GHz at a frequency of 38 GHz. Joshi [27] reports a 1 GHz electronic tuning range for a full height waveguide cavity at X-band showing less output power variation than the lower Q-factor cavities.

CHAPTER 3

3. THE PRACTICAL OSCILLATOR

3.1 Introduction

Two different varactor controlled waveguide oscillator configurations have been researched in detail. It has been found that the one configuration presented certain unwanted technical problems and therefore the other configuration was chosen for the datalink. This chapter explains why the two configurations were chosen and presents the experimentally derived characteristics of each configuration with respect to changes in certain physical dimensions of the cavities. It then attempts to explain the phenomena that occurred during the course of the experiments.

3.2 Different Waveguide Oscillator Configurations

There are many ways of the physical implementation of the waveguide Gunn oscillator. One implementation would be to place the Gunn-effect device and the varactor along the centre of the broad side of the waveguide. With one side of the waveguide short-circuited with a metal plate and the other end open, the varactor can be placed closest to the short-circuit and the Gunn-effect device closest to the open end or vice versa. These combinations have been researched

by Templin and Gunshor [28] who found that if the varactor was placed closest to the short-circuit, electronic tuning was smoother than mechanical tuning with the short-circuit. With the Gunn-effect device closest to the short-circuit, mechanical tuning was smoother than electronic tuning.

In another configuration the Gunn-effect device and the varactor were placed next to each other on the broad-side of the waveguide [27,29]. Although the electronic and mechanical tuning characteristics were 'well behaved' in this configuration, the electronic tuning range is excessively high (1 GHz at X-band). This resulted in a reduced oscillator Q-factor and poorer FM noise performance.

Other researchers [30] investigated oscillators in reduced height waveguides where Gunn-effect device and varactor were placed behind each other along the centre of the waveguide. The effect of reducing the height of the waveguide was an increase of electronic tuning range with an accompanying reduction of oscillator Q-factor. Even larger tuning ranges (1.95 GHz at X-band) were achieved by placing the Gunn-effect device and the varactor next to each other in a reduced height waveguide [25].

The final choice of the configuration was determined by the design specifications. The tuning range had to be relatively small (±250 MHz) and as linear as possible. The oscillator had to be low noise and therefore a high Q-factor was necessary. The possibility of using either reduced height waveguide or placing Gunn-effect device and varactor next to each other were therefore ruled out from the start. It has

been decided to use full height waveguide and placing the Gunn-effect device and the varactor behind each other along the centre of the broadside of the waveguide with the varactor closest to the short-circuit. This has been done to ensure that electronic tuning is as smooth as possible, as it was of importance to the functional design of the datalink. In this way moderate tuning ranges are achievable, yet high Q-factor and good stability are possible.

3.3 The Two Oscillator Concepts

Both the oscillators use standard full height waveguide cavities and are manufactured from brass. The basic difference between the two concepts is that the Gunn effect device is in the one case mounted on the bottom of the waveguide and in the other case mounted on a post in the centre of the waveguide. The two configurations are presented in Fig.16 and Fig.17.

Both oscillators consist of a short-circuit plate and then the varactor which is mounted on the floor of the waveguide cavity and held there by a choke. The Gunn effect device is mounted on the floor of the waveguide, or in the other case, on a post in the waveguide and both are held there by a choke.

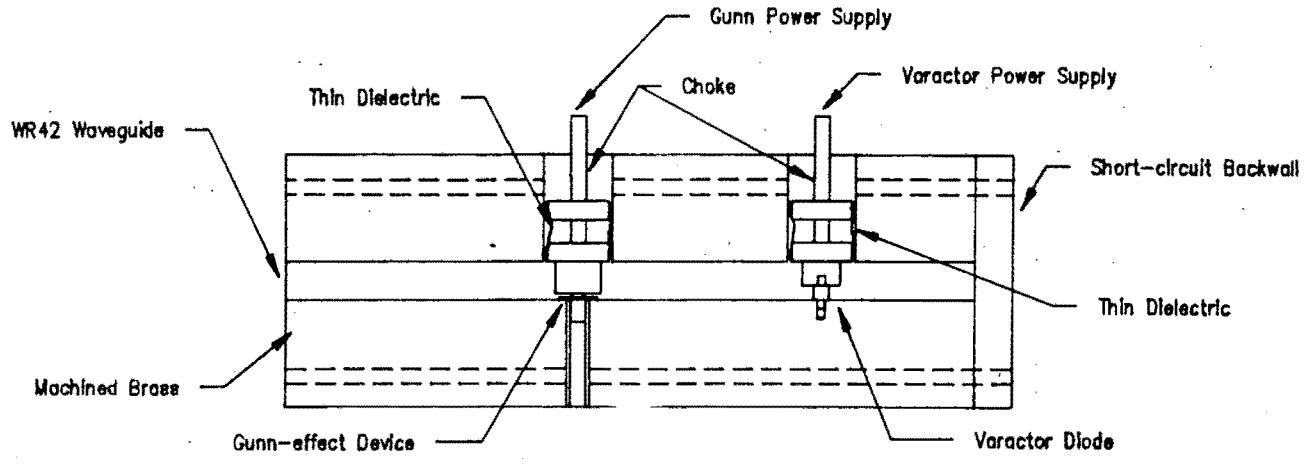

Fig. 16 Cavity Oscillator Design with Gunn-effect Device on the Floor of the Waveguide.

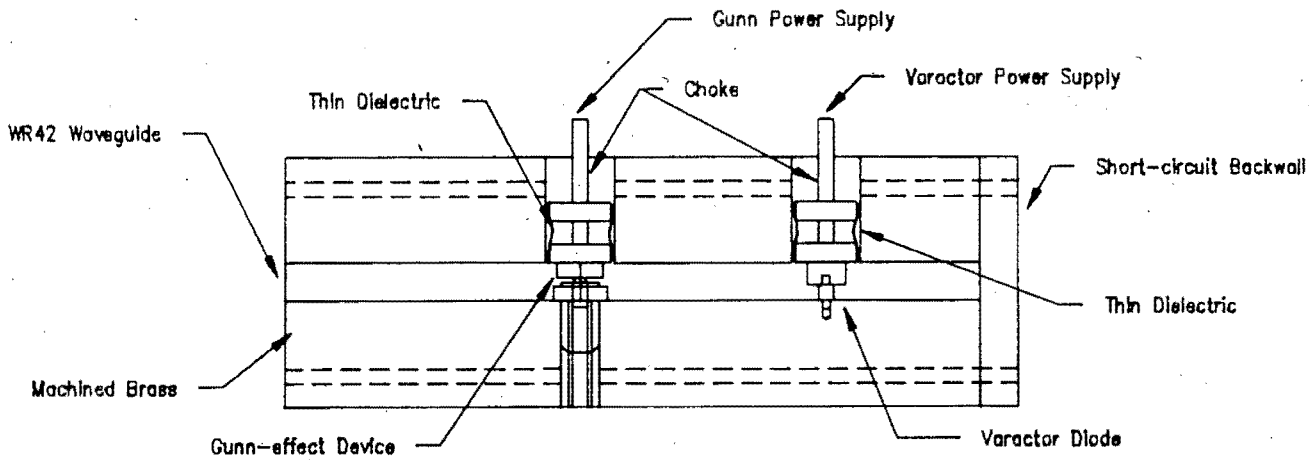

Fig. 17 Cavity Oscillator Design with Gunn-effect Device mounted in the Centre of the Waveguide.

The chokes are electrically insulated with plastic heat-shrink dielectric from the cavity as they carry the bias to

The basic test-setup is as shown in Fig.19. It consists of the Gunn device/varactor cavity with a copper heatsink, a piece of standard WR42 waveguide, a cross-coupler, an attenuator, a termination and two waveguide-to-coax adapters. The cross-coupler, the attenuator and the termination had to be designed, fabricated, tested and calibrated before the experiments.

The Gunn-effect device type that has been selected for the oscillator is the MA 49180-148 from Microwave Associates with an nominal output power of 100 mW. The varactor diode is the MA 45225-30 also from Microwave Associates. Both specification sheets are given in Appendix A (pg.144).

3.4.1 The Cross-coupler

The cross-coupler as shown in Fig.20 consists of two brass blocks in which there are slots of standard sized waveguide. The two blocks fit together such that the waveguide slots are at right angles to each other. Between the two blocks is a thin (0.6mm) brass shim with two crosses cut in it as shown in Fig.20.

The crosses in the shim are a quarter wavelength apart in each direction of the waveguides. The functional principle of the directionality of the cross-coupler is based on the theory that two plane waves subtract each other (destructive interference) when their phase differ by half a wavelength. The slots are used instead of round holes as this increases

the coupling as slots are more effective radiators than round holes [31,32].

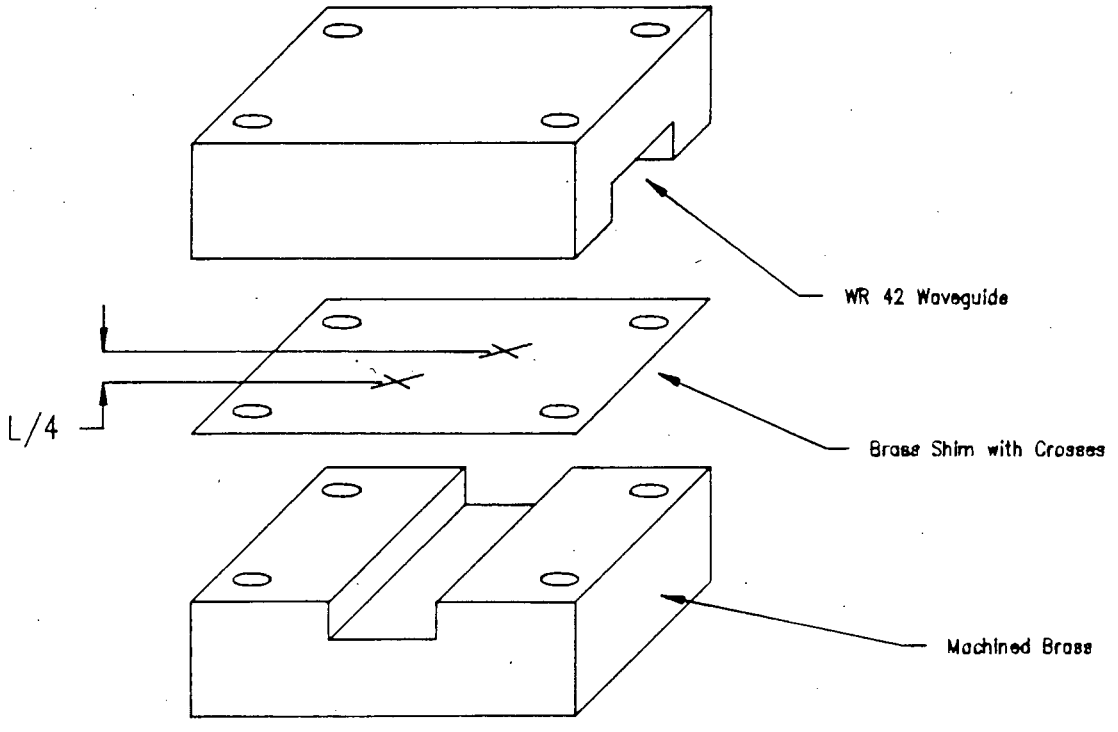

Fig. 20 The Cross-coupler Assembly.

The design details and s-parameters are given in Appendix B (pg.146). In summary, the calibration yielded the results that the cross-coupler has an insertion loss of 0.1 dB, an isolation of 20 dB and a coupling of 9 dB.

3.4.2 The Attenuator

An attenuator with an attenuation of approximately 3 dB was needed for the test-setup as the powermeter had a maximum

readable power input of 20 dBm and output powerlevels in the range of 20 dBm were expected.

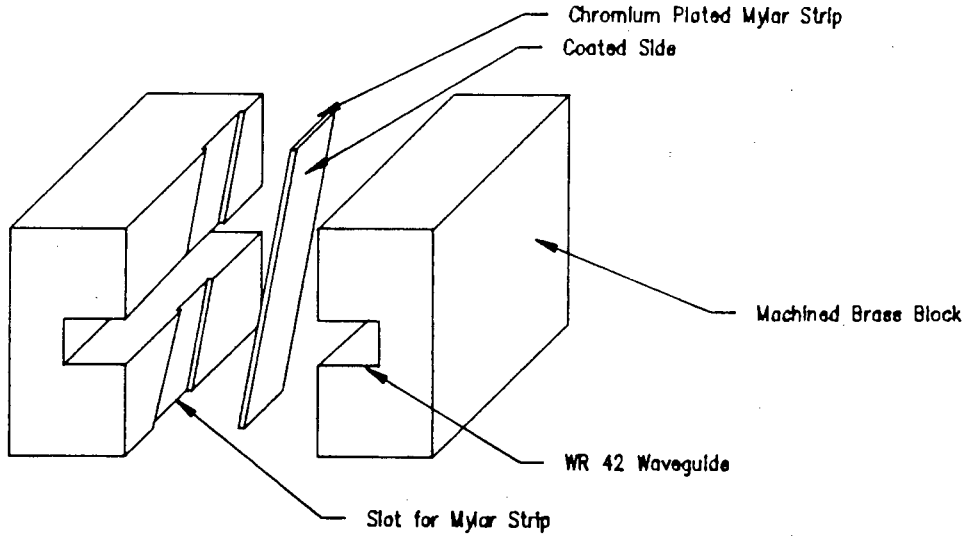

Fig. 21 The Attenuator Assembly.

The attenuation of the attenuator in Fig.21 is achieved by placing a parallel strip of mylar, coated on one side with chromium, at an angle into the waveguide. It is important that the chromium side of the strip is exactly in the centre of the waveguide as the influence on the electromagnetic wave is a maximum. Moving the metallic side of the strip slightly off centre reduces the effectiveness of the attenuator by a large amount (from 20dB to 3dB for a 20 dB attenuator).

The angle at which the strip is placed into the waveguide has to be as flat as possible to reduce the reflection due to mismatch caused by the insertion of the strip. For that

reason the length of the attenuator has to be longer than one waveguide wavelength [31].

In such a way an attenuation of 4.1dB was obtained with an input return loss of better than 20 dB. The design details and s-parameters are given in Appendix B (pg.146).

3.4.3 The Termination

The termination (Fig.22) is used to terminate the unused port of the cross-coupler into a matched load. The reason for this being that changing external conditions may not influence (like frequency pulling) the measurement.

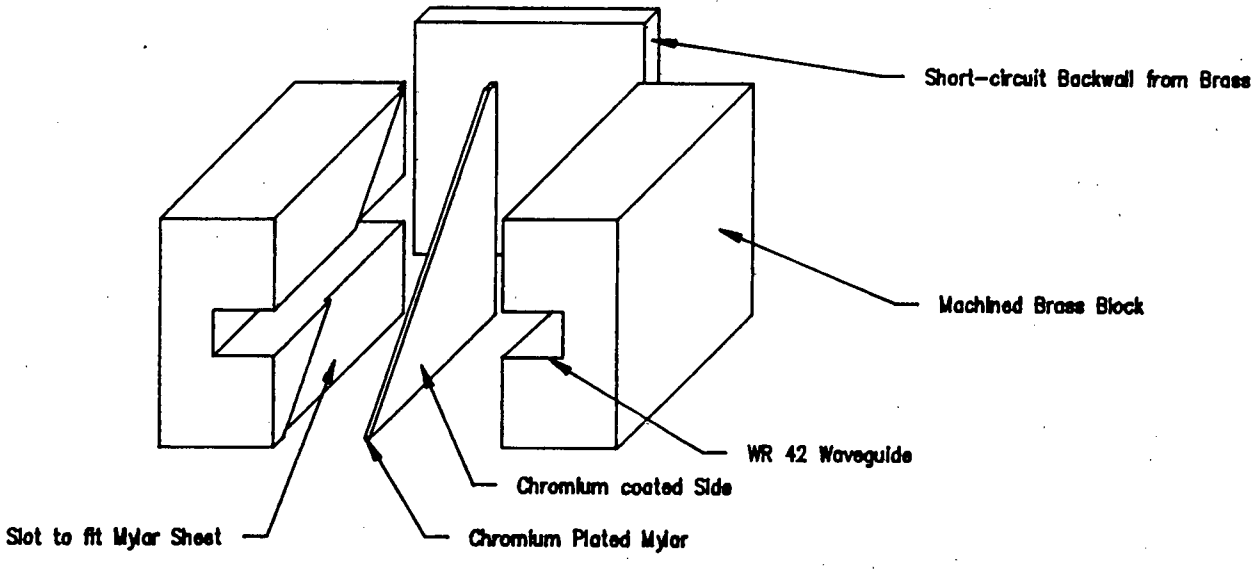

Fig. 22 The Termination.

The termination is designed in very much the same way as the attenuator and based on the same principles. It basically consists of a very wide strip of the chromium coated mylar and one side of the waveguide is simply closed with a metal plate acting as a short-circuit. In the case of the termination the return loss at the input port is however the most important design feature. A return loss of better than 30 dB was achieved. The design details and s-parameters are given in Appendix B (pg.146).

3.5 The Test-procedure

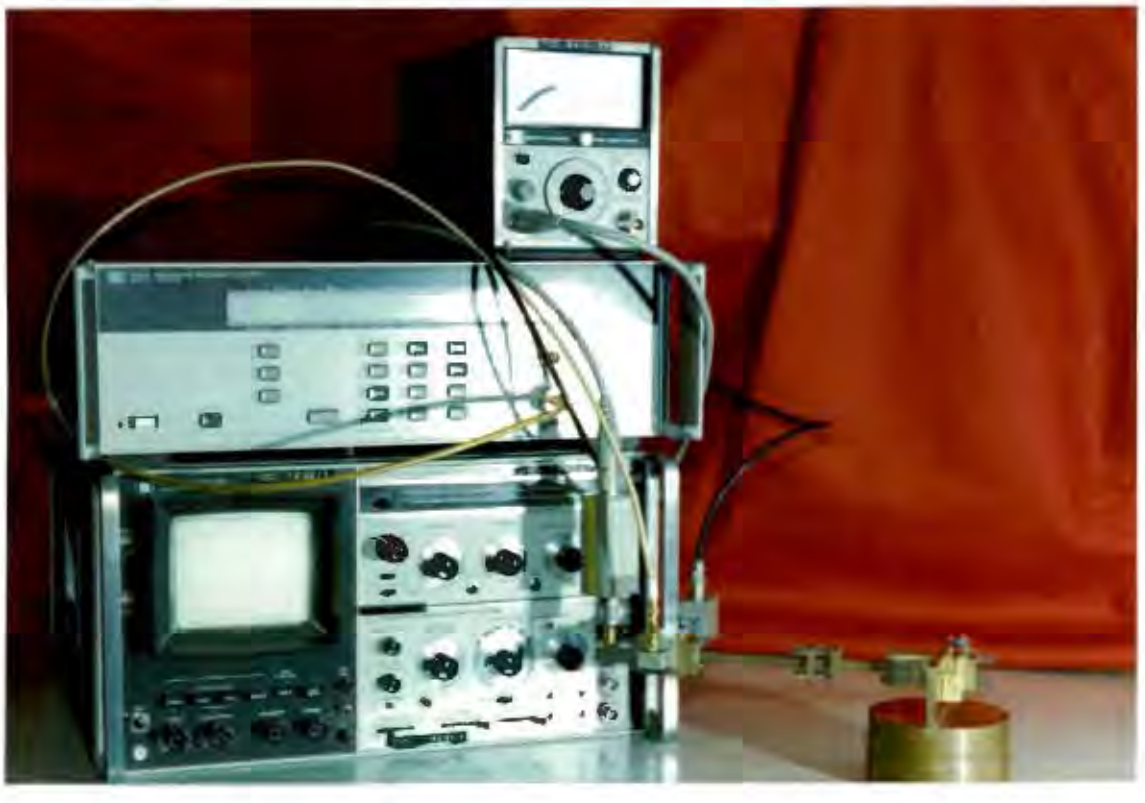

Fig. 23 The Test-setup.

With the test-setup as described above and as shown on the photograph (Fig.23) several dimensions of the cavity have been changed to establish firstly the characteristics of the cavity and secondly to determine a design procedure to fabricate oscillators with the required specifications.

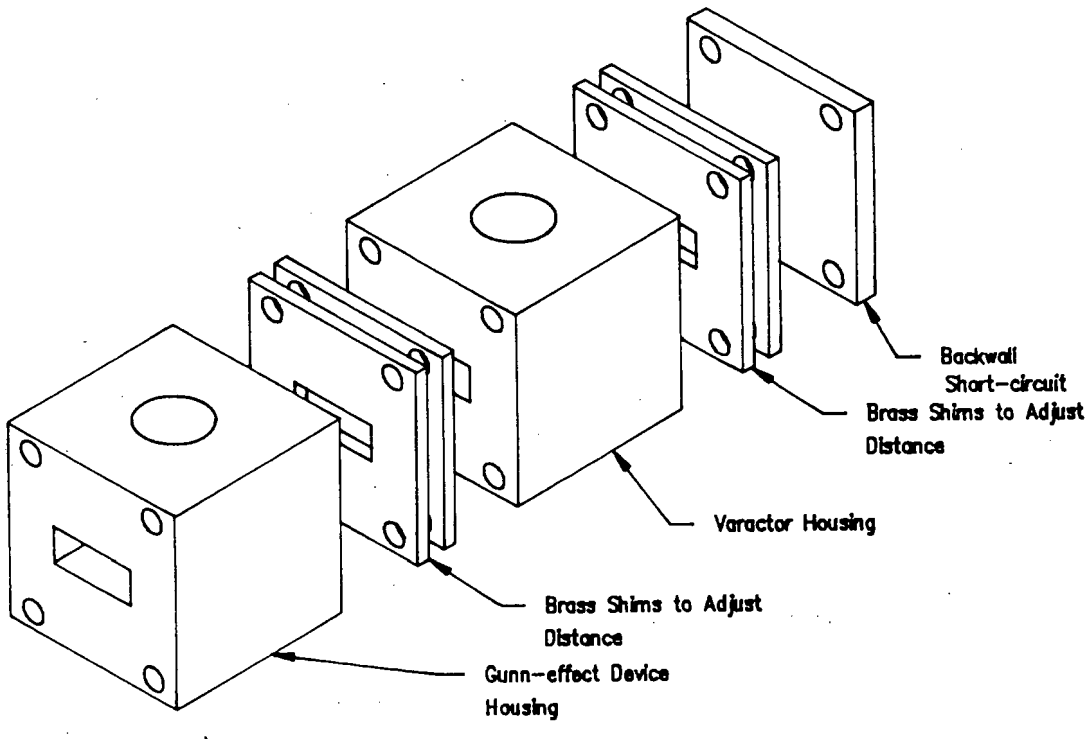

Fig. 24 Method of adjusting the Cavity Lengths by using Brass Shims.

In both oscillator configurations the distance between the Gunn-effect device and the varactor have been changed as well as the distance between short-circuit and the varactor. This has been achieved with a set of machined brass shims as shown in Fig.24. The set of shims consists of shims from 1.00 mm width to 2.00 mm width in steps of 0.1 mm as well as a set of shims of widths 1.00 mm, 2.00 mm, 2.50 mm, 3.00mm,

4.00 mm, 6.00mm and 8.00 mm. The set was selected to insure that there were always a pair of shims between varactor and Gunn-effect device and between varactor and short-circuit backwall, so that the only changing factor during the experiment was the distance and not the number of shims used. This was to isolate the test aim and to reduce experimental error.

The parts of the varactor choke and the Gunn-effect device choke that are protruding into the waveguide have also been varied in size. This was done by inserting a different choke with the diameter that protrudes into the waveguide having each time a different size. In the case of the Gunn-effect device being mounted on a post off the floor of the waveguide, the diameter of the part of the post that protrudes into the waveguide has also been varied.

The above variations in physical dimensions of the cavities were performed in independent experiments as to isolate the effects of each change.

Measurements of power, frequency, varactor voltage and Gunn-effect device current were recorded as well as all the changes in physical dimensions of the cavity. The test results were recorded and entered into an electronic spreadsheet (LOTUS 1-2-3) and the data was immediately analysed. A copy of the spreadsheet is attached in Appendix C (pg.150).

3.6 An intuitive Theory for Gunn Oscillator Characteristics

An intuitive analysis of cavity Gunn oscillators can be done using the standing wave pattern that is generated inside the waveguide. If a simple oscillator circuit is being considered with only a mounted Gunn-effect device and a sliding short-circuit inside the waveguide, it can be reasonably assumed that the electric field is at a minimum at the short-circuit. For the space between the Gunn-effect device and the short-circuit backwall to form a resonant cavity the distance between the active device and the short-circuit must be normally half a waveguide wavelength long.

If the short-circuit backwall is changed in position it is obvious that as the distance between Gunn-effect device and backwall increases, the waveguide wavelength increases and therefore the resonant frequency decreases.

A problem occurs at the point where the distance between the Gunn-effect device and the backwall becomes so long that the distance is a multiple of half a waveguide wavelength. The theoretical graph of frequency versus distance between Gunn-effect device and backwall is shown in Fig. 25. The graph is derived from the relation between the wavelength (L) of an electromagnetic wave and the waveguide wavelength (L_g)

$$L = L_g/\sqrt{[1 + (L_g/2a)^2]} \qquad .... (6)$$

Where a is the longer of the two inside dimensions of a rectangular waveguide.

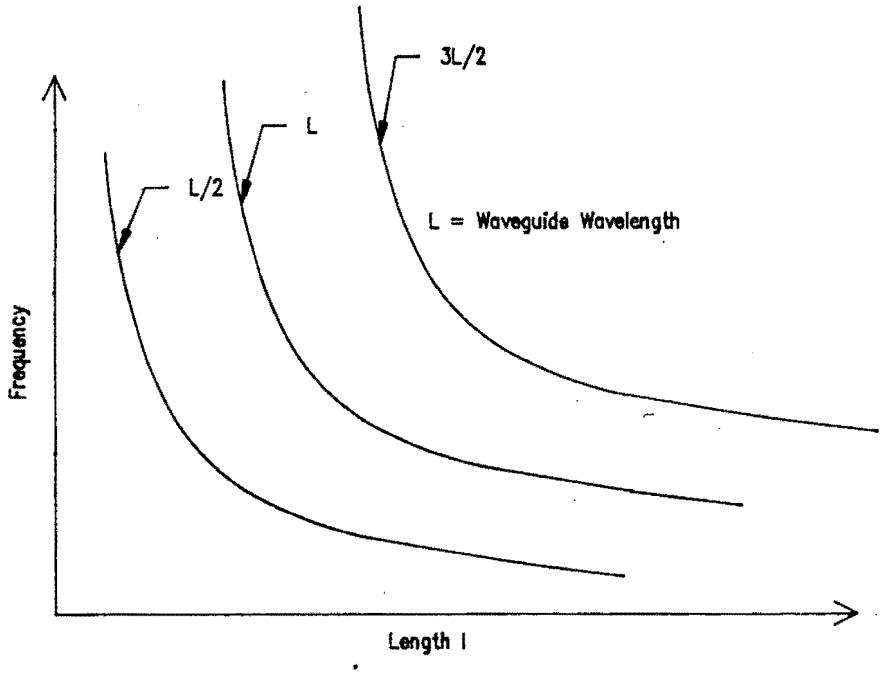

Fig. 25 Theoretical Tuning Curves for varying the Length of the Cavity.

The family of curves depicted in Fig. 25 indicate that there is for a certain backwall distance adjusted, more than one frequency of operation is possible. Alternatively, the same frequency of oscillation can occur at more than one position of the short-circuit. It can therefore be expected that the tuning of the Gunn oscillator is not smooth over whole mechanical tuning range but that the frequency will jump from one oscillation mode or cavity mode to the other under certain conditions.

Introducing a varactor diode between the backwall and the Gunn-effect device does not complicate the matter if the varactor diode is thought of as a simple variable reactance

which is inserted into the cavity. However if the resonance condition of the cavity is marginally in one mode, any changes in the reactance of the varactor due to supply voltage changes will cause the oscillation conditions to change and a jump in output frequency can be expected.

How these phenomena affect the practical oscillator and what governs them will be investigated in the following sections.

3.7 Variation of the Distance between Varactor and Backwall Short-circuit

3.7.1 Gunn-effect Device on the Floor of Waveguide

The summarised results of these experiments are shown in Fig.26. Graph (a) displays the output frequency versus the distance between the short-circuit backwall and the varactor diode. This graph shows that the frequency of the oscillator changes only very slowly with increasing distance. A maximum frequency variation of 115 MHz over a mechanical adjustment range of 8.5 mm can be measured. But the most significant feature of the graph is that the frequency increases slowly with increasing distance. This contradicts the theory outlined in section 3.6 and none of the modes described in that section demonstrate this behaviour. The only conclusion that can be made at this stage is that the oscillator operated in another, yet undescribed mode.

(a) Frequency

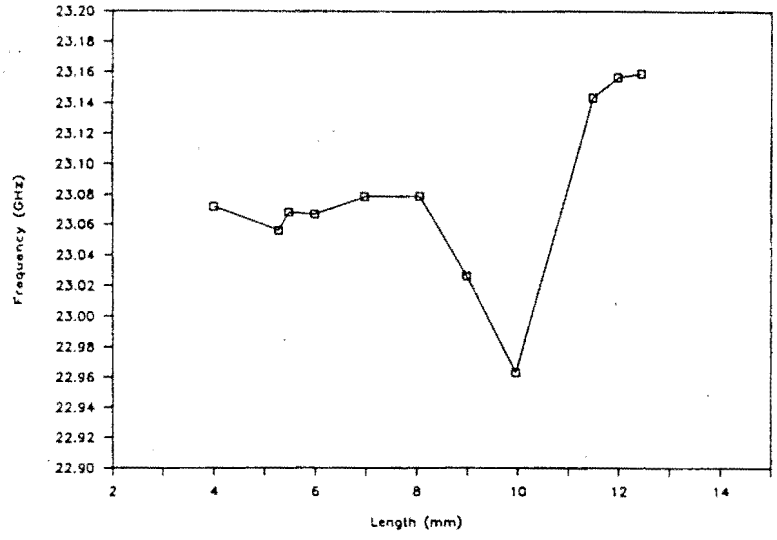

(b) Power

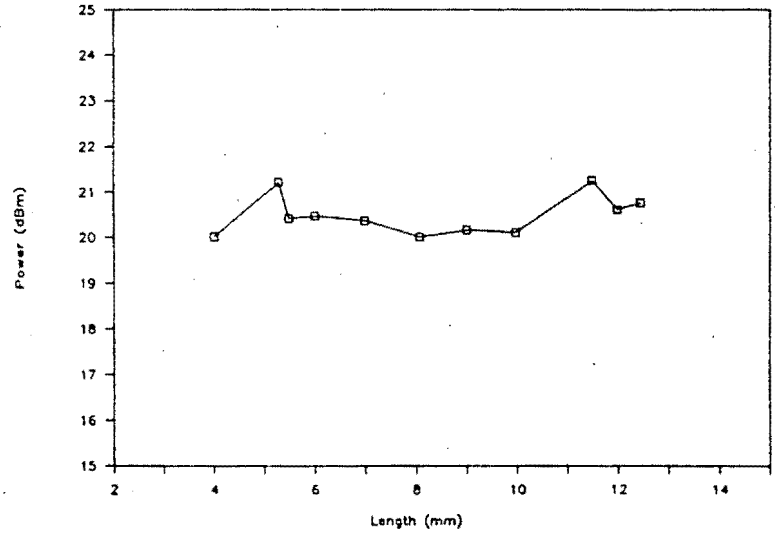

(c) Electronic Tuning Range

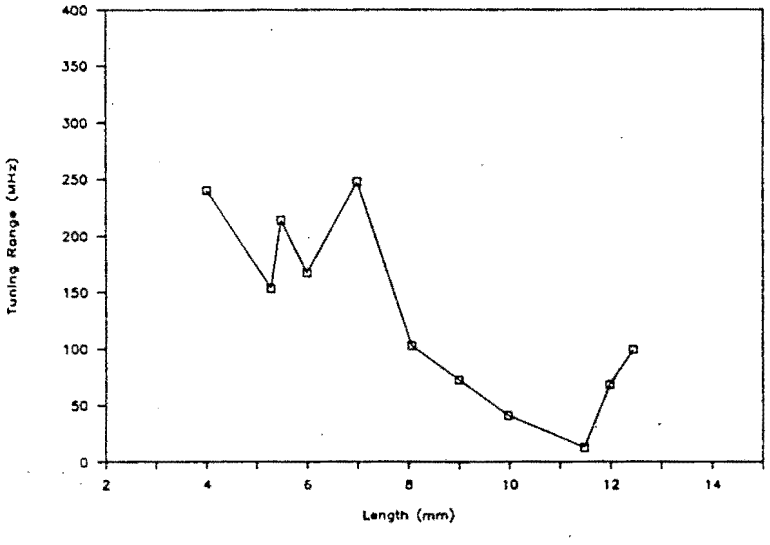

Fig. 26 Variation of Distance between Backwall and Varactor, Gunn-effect Device on Floor.

The variation of power versus the variable length is shown in graph (b) of Fig.26. The power output remains fairly constant at 20.5 dBm and varies only by 1.25 dBm over the variable distance. Only two small power peaks at the distances of 5.0 mm and 11.5 mm are of significance.

Graph (c) of Fig.26 depicts the tuning range versus the variable length. It is important to note that for the shorter distances between varactor and backwall relatively high tuning ranges (approx. 200 MHz) are achieved. Increasing the distance reduces the tuning range up to a distance of 11.5 mm after which the tuning range increases again.

3.7.2 Gunn-effect Device in the Centre of Waveguide

The results of the second cavity configuration are shown in Fig.27. Graph (a) depicts the expected decrease of frequency when the distance between varactor diode and backwall is increased as outlined in section 3.6. The characteristic hyperbolic decrease in frequency as presented in Fig. 25 however is only apparent from distances longer than 9 mm. For shorter distances the change in frequency decreases till it almost levels out. The change in frequency that can be achieved in this configuration is 1.18 GHz over a mechanical tuning range of 4.5 mm. It is also important to note that the mechanical tuning over that range is smooth and no frequency jumps have been measured.

(a) Frequency

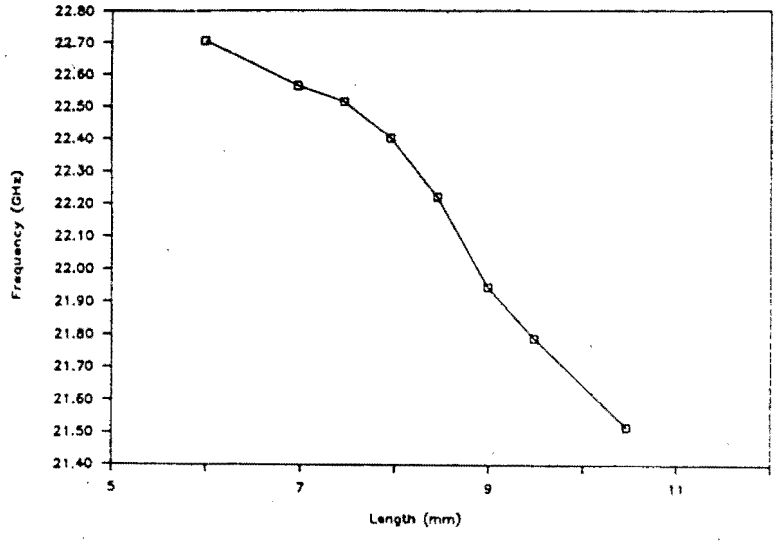

(b) Power

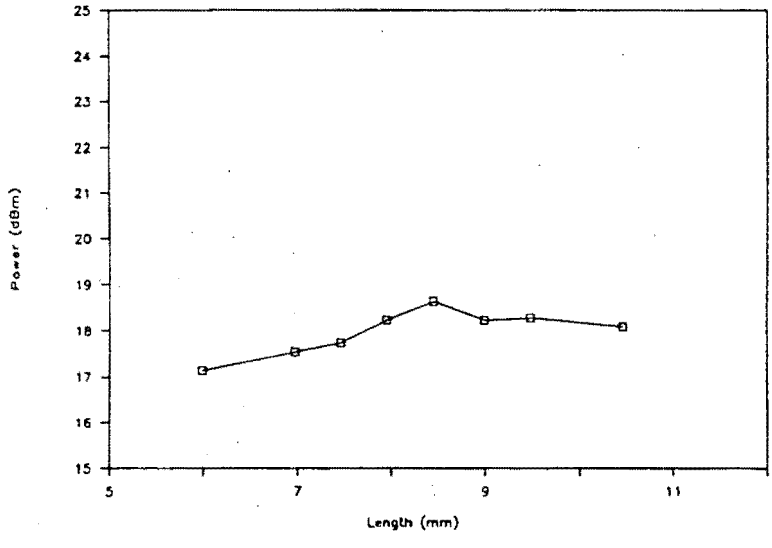

(c) Electronic Tuning Range

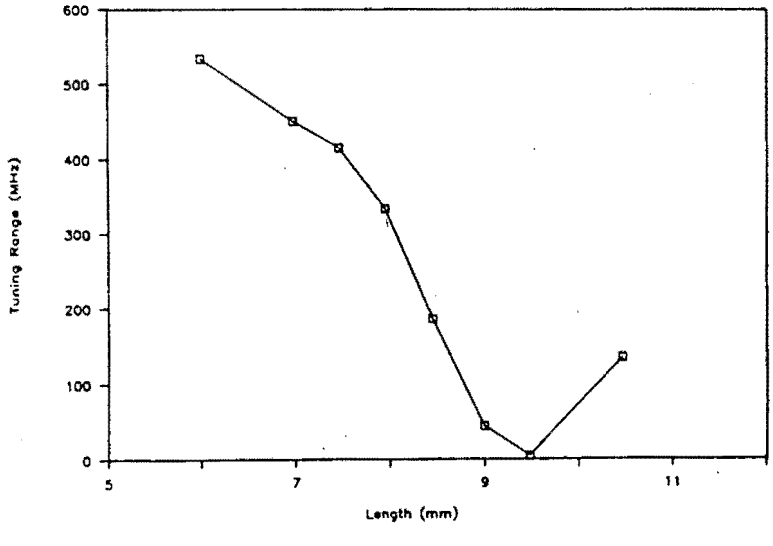

Fig. 27 Variation of Distance between Backwall and Varactor, Gunn-effect Device in Centre.

The power output varies only by 1.5 dBm over the mechanical tuning range and the mean output power is approximately 18dBm. This is shown in graph (b) of Fig.27. It can also be seen that the power output increases slightly as the variable length is increased.

A large tuning range (550 MHz) is obtained at close distances of the backwall to the varactor diode as presented in graph (c) of Fig.27. The tuning range then decreases to a minimum at a distance of 9.5 mm and then increases again with increasing length.

3.8 Variation of the Distance between Varactor and Gunn-effect device

3.8.1 Gunn-effect Device on the Floor of Waveguide

The summarised results of these experiments are shown in Fig.28. Graph (a) of Fig.28 shows the frequency (measured at 30V constant varactor voltage) versus the spacing between Gunn-effect device and the varactor. The graph is not smooth and frequency jumps as described in section 3.6 are present. After a rapid decrease of frequency, such a mode jump is evident in the sudden frequency increase at a spacing of 13 mm. Further increasing the distance the frequency then decreases as before. The measured frequency change over the mechanical tuning range of 5.5 mm is 2.3 GHz.

(a) Frequency

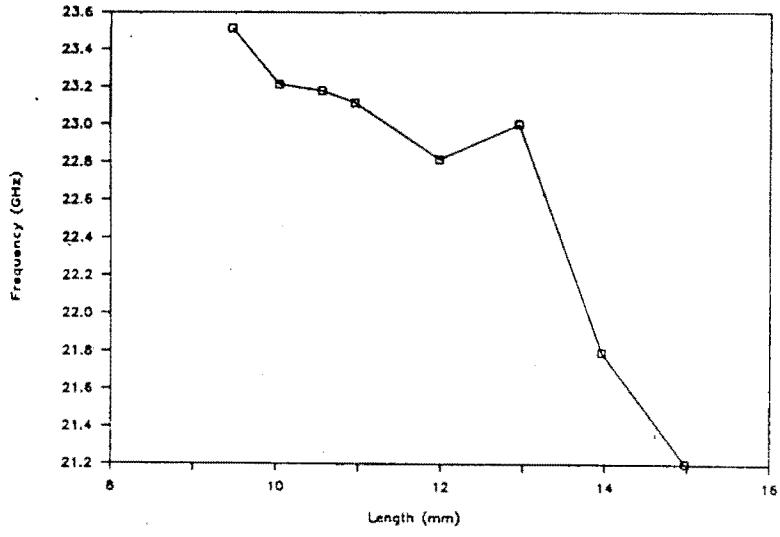

(b) Power

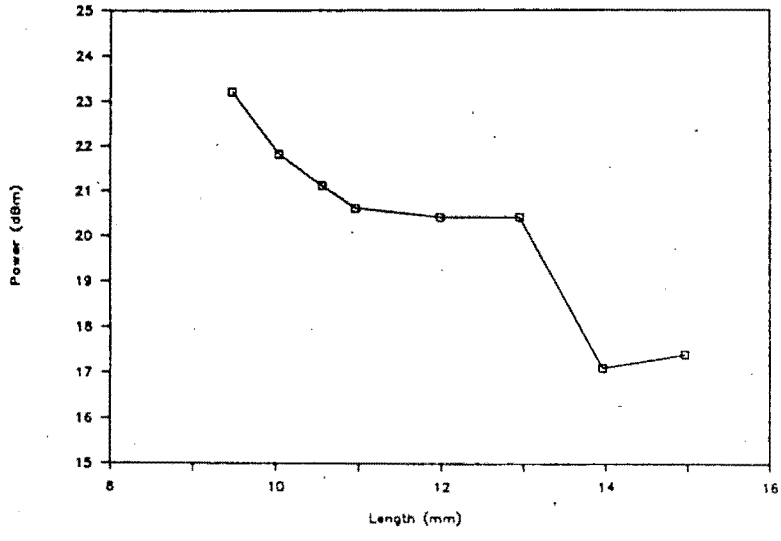

(c) Electronic Tuning Range

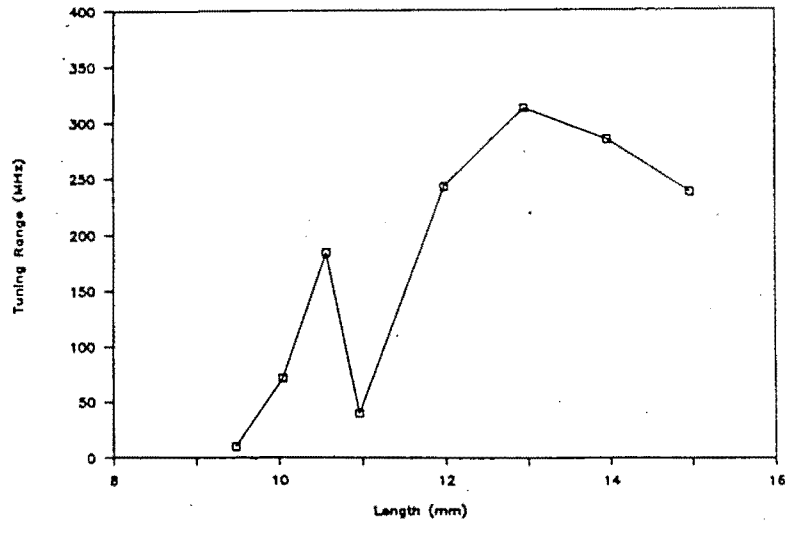

Fig. 28 Variation of Distance between Gunn-effect Device and Varactor, Gunn-effect Device on Floor.

Graph (b) in Fig.28 shows the microwave power output versus the variable length. As in the frequency response the variation of the output power does not present a smooth function. It is significant that a sudden power drop occurs at a distance of 13 mm which corresponds to the sudden frequency jump at 13 mm in graph (a).

The tuning range versus the spacing between the varactor diode and the Gunn-effect device is presented in graph (c) of Fig.28. After having a very low tuning range at short distances the range increases to a peak at 13 mm with increasing distance. Further increasing the distance decreases the tuning range again. It is important to note that the maximum tuning range occurs at the same distance at which sudden frequency and output power changes happen.

3.8.2 Gunn-effect Device in the Centre of Waveguide

The frequency response versus the variable length of this cavity configuration is displayed in graph (a) of Fig.29. The response is smooth and the frequency decreases as the distance between the varactor and Gunn-effect device increases. The mechanical tuning of 3.5 mm of the cavity produces a frequency change of 1.57 GHz.

The microwave output power in graph (b) is on the average 18 dBm and peaks at 10.5 mm length. The power variation of 1.65

(a) Frequency

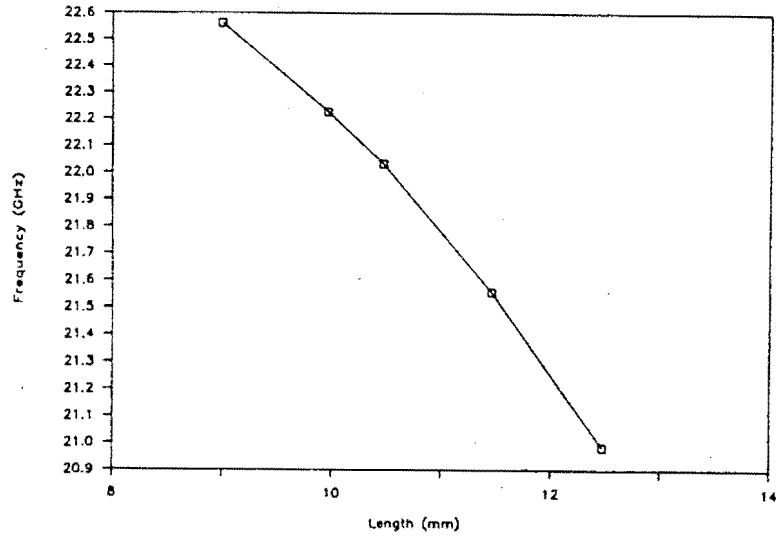

(b) Power

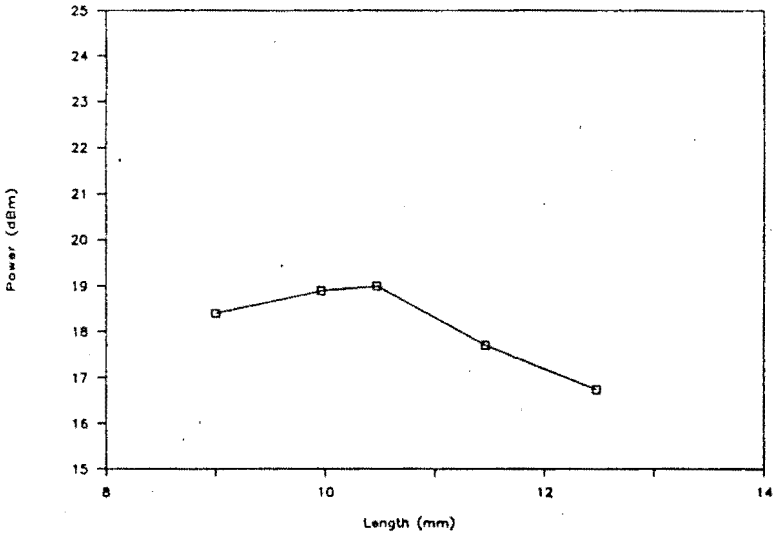

(c) Electronic Tuning Range

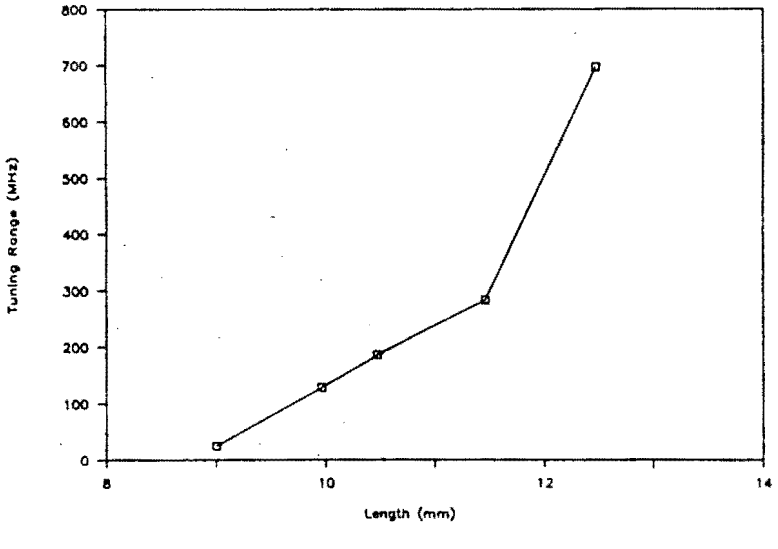

Fig. 29 Variation of Distance between Gunn-effect Device and Varactor, Gunn-effect Device in Centre.

dBm over the mechanical tuning range does not display any jumps or mode changes. This corresponds to the smooth frequency tuning in graph (a).

Graph (c) depicts the electronic tuning range versus the variable length. The tuning range is increasing very steeply with increasing distance between the varactor diode and the Gunn-effect device. At a distance of 12.5 mm between the devices the tuning range increases very sharply to almost 700 MHz in comparison to the relatively linear rise of tuning range with increasing distance.

3.9 Comparison of Results of varying Cavity Lengths

a) Frequency

The most significant difference between the two configurations occurs when the distance between varactor diode and backwall is changed. While the frequency of the cavity configuration with the Gunn-effect device mounted on the bottom of the waveguide changes only by 115 MHz over a mechanical tuning range of 8.5 mm (or 13.5 MHz/mm), the other configuration changes by 1150 MHz over a mechanical tuning range of 4.5 mm (or 255 MHz/mm). This information alone leads to the belief that there is a different oscillation mechanism responsible in each of the cavity configurations.

c) Tuning Range

The family of curves displaying the electronic tuning range of the two oscillator configurations show that with the Gunn-effect device mounted on a post in the centre of the waveguide far higher tuning ranges can be achieved. While the maximum tuning range measured in the configuration with the Gunn-effect device mounted on the floor of the waveguide was approximately 320 MHz a maximum tuning range of 700 MHz was obtained with the other configuration.

When the distance between the backwall and the varactor is changed in both configurations the tuning range is high when the backwall is close to the varactor. This then drops to a minimum and then the tuning range increases again. However if the distance between the two semiconductors is increased both cavity configurations display the characteristic of increasing the tuning range. Another important feature is that frequency jumps or mode jumps correspond to the place where the electronic tuning range is either at a minimum or at a maximum. This is seen in the graphs where the Gunn-effect device is mounted on the bottom of the waveguide, as the other configuration does not display the characteristics of mode jumping very clearly.

To summarise, the configuration where the Gunn-effect device is mounted on a post in the centre of the waveguide is in general more 'well behaved', displaying a wider mechanical tuning range, higher electronic tuning range and less mode

jumping although the microwave output power is lower than the other configuration.

3.10 Variation of the Varactor Post Diameter

3.10.1 Gunn-effect Device on the Floor of Waveguide

The summarised results of this series of experiments are presented in Fig.30. Graph (a) shows the frequency versus the varactor choke diameter. The frequency decreases fairly consistently with increasing varactor post diameter. From a post diameter of 3 mm to a post diameter of 5.7 mm the frequency decreases by 427 MHz.

The microwave output power as shown in graph (b) of Fig.30 decreases as the post is increased. The power varies by 3.05 dBm over the range of varactor posts.

The tuning range increases as the varactor post increases as shown in graph (c). The sudden drop in electronic tuning range for the largest varactor post diameter is due to a mode jump which occurs if the varactor voltage is dropped below 12V.

(a) Frequency

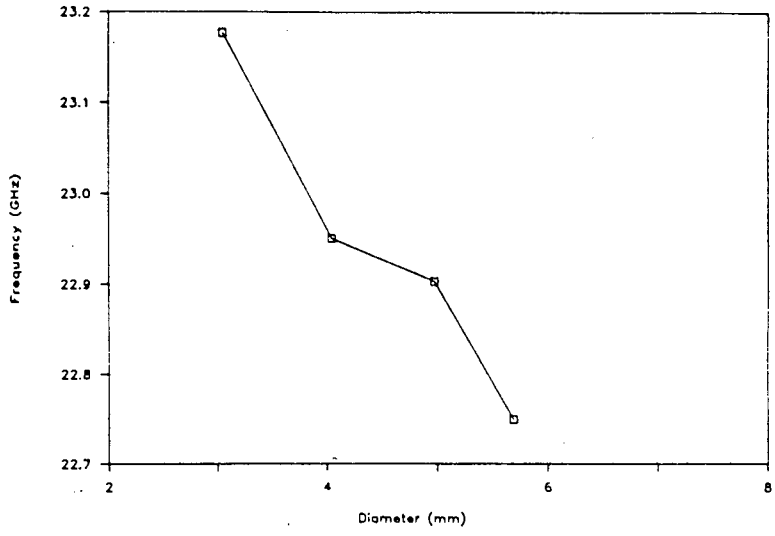

(b) Power

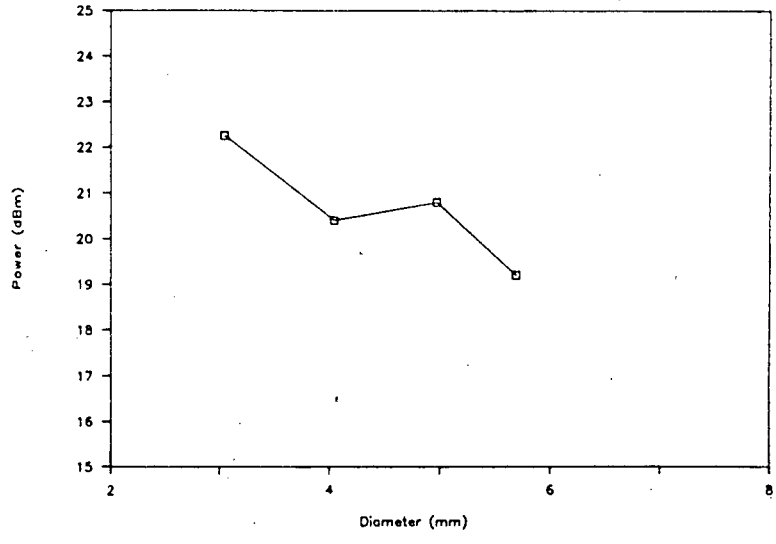

(c) Electronic Tuning Range

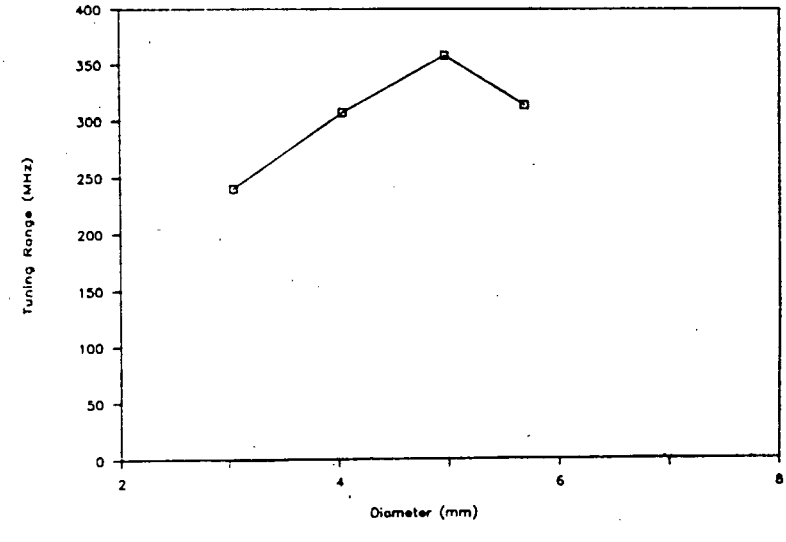

Fig. 30 Variation of Varactor Choke Post Diameter, Gunn-effect Device on Floor.

3.10.2 Gunn-effect Device in the Centre of Waveguide

The frequency decreases with increasing varactor post diameter as shown in graph (a) Fig.31. A variation of 496 MHz over the range of varactor posts was measured. It is of interest that if the varactor post diameter is small the effect on the frequency is not as substantial as when the diameter is large. This is evident from the changing slope of the frequency response.

The output power varies only by 1.5 dBm as the varactor post diameter is changed as shown in graph (b).

The tuning range in graph (c) decreases with increasing varactor post diameter.

(a) Frequency

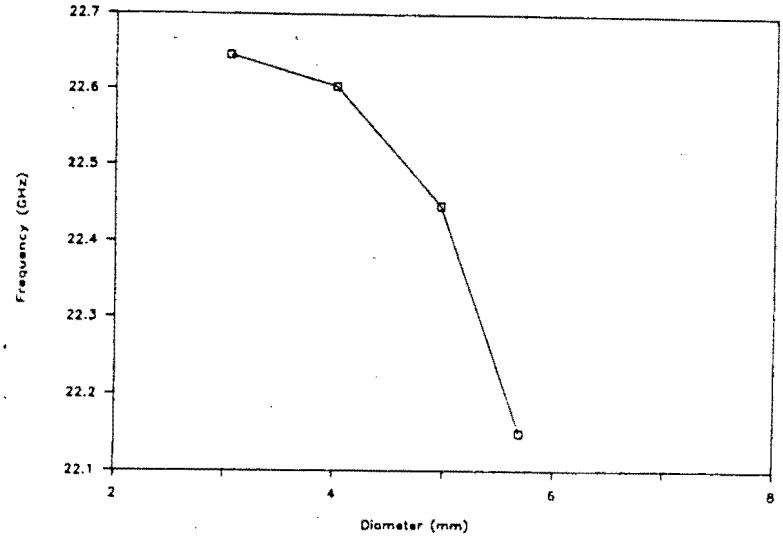

(b) Power

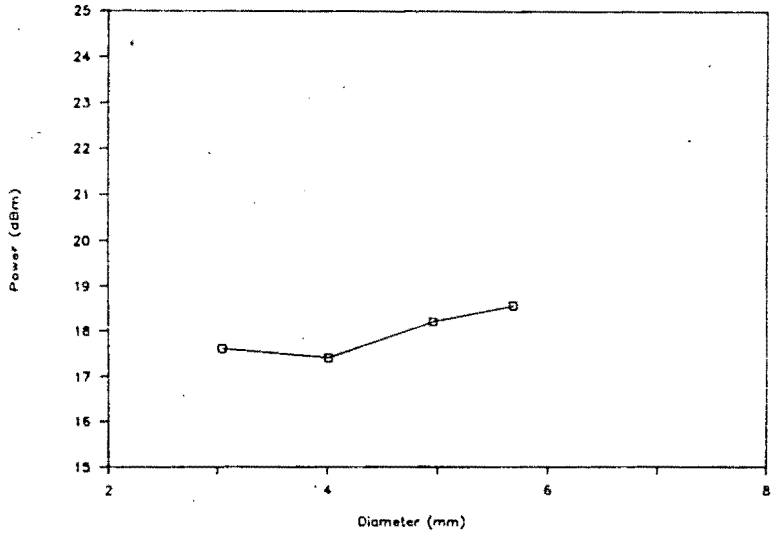

(c) Electronic Tuning Range

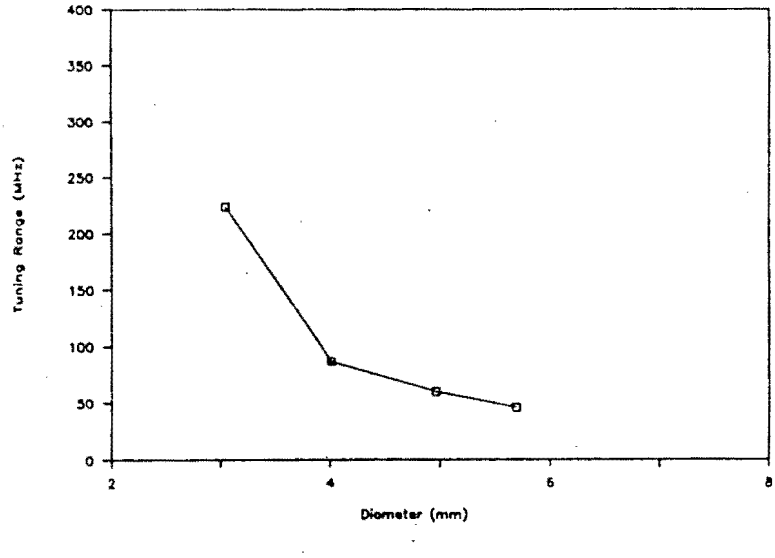

Fig. 31 Variation of Varactor Choke Post Diameter, Gunn-effect Device in Centre.

3.11 Variation of the Gunn-effect Device Post Diameter(s)

3.11.1 Gunn-effect Device on the Floor of Waveguide

The summarised results of these experiments are presented in Fig. 32. Graph (a) depicts the frequency response of the oscillator. As the Gunn post diameter is increased the frequency of the oscillator increases except for the step from 3 mm to 4 mm diameter where the frequency decreases. The latter can be attributed to mode jumping which is so prominent in this cavity configuration. A feature of this graph is the immense effect the variation of the Gunn post diameter has on the frequency. When the Gunn post diameter is increased from 3 mm to 5.7 mm the frequency changes over 7 GHz.

The output power in graph (b) takes on very much the same shape as the frequency response. After an initial decrease of output power it increases to almost 23 dBm with increasing post diameter.

Graph (c) displays the variation of the electronic tuning range versus the Gunn post diameter. As expected the tuning range takes on the same erratic characteristic as the frequency response. The tuning range varies from a few

(a) Frequency

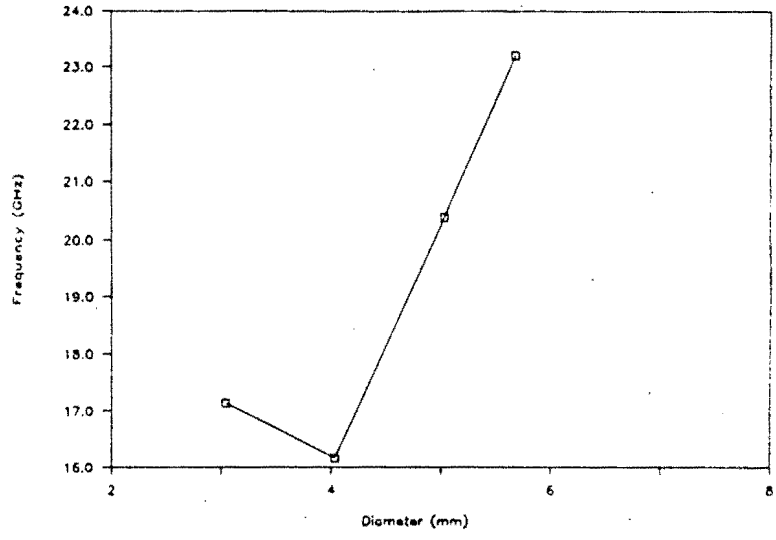

(b) Power

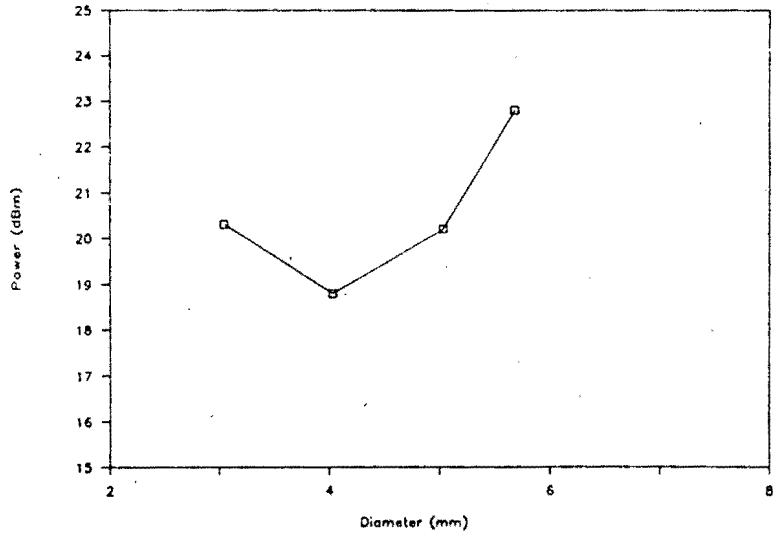

(c) Electronic Tuning Range

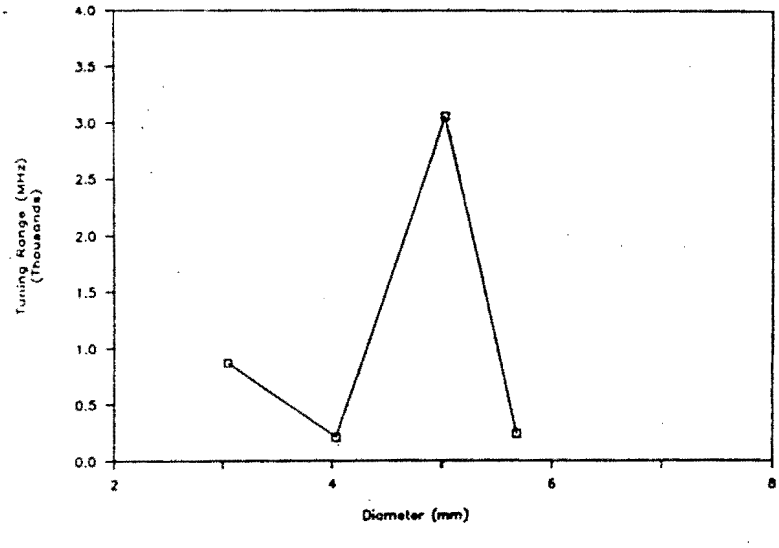

Fig. 32 Variation of Gunn Choke Post Diameter, Gunn-effect Device on Floor.

hundred MHz to almost 3 GHz (the latter tuning range due to a mode jump) and does not display any particular pattern.

3.11.2 Gunn-effect Device in the Centre of Waveguide

There are two sets of summarised experimental data in this series of experiments because the diameter of the post of the Gunn choke as well as the diameter of the post in which the Gunn-effect device is mounted is varied. The data when the post of the Gunn choke is varied is presented in Fig. 33.

Graph (a) shows the frequency response with varying Gunn choke post diameter. The frequency roughly decreases with increasing Gunn choke post diameter. The graph is however not smooth and a mode jump occurs. A frequency change of 496 MHz can be measured over the range of Gunn chokes used.

The output power in graph (b) remains relatively constant around 18 dBm when the post diameter is changed. Only the largest post diameter increases the output power more suddenly which is due to the mode jump that is also evident in the frequency response curve.

The tuning range in graph (c) remains fairly constant around 100 MHz and only for the largest post diameter when the mode jump occurs the tuning range increases suddenly to 190 MHz.

(a) Frequency

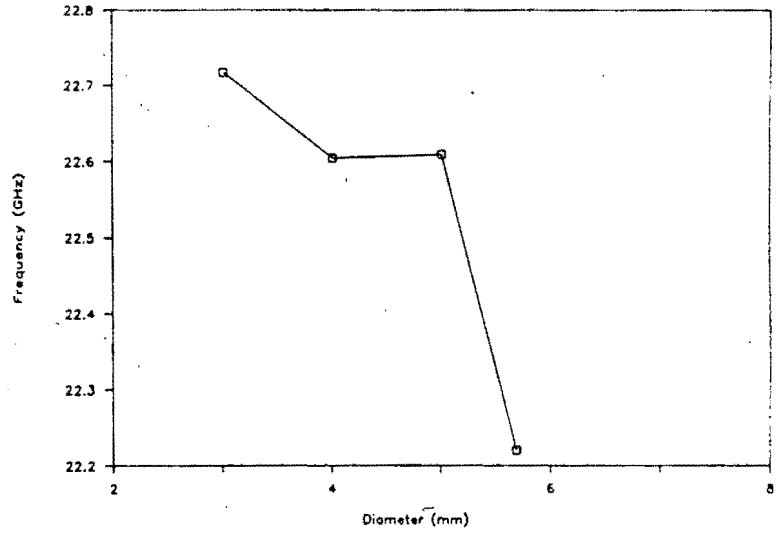

(b) Power

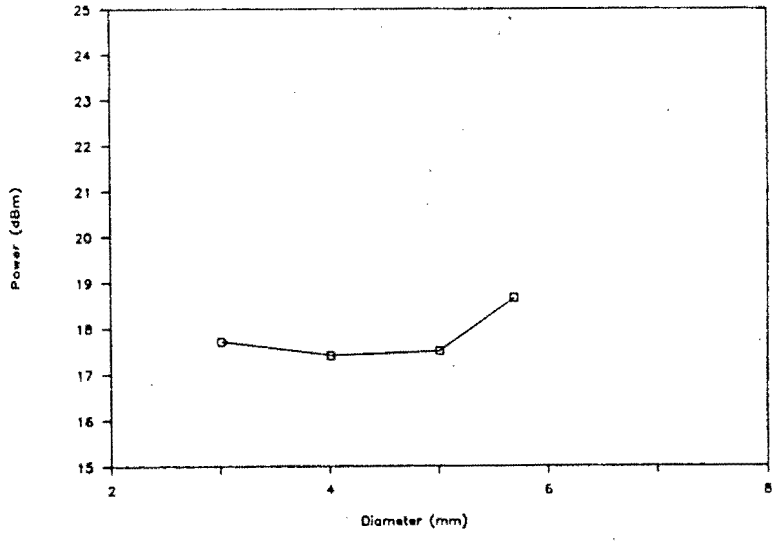

(c) Electronic Tuning Range

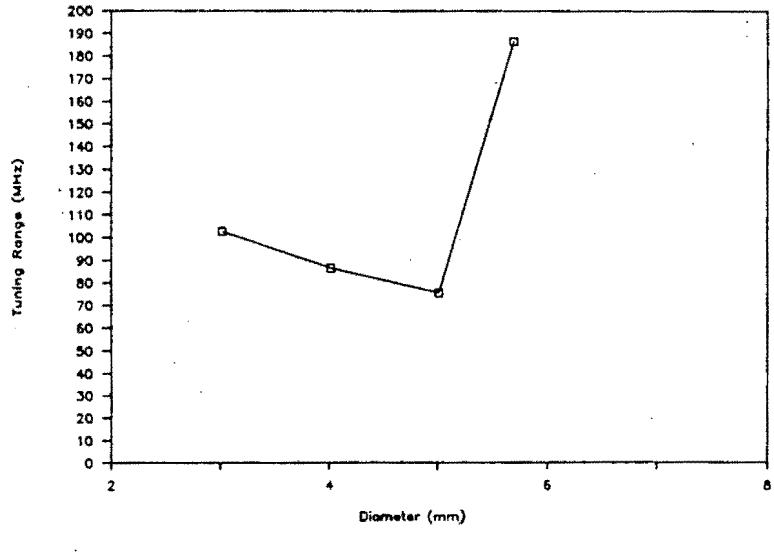

Fig. 33 Variation of Top Gunn Choke Post Diameter, Gunn-effect Device in Centre.

The variation of frequency, power and tuning range when the diameter of the post in which the Gunn-effect device is mounted is changed is presented in Fig. 34. Graph (a) shows the frequency variation when this post diameter is changed. The response curve is very much like the curve when the Gunn choke post diameter is varied except that no mode jumping occurs. The frequency decreases by 219 MHz when the post diameter is increased from 4 mm to 5.7 mm.

The power output increases as the post diameter is increased as shown in graph (b), reaching a maximum of 18 dBm for maximum post diameter.

Tuning range increases from 70 MHz to 105 MHz as the post diameter is increased as can be seen on graph (c).

(a) Frequency

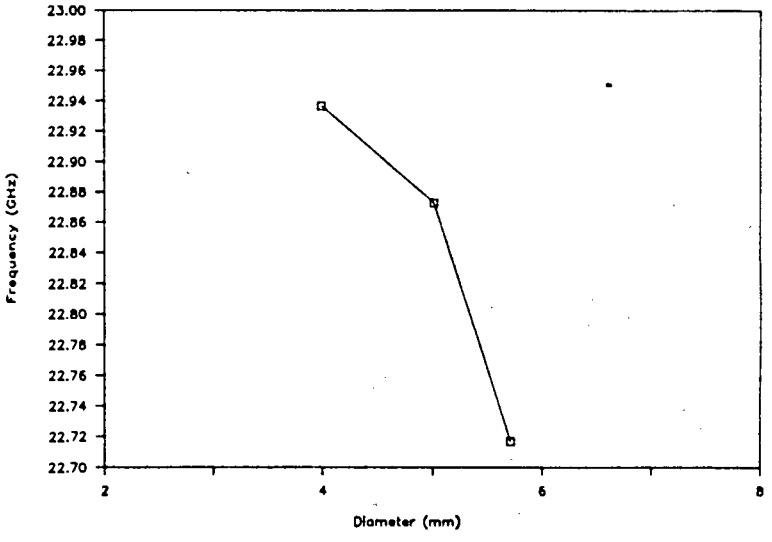

(b) Power

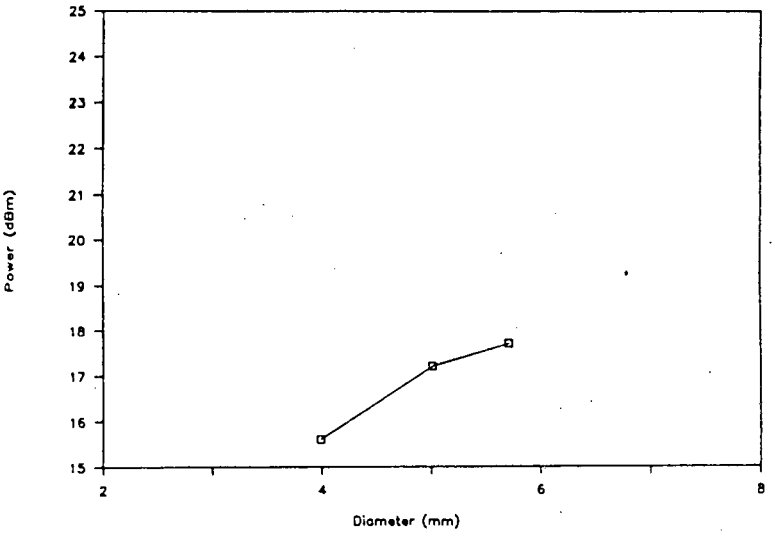

(c) Electronic Tuning Range

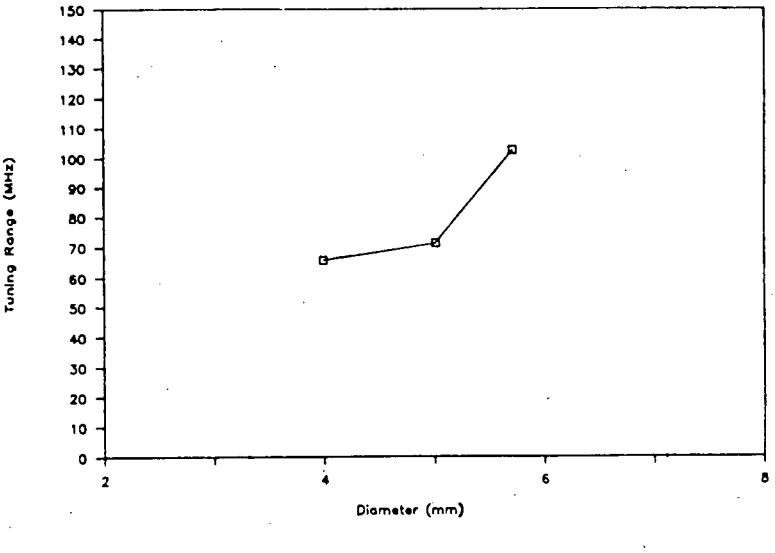

Fig. 34 Variation of Bottom Gunn Post Diameter, Gunn-effect Device in Centre.

3.12 Comparison of Results of varying Post Diameters

The comparison of the two cavity configurations with respect to the variation of the varactor post diameter shows again that the cavity with the Gunn-effect device mounted on the bottom of the waveguide is more prone to mode jumps. This can be seen when the two frequency response curves are compared. While the curve is smoothly varying from a small slope to a high slope in case where the Gunn-effect device is mounted in the centre of the waveguide, the frequency response of the other cavity configuration displays a discontinuity in form of a step in the curve. This is better illustrated when two typical tuning curves of frequency versus varactor voltage are compared.

While the power output of the oscillator with the Gunn-effect device mounted on the bottom of the waveguide is high (20 dBm plus), the power output varies much more than in the other oscillator configuration where the output power varies around 18 dBm.

For the variation of the varactor post diameter there is however a prominent difference between the two configurations regarding the electronic tuning range. While the electronic tuning range decreases with increasing varactor post diameter when the Gunn-effect device is mounted in the centre of the waveguide the exact opposite is true for the other oscillator configuration. This can be

seen as another proof that the oscillation modes in the two cavities differ.

More proof of the difference of oscillation mode can be found when the characteristics of the two oscillators are compared with respect to the changes in the Gunn choke post diameter. While the frequency response of the cavity configuration with Gunn-effect device mounted on a post in the centre of the waveguide is only moderate (500 MHz) the frequency response of the other cavity configuration is excessive and covers almost 7 GHz. This is reflected in the tuning range of the two oscillator configurations where in the latter configuration the electronic tuning is erratic and prone to mode jumps. The other configuration has an electronic tuning range which increases only up to 200 MHz.

Varying the bottom post diameter of the one configuration where the Gunn-effect device is mounted in the centre of the waveguide does not provide more information, it merely confirms the characteristics that were established when the Gunn choke diameter was changed.

3.13 Mechanical Tuning with Sliding Short-circuit

Adjustment of the frequency as in section 3.7 has also been measured with a sliding short-circuit as depicted in Fig. 35. The design of the quarter wavelength choke elements is determined using the same method as in the design of the chokes for the varactor diode and the Gunn-effect device. The sliding short-circuit is then covered with a thin

dielectric for insulation. It has been found that the fine adjustment of the oscillator was easier this way, rather than adjusting the oscillator with shims. The reason that a sliding short-circuit has not been used in all experiments particularly in section 3.7 was, that the required mechanical test apparatus was not freely available.

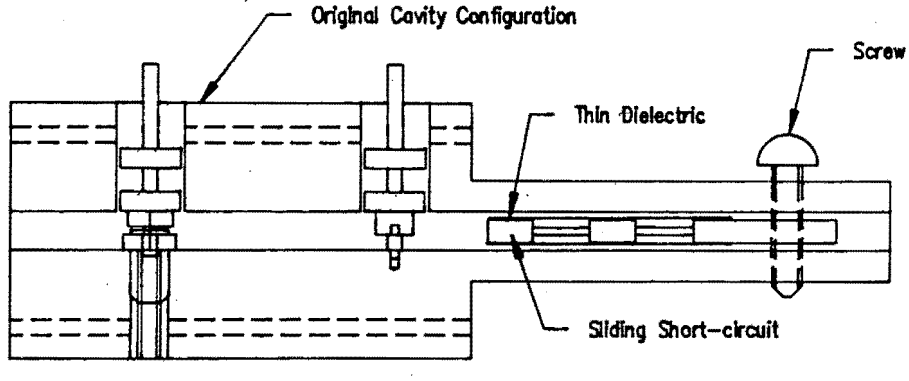

Fig. 35 Oscillator Configuration with Sliding Short-circuit.

Adjusting the frequency with the sliding short-circuit and observing the frequency shift on a spectrum analyser pictures the mode jumping of the oscillator very clearly. If the sliding short-circuit is inserted into the waveguide, the frequency increases up to a point where the oscillator becomes very noisy and low in output power and then it jumps suddenly back to a lower frequency. Further insertion of the sliding short-circuit causes the frequency to rise again. An interesting difference occurs however when the short-circuit is withdrawn slowly from the cavity. The mode jumps do not occur at the same physical distance between the varactor and the sliding short-circuit as when the short-circuit is inserted. This is shown graphically in Fig. 36. There is

thus a hysteresis effect when the short-circuit backwall is adjusted.

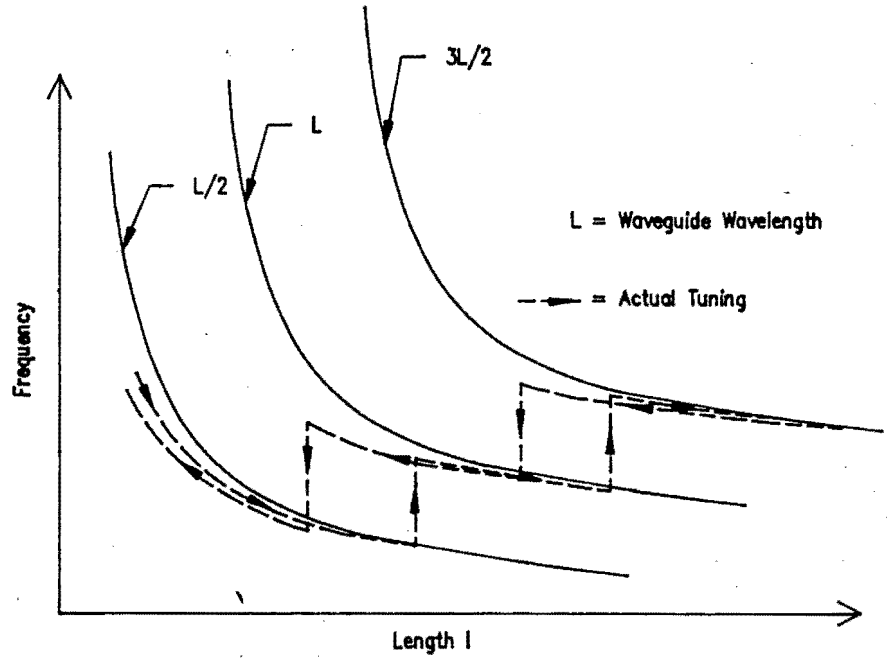

Fig. 36 Frequency Tuning Curves and Hysteresis for Sliding Short-circuit Configuration.

3.14 Frequency Phenomena of Gunn-effect Oscillators

The results in the previous sections of more that 100 individual experiments show very clearly that there are certain characteristics of Gunn oscillators which can present problems for trouble-free operation of the unit. These are for example mode jumping and erratic frequency responses. These problems are discussed in the next two

sections and present a theory for this Gunn oscillator behaviour.

3.14.1 Hysteresis and Mode-switching

The experimental results described in the previous sections show that the Gunn oscillators, particularly the configuration with the Gunn-effect device mounted on the bottom of the waveguide, are not easy to tune and to adjust because they exhibit mode jumping which can be observed in sudden changes in frequency, output power and tuning range.

During normal operation the above two cavity oscillators will oscillate at a frequency which is determined by the condition that the cavity length be an integral number of half-wavelengths long. By altering the cavity length the oscillator can be tuned to any frequency in the band of interest assuming that the diode negative resistance is always adequate to match the load resistance presented to it by the circuit. This is as described in section 3.6.

The mode jumps that are predicted in section 3.6 and which have been experimentally verified in the subsequent sections have been reported by several authors [30,33,34,35].

The conditions for circuit controlled steady state oscillations with w the angular frequency are as follows [28].

If $G_l(w)$ and $B_l(w)$ are the real and imaginary parts respectively of the load admittance at the device terminals (the Gunn-effect device) and $G_d(w)$ and $B_d(w)$ are the real and imaginary parts respectively of the device admittance then,

$$G_l(w) + G_d(w) = 0 \qquad .... (7)$$

$$B_l(w) + B_d(w) = 0 \qquad .... (8)$$

$G_d(w)$ is a negative quantity. In addition to these requirements for steady state oscillations, for stable oscillations the following must be true.

$$\delta B(w)/\delta w > 0 \qquad .... (9)$$

Where $B(w)$ is the total admittance $B_l(w) + B_d(w)$.

This means that stable operation will occur if a voltage fluctuation dV produces a change in the oscillator admittance, which is compensated for by a frequency shift df to an operating point where the circuit and oscillator admittance again sum to zero. The operating point is unstable if the admittance changes are of the same sign.

For every short-circuit position in the cavity the load susceptance $B_l(w)$ can be calculated as a function of frequency. This can be calculated for all the waveguide modes [35]. A particular mode divides the distance between short-circuit backwall and active device into an integral

number of half waveguide wavelengths. If the distance between short-circuit backwall and the active device is constant and it is divided into an integral number of half waveguide wavelengths, n, then the higher mode divides the distance into n + 1 half waveguide wavelengths and the lower mode into n - 1 half waveguide wavelengths.

Some of the load susceptance curves due to the different waveguide modes fall within the same frequency band. Therefore, if at a short-circuit position in the cavity for a particular waveguide mode and frequency, either the oscillation criterion (8) or the stability criterion (9) is not met then the frequency changes so that both criteria are met. The condition of zero total susceptance can however not always be satisfied in the current waveguide oscillation mode, but in the next higher (or lower) mode. The frequency though, does not change gradually into the next mode, it jumps to the appropriate frequency so that stable oscillation occurs. Frequency jumps of up to 2.5 GHz at an operating frequency of 22 GHz have been observed during the experiments.

If the oscillator changes into a different mode the power output of the oscillator also changes. This has been observed experimentally as described in the previous sections (3.7 through to 3.11). Again the output power jumps suddenly from one value to another instead of changing gradually.

There are two other effects that occur simultaneously with the frequency jump due to mode switching. Just before the

mode switch occurs the electronic tuning range is very large and after the mode jump the tuning range is low again. Together with the large tuning range it can also be observed that the oscillator output becomes very noisy.

The last two characteristics, a large electronic tuning range and a noisy oscillator, lead to the conclusion that before the mode switch occurs, the Q-factor of the oscillator is low. It can be shown [34] that the loaded Q of the cavity oscillator can be calculated from,

$$Q_l = \delta B_l f / 2\delta f G_l \qquad \ldots\ (10)$$

where G_l is the load conductance and δB_l is the change of the load susceptance seen by the device. This equation means also that during stable oscillation the lower the slope of the load susceptance versus frequency curve the lower is the loaded Q-factor of the oscillator. It has been found [34] that at points on the load susceptance curve where the mode switches the slope of that curve is very low. This then explains the wide tuning range and the poor noise performance of the oscillator just before mode switching.

Another approach to understand mode switching of the cavity oscillator is not only to fulfil the two criteria for oscillation (8) and (9) but also the condition that the load conductance can never be greater than or equal the absolute value of the device conductance [33]. There are two further conditions that predict the oscillation frequency in a multiresonant circuit such as the cavity oscillator.

Firstly, as the load conductance approaches the device conductance the output power increases with a maximum power output when the two conductances are equal. Secondly, under multiresonant circuit conditions the oscillator will always operate in that mode for which the load conductance is at its highest value. This theory explains therefore the power jumps that occur with the sudden frequency change during a mode jump.

Hysteresis in the mechanical tuning characteristic as observed in section 3.13 can also be explained with the help of the above theory. It must be kept in mind that the device susceptance is not a constant, it is a function of frequency. If therefore a particular mode switch is considered the oscillator changes from one frequency to the other. The device susceptance changes accordingly and therefore the next mode switch will not occur at the same short-circuit position.

Although negative resistance oscillators have been analysed [36,37] in depth, an exact theory for mode switching and hysteresis in Gunn oscillators is not easy to obtain. The main reason for this is that the circuit elements of the oscillator at high frequencies are of a distributive nature which complicates the formulation of a simple circuit. It is also understandable that at high frequencies many unwanted circuit elements affect the satisfactory operation of the oscillator. The effect of parasitic elements which are mainly due to elements introduced by the package of the active devices and the reactances of the mounting posts is to alter the waveguide wavelength tuning curves that have

been discussed in section 3.6. The effect of parasitics is to lower the slope of the tuning curves as shown in Fig. 37. This promotes a lower sensitivity to mechanical tuning as well as mode switching because more of the waveguide wavelength tuning curves fall within the frequency band of interest over some mechanical tuning distance x. If tuning range is the main concern in an oscillator then by reducing the waveguide height to the height of the package of the active device, the parasitic reactance of the posts are eliminated and large tuning ranges are possible.

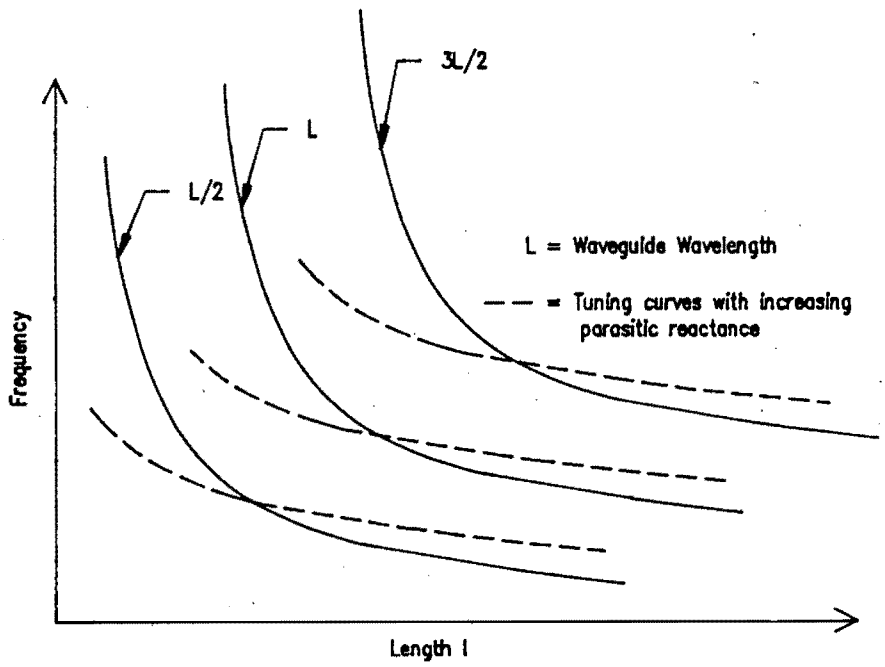

Fig. 37 The Effect of Parasitics on the Mechanical Tuning Curves.

3.14.2 Frequency Saturation Effects

Experiments described in sections 3.7 and 3.8 show that there is a difference in performance when the Gunn-effect device is mounted on the bottom of the waveguide or when the Gunn-effect device is mounted on a post in the centre of the waveguide. The main differences are that with the Gunn-effect device mounted on the bottom of the waveguide the oscillator had a higher power output, a relative insensitivity of frequency to mechanical tuning, a larger amount of mode switching and relative low electronic tuning ranges.

The above described characteristics are well known in literature [30,33] and are described as frequency saturation effects. An explanation of why frequency saturation exists can be found in the concept that the cavity oscillator can support modes of oscillation which do not necessarily divide the distance between the backwall and the active device into an integral number of half waveguide wavelengths. The other modes are essentially resonances in the local region of the mount of the Gunn-effect device which divides the height of the waveguide into half of a waveguide wavelength.

Experiments [30,33] have been conducted and by lowering the waveguide height the saturation frequency was shown to increase. By comparing the characteristics of a coaxial Gunn oscillator with the characteristics of a waveguide oscillator in which the Gunn-effect device was mounted on the floor of the waveguide it was shown [30] that saturation frequencies of both cavities were the same. This was the

main proof that there exists a resonance in the local region of the mount of the Gunn-effect device which is independent of the length of the waveguide cavity. It was concluded the mode is a simple coaxial mode with the mounting post as the centre conductor and the top and the bottom of the waveguide the end planes.

This mode would not cause any problems in oscillator performance if the saturation frequency does not lie within the frequency band of interest. The solution of the problem is either to use reduced waveguide height cavities which results in a lower Q-factor or to move the Gunn-effect device off the floor of the waveguide to its centre which increases the frequency at which the coaxial circuit resonates. This increase of resonance frequency is sufficient to remove the possibility that the Gunn-effect device can establish an oscillation with it.

The comparison of the results of the two waveguide cavities that have been designed, built and tested show exactly the behaviour that has been described above. The mounting configuration where the Gunn-effect device is mounted on a post in the centre of the waveguide has got a wider mechanical tuning range, larger electronic tuning range (due better coupling into the waveguide resonance mode) and less mode switching.

The lower output power of the oscillator in this configuration is due to the fact that the Gunn-effect device is not as effectively coupled into the waveguide as when it is mounted on the floor of the waveguide. This mounting

configuration also provides a problem in heatsinking which is not as effective as when the Gunn-effect device is mounted on the floor of the waveguide. This trade-off has however been made in favour of the improved frequency performance of the oscillator in this configuration.

3.15 Summarised Characteristics of the Gunn Oscillators

This section investigates how the Gunn oscillator characteristics and performance can be explained in terms of the standing wave pattern that is generated in the waveguide.

Section 3.7 shows the characteristics when the distance between the varactor and the short-circuit backwall is changed. The two oscillator configurations have in common that for close distances of the backwall to the varactor the electronic tuning range is in general large, it then drops to a minimum with increasing distance after which the electronic tuning range increases again.

In both cases the minimum of the tuning range occurs at a distance from the backwall which corresponds approximately to half a waveguide wavelength of the centre frequency of the oscillator (10.5 mm). This can readily be explained as a magnitude minimum of the electromagnetic field occurs at the position where the varactor is located and therefore the varactor is coupled only weakly to the electromagnetic field in the waveguide and the oscillator circuit. If the backwall is moved in either direction from this position, the

coupling of the varactor to the circuit increases and therefore the electronic tuning range increases as well.

In the case of the Gunn-effect device being mounted at the bottom of the waveguide the minimum tuning range at a distance of 10.5 mm corresponds to a peak in output power. The varactor is at this point only weakly coupled to the circuit and therefore contributes the least loss to the circuit due to its series resistance hence the peak in power output at this point.

When one compares the frequency responses versus length of sections 3.7 and 3.8 it can immediately be seen that when the distance between the two semiconductors is changed the effect on the frequency is much larger than when the distance between the short-circuit backwall and the varactor is changed. Table 1 illustrates the relationship between the distance between the two semiconductors and the centre frequency of the oscillator.

Distance between the devices.	Half waveguide wavelength from measured Frequency.
9.0	10.83
9.96	11.13
10.47	11.32
11.46	11.80
12.47	12.44

Table 1 The Relationship between Waveguide Wavelength and Distance between the Semiconductors.

For purpose of comparison the corresponding values when the distance between backwall and varactor is changed, is presented in Table 2.

Spacing between Varactor and backwall	Half waveguide wavelength from measured frequency
5.99	10.71
6.97	10.83
7.46	10.87
7.95	10.97
8.45	11.14
8.99	11.40
9.48	11.56
10.46	11.84

Table 2 The Relationship between Waveguide Wavelength and Distance between Varactor and Backwall.

Referring to Table 2 the distance between the varactor and the Gunn-effect device is a constant 10.47 mm.

Summarising, it can thus be said that the distance between the varactor and Gunn-effect device sets the centre frequency of the Gunn oscillator. The distance between the backwall and the varactor, although influencing the centre frequency as well, sets mainly the electronic tuning range of the oscillator. This is in accordance with previously published work [28].

The varactor post diameter has a less obvious effect on the oscillator characteristics. From the experimental results in section 3.10 it can be seen that the centre frequency decreases as the diameter of the varactor post is increased.

This shift in frequency is due to the increased reactance that the increasing diameter of the varactor post provides.

The electronic tuning range is influenced in two ways by the increasing diameter of the varactor post. With the Gunn-effect device mounted on the floor of the waveguide the trend of the tuning range is to increase, while in the other configuration the tuning range decreases. This behaviour can be understood when one considers the coaxial local resonance mode when the Gunn-effect device is mounted on the floor of the waveguide and the waveguide circuit resonance when the Gunn-effect device is mounted in the centre of the waveguide on a post. The larger the diameter of the varactor post the stronger the varactor is coupled into that mode. In the other configuration however the increase of the post reactance swamps the reactance of the varactor and therefore the tuning range decreases.

A similar effect due to the two resonance modes can be observed when the post diameter of the Gunn-effect device is increased. The centre frequency decreases and output power variations are minimal when the post diameter is increased in the configuration where the Gunn-effect device is mounted on a post in the centre of the waveguide. The reason for the decrease in frequency is again due to the increased post reactance. The sudden increase of tuning range for the largest post diameter is due to a mode switch and therefore must not be confused with the general trend of decreasing tuning range due to increased circuit reactance.

The effect on frequency, power and tuning range for changing post size of the Gunn-effect device is large when the Gunn-effect device is mounted on the floor. The reason for this is that the post operating as the centre conductor of the coaxial resonance mode that is present in this configuration. The trends are not clearly defined except that the change in centre frequency and electronic tuning range are very large.

3.16 Conclusion

This chapter has described in detail the characteristics of the two Gunn oscillator configurations. Using the information in this chapter a Gunn oscillator with the required frequency, power and tuning range can be constructed. The chapter proved conclusively that when the Gunn-effect device is mounted on a post in the centre of the waveguide the problems of mode switching and frequency saturation are greatly reduced. The two trade-offs of a lowered power output and an inferior heatsinking capability were accepted in favour of the improved frequency characteristics.

CHAPTER 4

4. LINEARISATION OF THE ELECTRONIC TUNING CHARACTERISTIC

4.1 Introduction

In the initial design specification it was required that the electronic tuning characteristic be as linear as possible. This was essential because the digital modulation technique that is employed needs a constant modulation index for good noise performance as well as meeting transmission regulations of the authorities.

Using more advanced, spectrally efficient modulation techniques, one of the prime requirements for the oscillator is a linear varactor voltage versus frequency characteristic. The necessity of a linear tuning characteristic is discussed with reference to the bandwidth efficient modulation method minimum shift keying (MSK). A method of linearising the normally highly non-linear characteristic is described.

4.2 Requirements and Characteristics of MSK

The physical implementation of a MSK system which is reported in detail elsewhere [38,39] results in the

transmitted bits being phase shifted by +90° or -90° from the previous bit depending on whether a binary zero or a binary one is transmitted. This results ultimately from the modulation index (h) of MSK defined to be h = 0.5 with the phase of the modulated signal given by πh [38]. If alternating zero's and one's are being transmitted it is clear that if the modulation index is not accurately h = 0.5 then the errors in the phase due to the modulation index will cancel and error free transmission is possible. If however long strings of zero's or one's are being transmitted the phase errors due to the incorrect modulation index accumulate with a resulting degradation the bit error rate.

The phase error that is produced by the error in the modulation index dh can be written as [38]:

$$\phi_e = \pi dh \qquad \ldots\ (1)$$

The phase error that accumulates due to long strings of binary one's or zero's of length S (from (1))is therefore:

$$\phi_{le} = \pi Sdh \qquad \ldots\ (2)$$

For no errors to occur due to these long strings the phase error in (2) must not exceed π/2. Therefore the following relationship for no additional bits in error can be deduced:

$$Sdh \leq 1/2 \qquad \ldots\ (3)$$

To asses by how much the modulation index can vary so that the system performance is not degraded, statistical calculations of the occurrence of long strings (of length S) of zero's and one's in a bit stream have to be made.

Before the calculations can be made it has been noted that many existing MSK modulators employ a technique to reduce the probability of long strings of zero's or one's occurring. The technique is to count the number of consecutive bits of equal state in the bitstream. As soon as the count reaches some threshold (e.g. 4 bits) the module inverts the following 4 bits. Since the identical function is performed twice the nett effect on the data is nil.

The probability distribution function of the value of a given 4-bit number is therefore examined. Because there are 16 different combinations of a 4-bit number the probability of any one combination occurring is 1/16.

Considering the worst case where consecutive, alternating 4-bit strings of zero's (0) and 4-bit strings of one's (15) occur, the following calculations can be made:

$$P(\text{4-bit string}) = P(0) + P(15) = 2(1/16) = 0.125$$

$$P(\text{8-bit string}) = P(0, \text{ then } 15) + P(15,0) = 2(1/16)(1/16)$$
$$= 7.81\times10^{-3}$$

$$P(\text{12-bit string}) = P(0,15,0) + P(15,0,15) = 2(1/16^3)$$
$$= 4.88\times10^{-4}$$

$$P(16\text{-bit string}) = P(0,15,0,15) + P(15,0,15,0) = 2(1/16^4)$$
$$= 3.05\times10^{-5}$$
$$P(20\text{-bit string}) = 1.91\times10^{-6}$$
$$P(24\text{-bit string}) = 1.19\times10^{-7}$$
$$P(28\text{-bit string}) = 7.45\times10^{-9}$$

For reliable digital transmission the bit error rate of the system has to be better than 1×10^{-7} [38]. As the modulation technique must not contribute to the bit error rate of the system it is sufficient for worst case conditions to ensure that the above described 28-bit string complies with the condition in (3). This yields the allowable variation of the modulation index dh. For no error occurring the variation of the modulation index must be:

$$0.482 \leq h \leq 0.518 \qquad \ldots. (4)$$

It must be noted that this analysis assumes for simplicity that once $\varnothing_e$ has exceeded $\pi/2$ radians and produced a bit error, its value is reset to zero.

The modulation index at a particular operating point on the voltage/frequency characteristic can be assumed constant as the modulation results only in small excursions from the operating voltage due to the large electronic tuning range of the Gunn oscillator. However due to the frequency drift of the Gunn oscillator with temperature the operating point on the voltage/frequency characteristic of the crystal

locked oscillator changes. If the electronic tuning range is not linear the modulation index (with the same modulation voltage applied to the varactor) will change according to the change of the slope of the voltage/frequency characteristic.

Slope changes in electronic tuning range of 1:5 are common with varactor controlled Gunn oscillators and to employ MSK as a modulation technique, linearisation of the voltage/frequency characteristic was attempted.

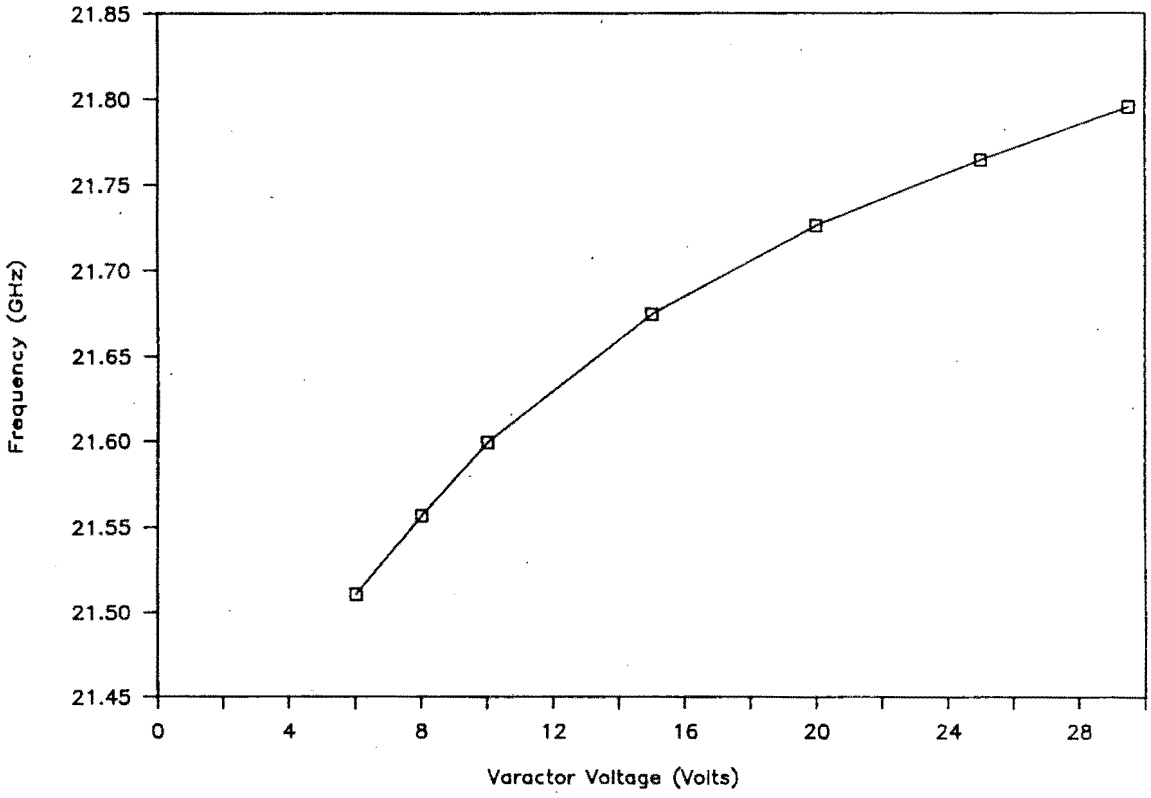

Fig. 38 Typical Non-linear Electronic Tuning Curve of Gunn Oscillators.

4.3 Linearisation of Electronic Tuning

When the Gunn-effect device is mounted on the bottom of the waveguide a typical electronic tuning curve is shown in Fig.38. The characteristic change in slope at low varactor voltages is caused by the drop in varactor Q-factor and due to the strong nonlinearity of the capacitance characteristic at low varactor voltages.

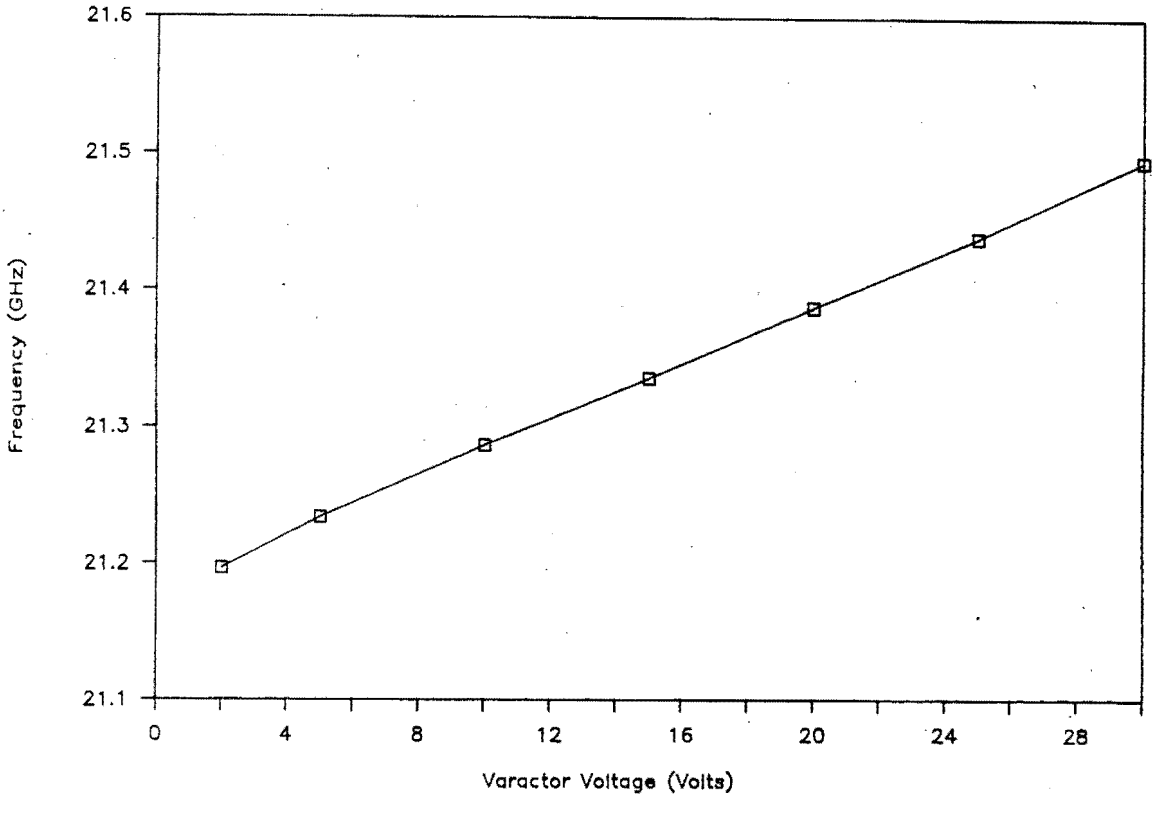

Fig. 39 Linearised Electronic Tuning Curve of Gunn Oscillator.

The electronic tuning characteristic in Fig.39 is typical of the cavity configuration where the Gunn-effect device is mounted on a post in the centre of the waveguide. The important feature of the curve being the linearity of the tuning curve.

If X_v is the varactor reactance, X_{eff} the effective circuit reactance made up of the active device, cavity and load reactance and V the varactor voltage then the change in frequency (δf) for a change in varactor voltage (δV) can be written as [40],

$$\delta f/\delta V = \frac{A\ [-\delta X_v/\delta f]}{[-\delta X_v/\delta f] + [\delta X_{eff}/\delta f]} \qquad .... (5)$$

Where A is a function of the coupling between the varactor and the circuit. From the equation (5) several conclusions can be made.

If the slopes of the effective circuit reactance X_{eff} and the slope of the varactor reactance X_v are made nearly equal and of opposite sign then large tuning ranges are possible. This method of obtaining large tuning ranges is called reactance compensation and has been suggested by Aitchison [41], who also reported an experimental result at X-Band [42].

For a linear tuning characteristic only a more general form of reactance compensation is required. From equation (5), linear tuning can be achieved in theory if the slope of the

effective circuit reactance is a multiple of the slope of the varactor reactance. By making the slopes equal and opposite as described earlier is only a special case of the linearisation of the electronic tuning characteristic.

One of the practical ways to linearise the tuning characteristic is to reduce the slope of the effective circuit reactance (In the limit the slope would be zero).

There are two ways in which the effective circuit reactance has been reduced. One way was to lift the active device off the floor of the waveguide to the centre of the waveguide by mounting it on a post. The effect of this was to cancel the series resonance due to the post of the active device if it would be mounted on the floor [33].

The other way the effective circuit reactance was lowered was achieved by reducing the diameter of both the varactor post and the Gunn-effect device choke post. It can be shown [43] that the larger the diameter of the posts the larger their reactance is. Also the larger their reactance is the larger is the slope $\delta X/\delta f$. The effect the Gunn choke post size has on the electronic tuning characteristic is shown in Fig. 40.

The effect of the variation of the varactor post on the linearity of the tuning characteristic is shown in Fig. 41. From the graph it is not easy to see that there is any change of linearity of the tuning characteristic. The reason for this is that with the variation of the varactor post not

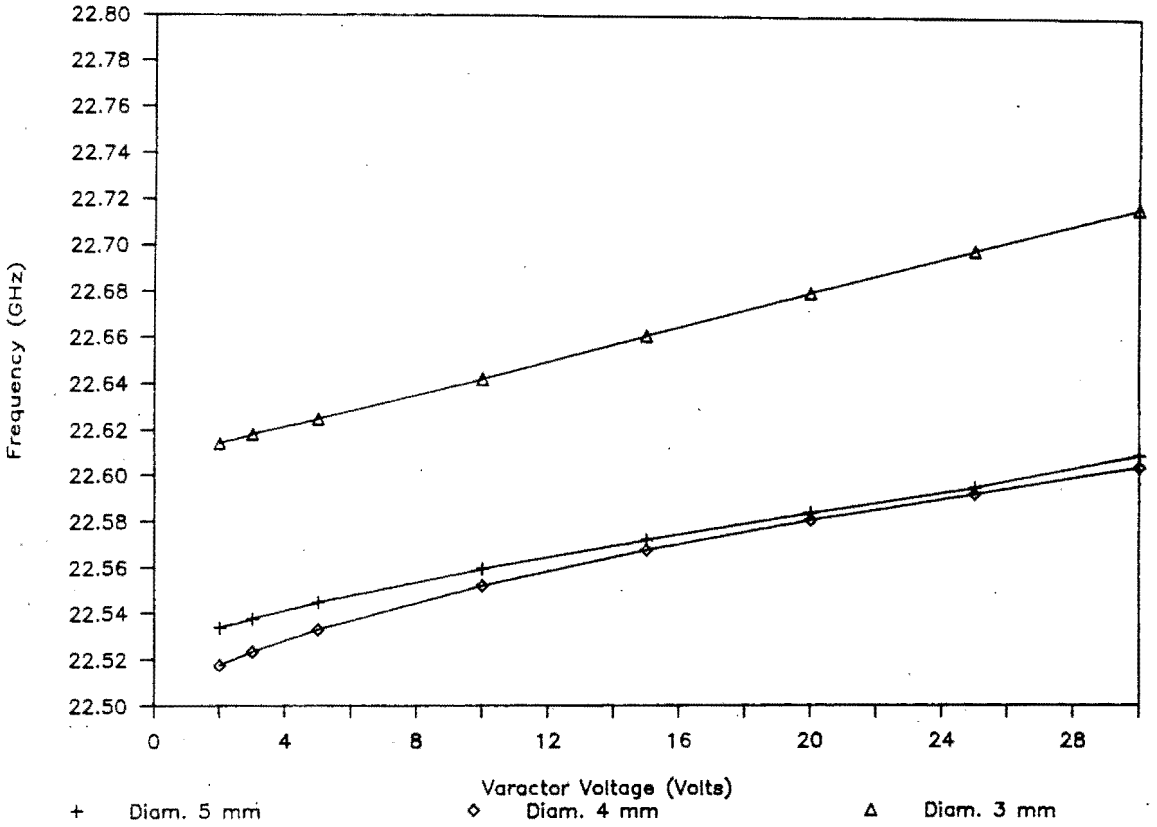

Fig. 40 Effect of the Gunn Post Diameter on the Electronic Tuning Characteristic.

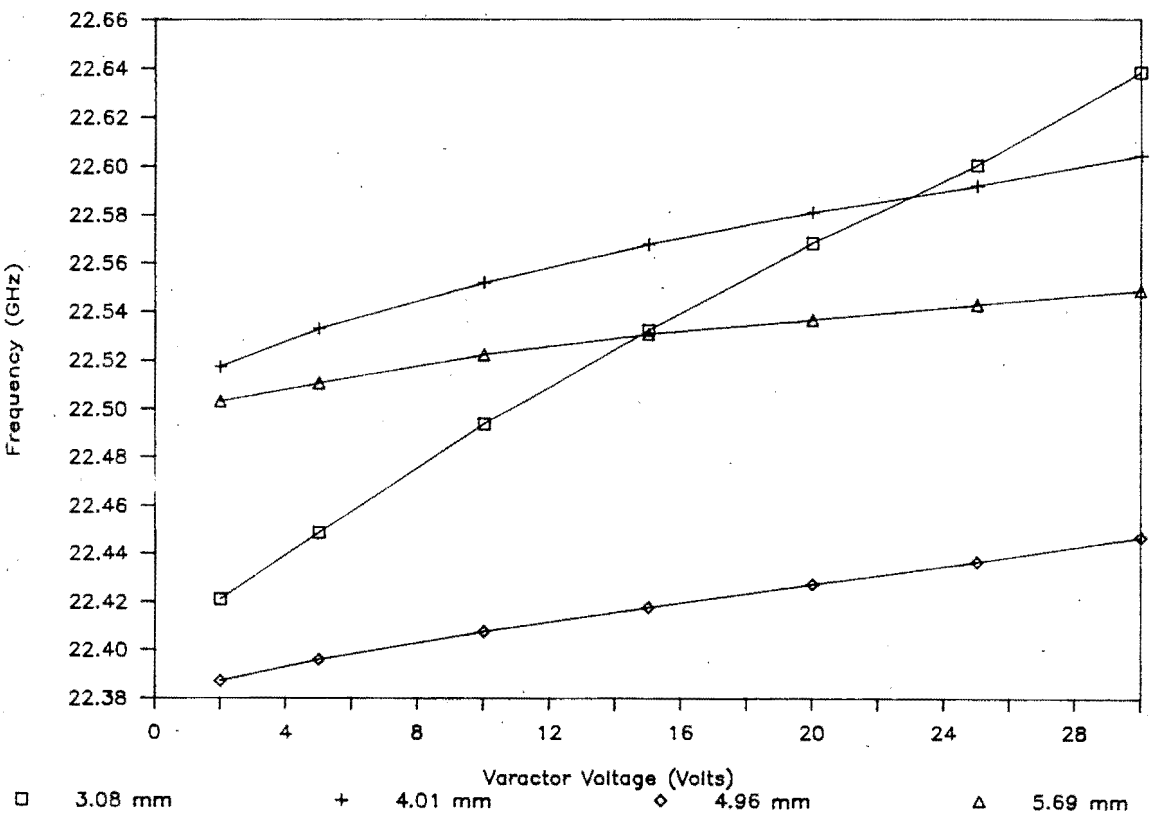

Fig. 41 Effect of the Varactor Post Diameter on the Electronic Tuning Range.

only the linearity changes but also the tuning range increases as the post diameter decreases. To investigate the linearity a statistical analysis of each curve has been made and the coefficient of linear regression has been determined with variation of the varactor post diameter as shown in Table 3.

Varactor Post Diameter (mm)	Coefficient of Linear Regression
3.08	0.998332
4.01	0.991177
4.96	0.998102
5.69	0.988588

Table 3 Variation of Coefficient of Linear Regression with Varactor Post Diameter.

As the value of the coefficient of linear regression increases it indicates the increasing linearity of the tuning characteristic. The table shows the maximum value for the coefficient of linear regression for the smallest varactor post diameter and the minimum value for the largest varactor post diameter.

4.4 Linearity and Variation of Modulation Index

To bring the linearisation of the voltage/frequency characteristic of the oscillator into context with the requirements for maximum allowable change in modulation index as outlined in section 4.2 a relationship between the two has to be derived.

The linearity of the voltage/frequency characteristic has been assessed by calculating the slope between consecutive measurements of voltage and frequency on graphs of Fig.40 and Fig.41. The values then have been averaged and maximum and minimum slopes have been noted.

Using the relationship that the modulation index h is given by:

$$h = df/f_b \qquad \ldots\ (6)$$

Where df is the frequency deviation and f_b the bit rate and also:

$$df = mc \qquad \ldots\ (7)$$

Where m is the slope of the voltage/frequency characteristic and c is the constant modulation voltage applied. Assuming that the modulation voltage is adjusted to a mean slope of the voltage/frequency characteristic, the modulation index of 0.5, together with (6) and (7) the following relationship can be deduced:

$$\delta h = \frac{0.5dm}{\text{mean slope}} \qquad \ldots\ (8)$$

Where δh is the change in modulation index from maximum to minimum and dm the change in slope from maximum to minimum of the voltage/frequency characteristic.

For a Gunn post diameter of 3.01 mm and a varactor post diameter of 4.01 mm (see Fig.40) the change δh of the modulation index over part of the curve is 0.0342 over a frequency range of 92 MHz. With the maximum change in modulation index being 0.036 (from section 4.2) the voltage/frequency characteristic is sufficiently linear to apply MSK directly to the crystal locked, varactor controlled Gunn oscillator, with a bit error rate of less than 10^{-7}.

4.5 Conclusion

Existing systems employing MSK as a modulation technique use linear VCO's at low frequencies and multiply up using an up-converter to the required frequency. Only that way sufficient tuning linearity can be achieved to keep the modulation index constant. The problem with this technique is that it is expensive, complicated to implement and at 23 GHz it is difficult to produce adequately high output powers for transmission. The advantages of the described system are that high output powers can be achieved readily and that the varactor controlled Gunn oscillator is relatively inexpensive to produce.

The chapter explains why high linearity is required when advanced modulation methods are used. This is described with special reference to minimum shift keying (MSK). A method of linearising the crystal locked, varactor controlled Gunn oscillator is presented and it is shown to be adequately linear for direct MSK modulation.

CHAPTER 5

5. TEMPERATURE COMPENSATION

5.1 Introduction

The Datalink units are to operate outdoors and for European conditions they are specified to be operational from -30°C to +55°C. The voltage controlled Gunn-effect oscillator therefore had to be tested over that temperature range.

The chapter firstly researches the theoretical effect of temperature on the Gunn-effect device. Then the results that temperature has on the Gunn-effect device from experimental data as well as a revised theory is presented. The experimental results of varying the temperature of the oscillator performance are shown and an investigation of the phenomena that occurred during the testing is presented. To conclude a method of temperature compensation is investigated. This has been carried out in an attempt to reduce the tuning range of the Gunn-effect oscillator to preserve the linear tuning characteristic of the oscillator (Chapter 4).

5.2 The Effect of Temperature on the Gunn-effect Device

The effect that the variation of ambient temperature has on Gunn-effect devices was first researched by Bott and Holliday [44]. They found that ranges of bias voltages exist over which power output is extremely sensitive to temperature changes.

One of the more obvious effects the temperature has on the device characteristics is on a quantum mechanical level. The theoretical discussion in the earlier chapters (Chapter 2 and Chapter 3) concerning the Gunn-effect have been made at or below room temperature. It has been found that the Gunn-effect is entirely dependent on the velocity-field characteristic of GaAs and therefore any changes in that characteristic with temperature will affect the devices performance.

The electron mobility is reduced as the temperature increases. This is shown on the graph of electron mobility μ versus temperature (Fig.42) [12]. It has also been expressed quantitatively in an empirically derived expression [44] as follows:

$$\mu = 2.25 \times 10^{6} / (273 + \theta) \ cm^{2}(Vs)^{-1}$$

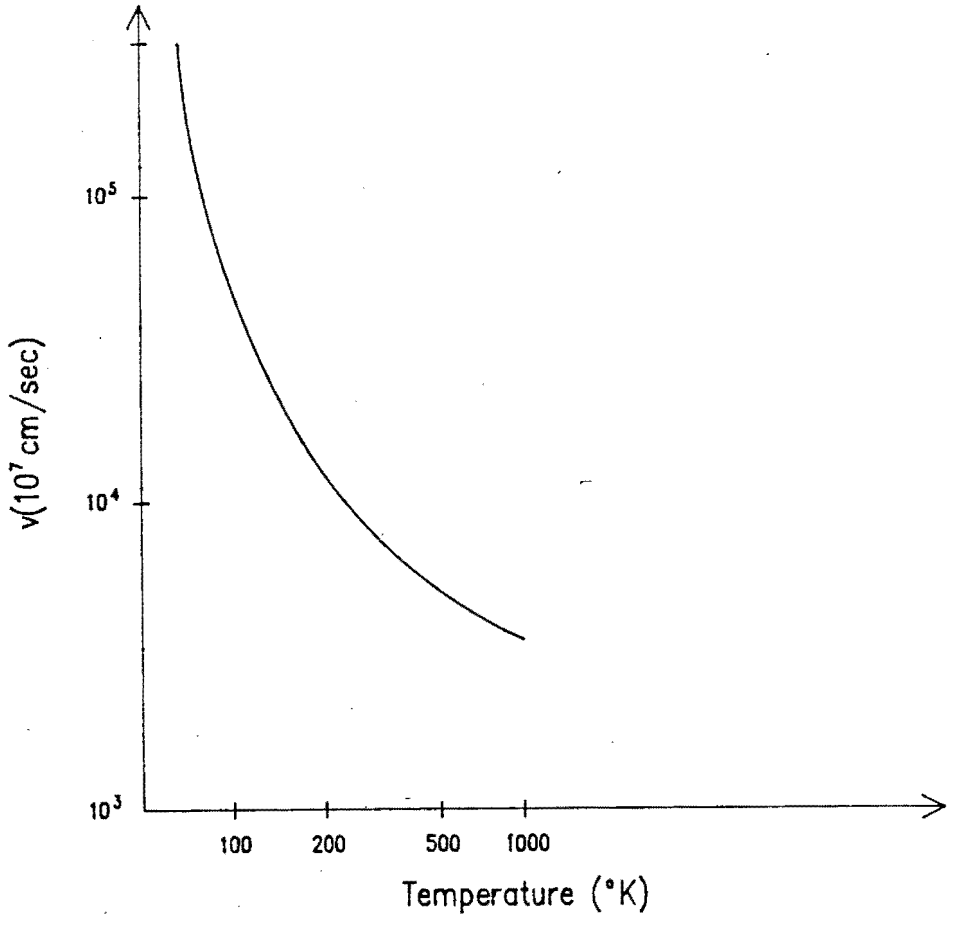

Fig. 42 Calculated Variation of GaAs Low-field Mobility with Temperature.

An analytic graph of electron velocity versus applied electric field is shown in Fig.43. An increase of temperature has the effect of reducing the electron mobility and therefore this will decrease the electron velocity. This will affect the low field characteristics but not the high field characteristics [45]. A family of curves of how the velocity/field characteristic is affected by temperature is also shown in Fig.43 [45].

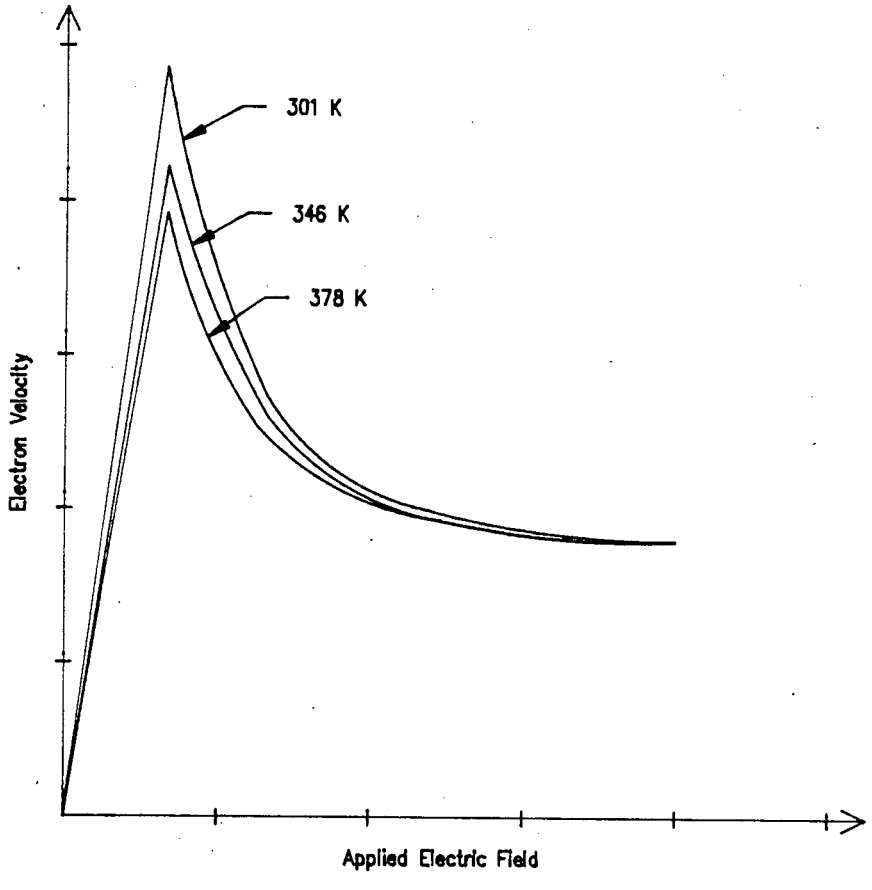

Fig. 43 Analytic Graph of Electron Velocity versus Applied Electric Field.

From Fig.43 it can be seen that the peak velocity is reduced with increasing temperature. This implies that the threshold will change with temperature. The reduction of peak velocity together with the almost invariant high field electron velocity means that the difference between the two velocities diminishes with increasing temperature. This means the slope of the negative differential mobility decreases with increasing temperature. As the negative differential mobility is the cause of the negative resistance phenomenon in GaAs, the temperature change will

thus affect the impedance of the device. The oscillator output power and frequency are therefore expected to change with temperature because impedance relations in the circuit have been modified.

5.3 Experimental Gunn-effect Device Characteristics

5.3.1 The Test-setup

Fig. 44 The Temperature Test Set-up.

The test-setup is essentially the same as in the prior experiments because the same parameters of the Gunn-effect

device are of interest. In addition to the previous test-setup an environmental chamber with a suitable thermometer was included for these experiments.

The test-setup (Fig.44) was arranged in such a way that only the Gunn-oscillator and varactor cavity was placed in the environmental chamber. This eliminated any experimental error due to temperature dependence of the test equipment. A heatsink was added to the cavity oscillator so that the temperature differential between the brass of the oscillator and the surrounding temperature was kept to a minimum.

The oscillator was sealed in a plastic bag to prevent the moisture that condensed during the warming cycle from -30°C entering the waveguide cavity . A thermocouple was placed in close proximity of the Gunn-effect device onto the brass casing of the oscillator to obtain an accurate measurement of the temperature. Good thermal contact was insured by the use of some heat conductive silicon grease between the brass casing of the oscillator and the thermocouple probe. The thermocouple was used because not only the temperature setting of the environmental chamber was inaccurate but it was also used because the Gunn oscillator did not have the very large heatsink of the previous experiments. This caused a larger temperature differential between the Gunn-oscillator housing and the surrounding air therefore the Gunn oscillator temperature could not be determined by controlling the air temperature.

5.3.2 The Experimental Results

Two different Gunn-effect devices were tested in a cavity in which the devices were centre mounted as described in Chapter 3. The physical dimensions of the cavity remained the same throughout the experiments. The temperature was then set at several chosen temperatures and with a constant voltage applied to the varactor, the voltage on the Gunn-effect device was varied and recordings of Gunn voltage, current, microwave output power and frequency were made. The results were then recorded on an electronic spreadsheet as previously (Chapter 3) described.

5.3.2.1 The I/V Characteristics of the Gunn-effect device

The I/V characteristics of the Gunn-effect device which was tested at the various temperatures are depicted in Fig. 45. The graph shows clearly that the negative slope, which is the negative resistance, changes from low to steep as the temperature decreases.

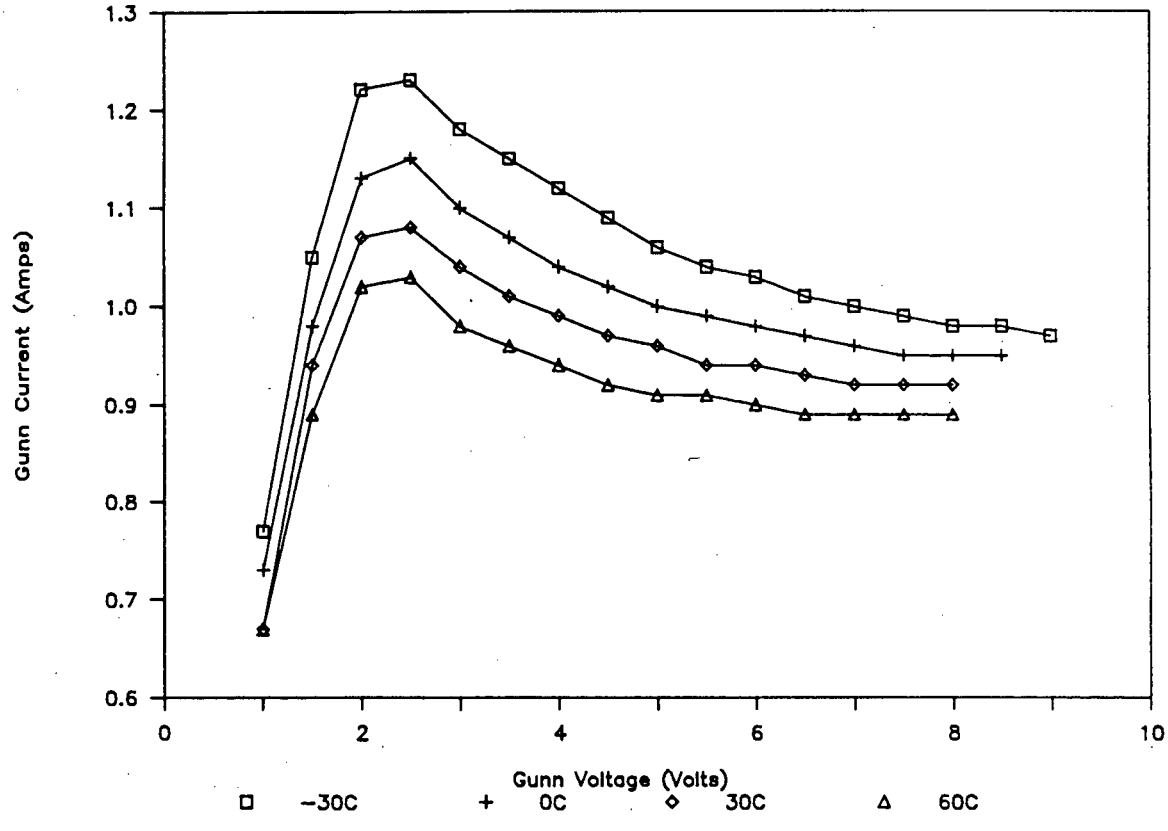

Fig. 45 The I/V Characteristic of the Gunn-effect Device with Temperature.

5.3.2.2 Frequency

The graph in Fig. 46 displays the frequency response of the Gunn-effect device when its bias voltage is varied at different temperatures. The frequency drift changes from 3.3 MHz/°C at a bias voltage of 3 V to the lowest frequency drift of 2.3 MHz/°C at a bias voltage of 6.5 V. The slope of the frequency variation at the various temperatures is

relatively constant. The slope ranges from 51 MHz/V at 60 °C to 68 MHz/V at -30 °C.

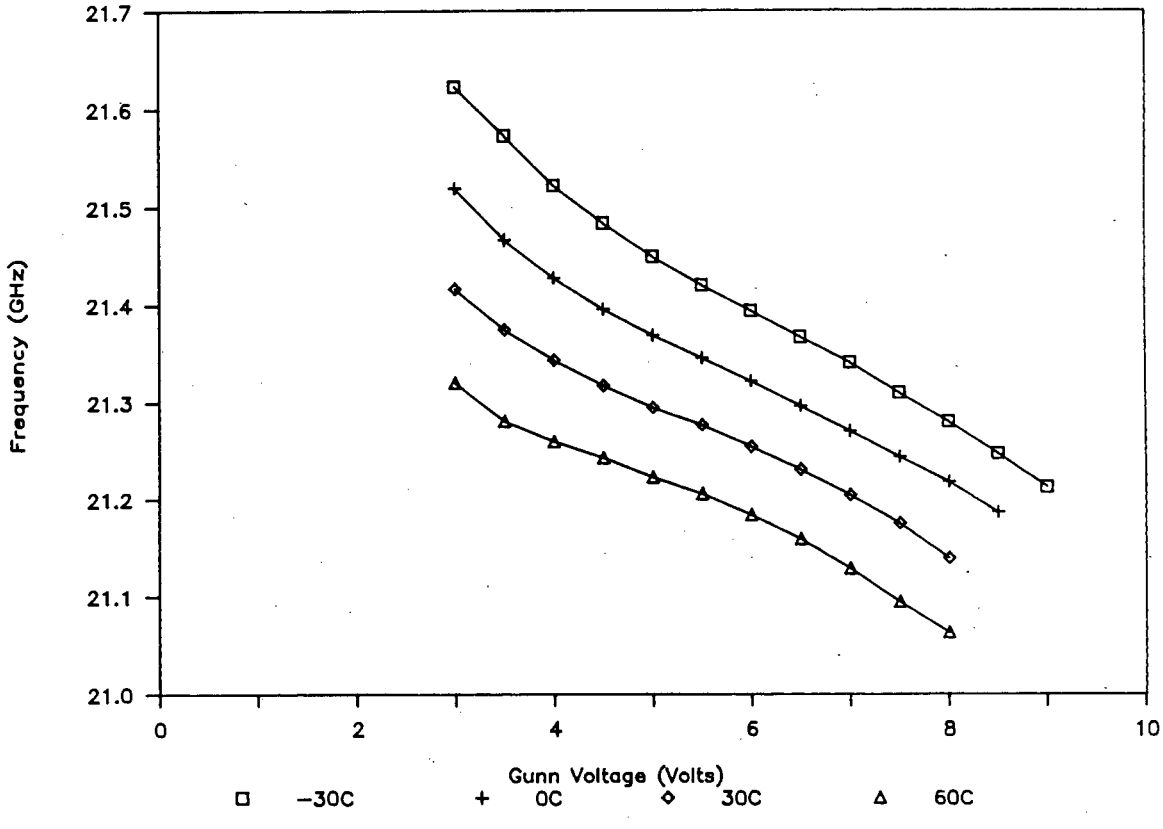

Fig. 46 Frequency versus Gunn-effect Device Bias Voltage with Temperature.

5.3.2.3 Power and Efficiency

The graphs displaying microwave output power and efficiency of the device are shown in Fig.47 and Fig.48 respectively. There are a few significant features about the two graphs. The graphs presenting the microwave output power at the various temperatures display a maximum. This maximum changes

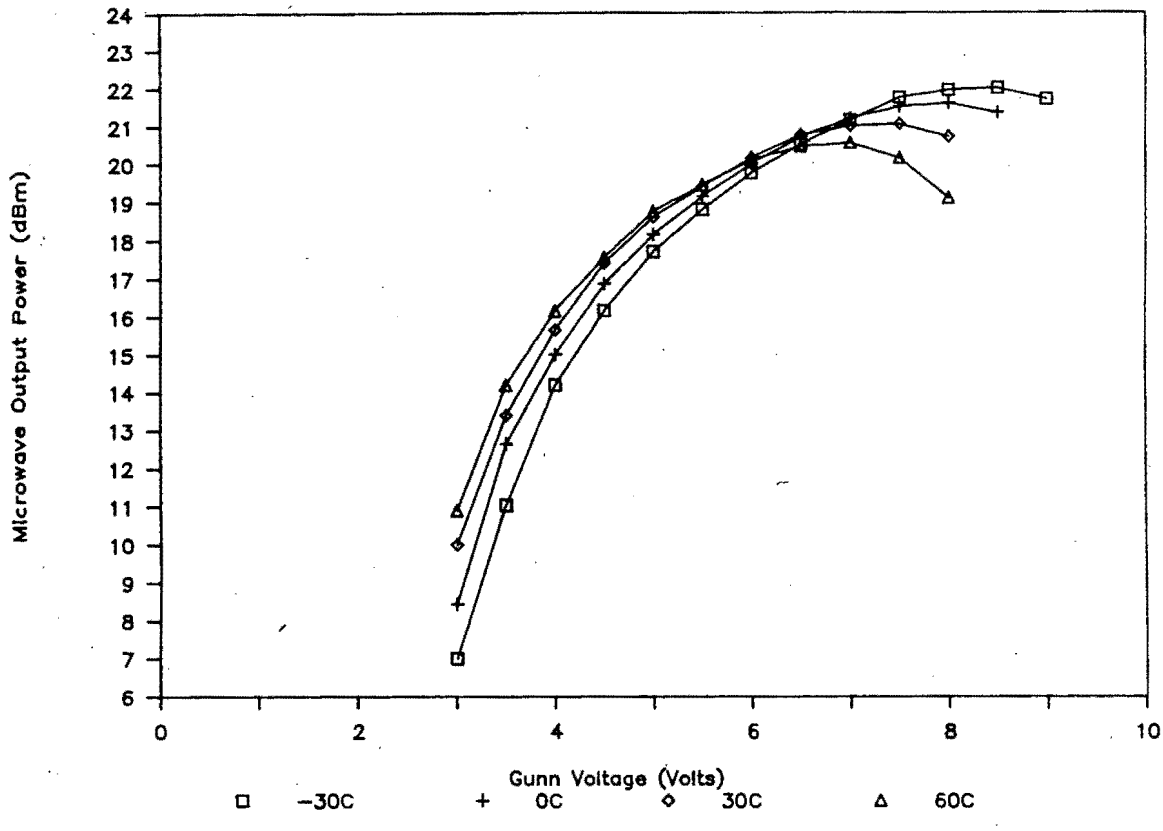

Fig. 47 Microwave Power versus Gunn-effect Device Bias Voltage with Temperature.

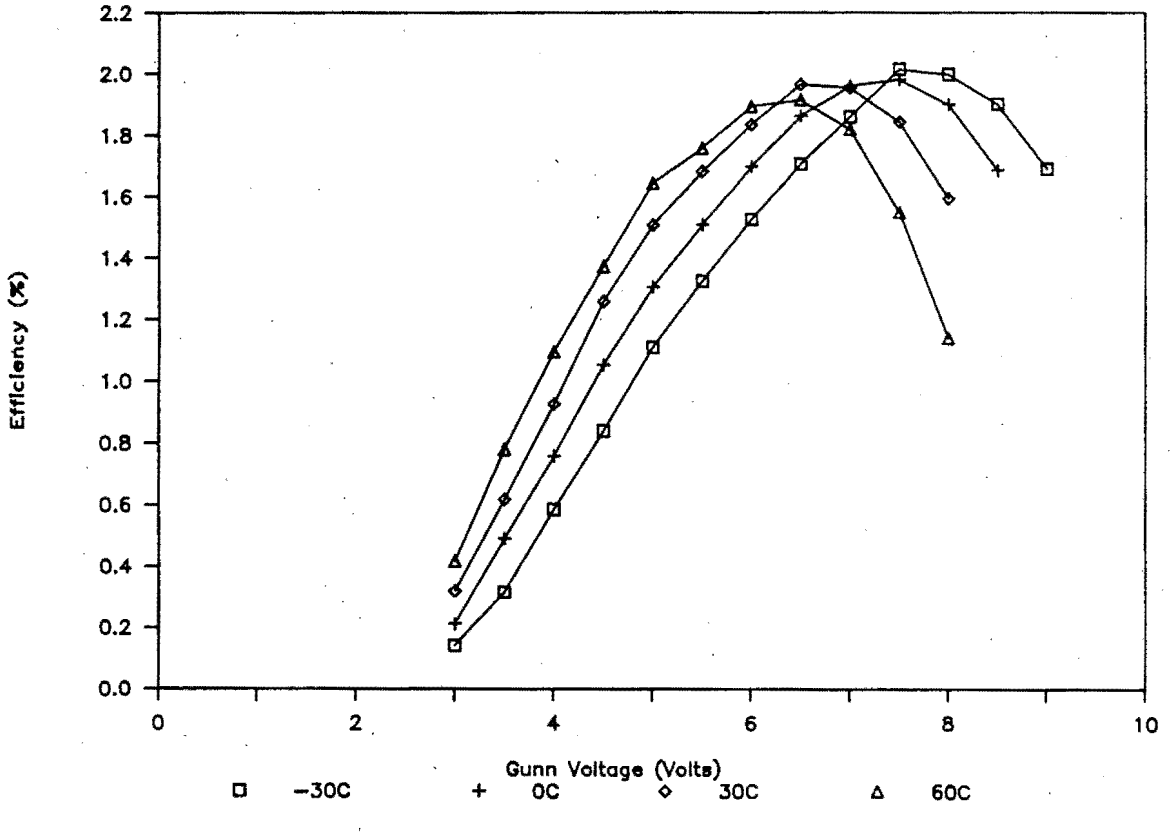

Fig. 48 Efficiency of Gunn-effect Device versus Bias Voltage with Temperature.

with temperature, occurring at 8.5 V at -30 °C (22.0 dBm) and at 7 V at 60 °C (20.55 dBm). Similarly the efficiency has also a maximum that varies with temperature, from 7.5 V at -30 °C (2.02%) to 6.5 V at 60 °C (1.92%).

5.4 A Revised Theory of Gunn-effect device Characteristics

The theory that is presented in section 5.2 is not adequate if it is analysed [45] and compared with the experimental results. Although the theory predicts adequately the shape of the experimental curves it does not predict the displacement of the output power curves with temperature.

Other studies [46] have been carried out and it has been found that Gunn-effect devices incorporate a series resistance which is temperature dependent. This series resistance is due to the contact imperfections of the device. Bird, Bolton and Edridge [47] compared devices with alloyed metal contacts and devices with grown n^+ epitaxial GaAs contacts. The study shows that whilst silver-tin contact devices had a temperature drift of 1 MHz/°C, this was reduced to 70 kHz/°C using n^+ contact devices. It is concluded from this that the low temperature drift and stability of the n^+ contact devices is due to the omission of the contact resistance.

Other experiments [48] show that the capacitance of the Gunn-effect device changes with temperature. Measurements indicate that the capacitance of the Gunn-effect device changes by 10^{-4} pF/°C. This represents a frequency change of

approximately -2 MHz/°C at 20 GHz if the Gunn-effect device is placed in a low Q cavity.

5.5 The Effect of Temperature on the Gunn Oscillator

5.5.1 Experimental Gunn Oscillator Characteristics

With the test-setup the same as in section 5.3.1 recordings of frequency, output power and electronic tuning range were made at various temperatures. The cavity tested was the configuration with the Gunn-effect device mounted on a post in the centre of the waveguide. A sliding short circuit was used instead of the fixed backwall. This was done to facilitate the initial frequency adjustment of the oscillator. The sliding short was then kept at a fixed position throughout the experiments.

5.5.1.1 Frequency

The results of this series of experiments is shown in Fig.49. It can be immediately be seen from the graph that the linearity as well as the slope of the electronic tuning characteristic is maintained. This is desirable as this means that the modulation index will not change with temperature. The oscillator presents an average frequency drift of -1.7 MHz/°C over the temperature range from -30 °C to +60 °C. At low temperatures the drift (-1.4 MHz/°C) is

however smaller than the drift (-2.1 MHz/°C) at high temperatures. The increased drift at high temperatures can be explained by the increased heating of the GaAs chip of the device due to the decreased efficiency of the oscillator at high temperatures (Section 5.3).

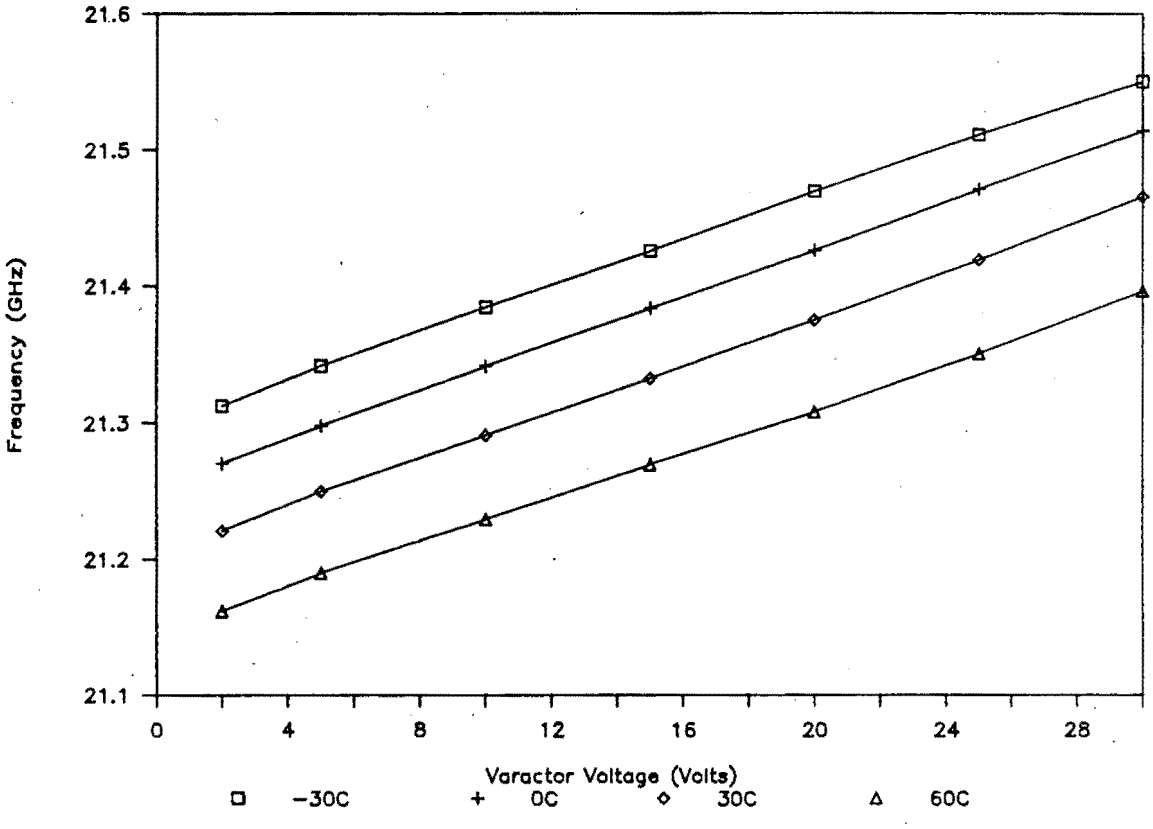

Fig. 49 Frequency versus Varactor Voltage of Gunn Oscillator with Temperature.

5.5.1.2 Power

The graphs displaying the output power are shown in Fig.50. An average drift of microwave output power of -0.01 dBm/°C

was measured. It must be noted that the drift of the output power is larger (-0.016 dBm/°C) at high temperatures than at low temperatures (-0.003 dBm/°C). The reasons for this are explained in section 5.3 where it was found that the maximum power output of an oscillator occurs at Gunn-effect device bias voltages that change with temperature Furthermore the output power drops very quickly at high temperatures if the bias voltage exceeds the maximum power point bias voltage. As the bias voltage is fixed the power will therefore change with temperature.

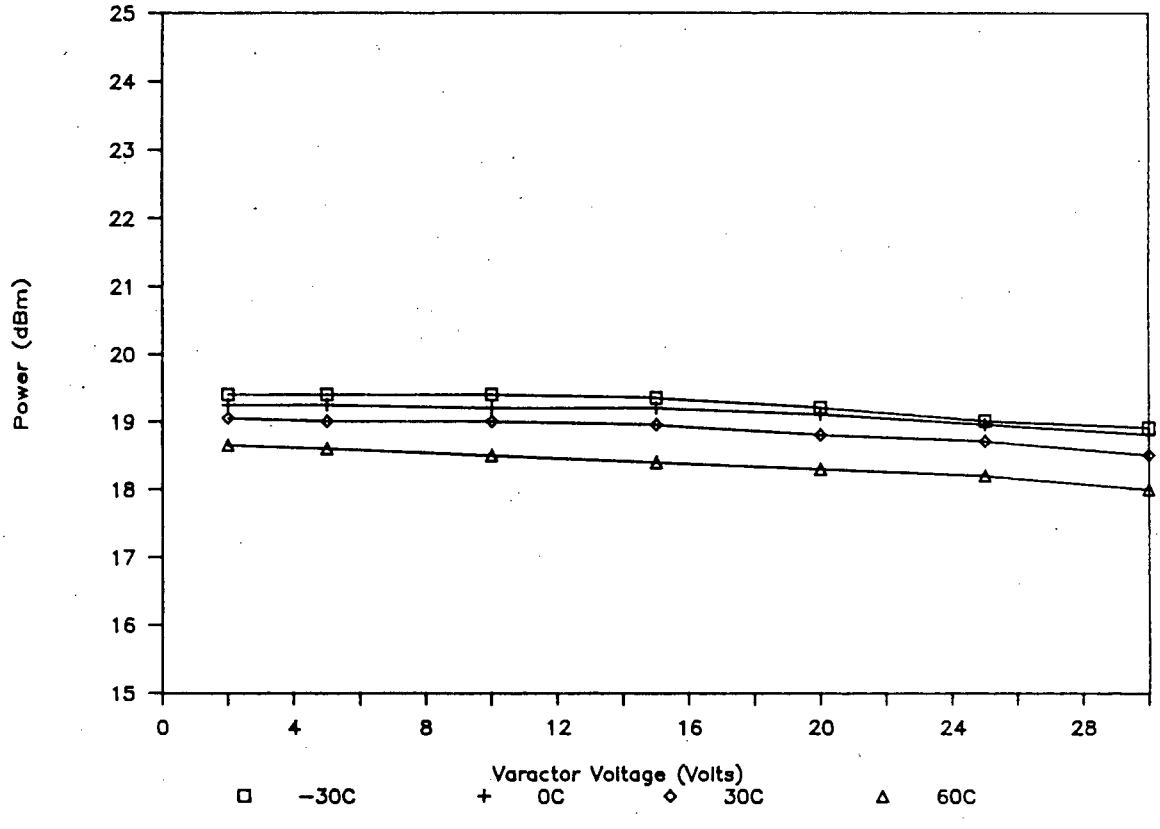

Fig. 50 Power versus Varactor Voltage of Gunn Oscillator with Temperature.

5.5.2 Mode Switching and Temperature

During the course of several experiments over the temperature range with different cavities, mode switching and start-up problems at low temperatures have become a problem. In particular, some oscillators started up in or switched to a high frequency mode at low temperatures others did not start to oscillate at low temperatures.

The reasons for this behaviour can be found in the changing impedance relations that occur with temperature variation. The changing impedance relations manifest themselves particularly in the variable optimum power point (Fig.47) and the modified I/V characteristic (Fig. 45).

If the bias voltage of the Gunn-effect device is too low, for example 6 V, then at low temperatures the oscillator is far removed from its optimum power output point (Fig.47). This means in turn that Gunn-effect device is not biased for its optimum negative conductance [48]. If the bias voltage at the low temperature is low enough, the negative conductance of the Gunn-effect device cannot match the circuit to sustain stable oscillation. The oscillator therefore fails to start to oscillate. It was shown that when the bias voltage of the Gunn-effect device was increased it was always possible to start oscillation of the Gunn oscillator at low temperatures.

The high frequency mode that occurred with some oscillators at low temperatures can also be explained in terms of the

changing impedance relations of the Gunn-effect device at low temperatures.

An investigation into the mode switching phenomenon at low temperatures revealed that if the bias voltage of the Gunn-effect device is increased appropriately the oscillator could be forced to mode switch into the desired frequency mode. The following table illustrates the temperature dependence of the bias voltage at which the oscillator switches from the higher frequency mode to the desired mode.

Temperature (°C)	Gunn Bias Voltage (Volts)
-30	8.181
-20	8.106
-10	7.951
0	7.743
10	7.585
20	7.405
30	7.239
40	7.073
50	6.957
60	6.793

Table 4 Temperature Dependence of Bias Voltage at which Mode Switch to desired Mode occurs.

To explain this circuit behaviour the theory outlined in chapter 3 has to be recalled and that the Gunn oscillator is a multiresonant circuit. When thus at a fixed bias voltage the temperature causes the negative conductance of the Gunn-effect device to change sufficiently the Gunn oscillator will jump into a different mode according to the set of rules outlined in chapter 3.

This mode switching has the same characteristics as the mode switching due to the sliding short-circuit. In this case only the negative conductance of the Gunn-effect device is changed by varying the bias on the devices. The oscillator also features hysteresis. This is shown in Table 5 which displays the bias voltage of the Gunn-effect device at which the oscillator jumps from the desired frequency mode to the high frequency mode.

Temperature (°C)	Gunn Bias Voltage (Volts)
-30	-
-20	-
-10	4.528
0	4.386
10	4.506
20	4.381
30	4.362
40	4.323
50	5.824
60	5.649

Table 5 Temperature Dependence of Bias Voltage at which Mode Switch to High Frequency Mode occurs.

The bias voltage at which the mode switch occurs as presented in Table 4 and Table 5 is highly dependent on the varactor bias voltage. This confirms the theory that the mode switch at low temperature is of the same nature, ie. circuit dependent, as those described in chapter 3.

5.6 Implications of the Experimental Results

The peak power output of the Gunn oscillator changes with temperature. This causes problems when a decision has to be made at which voltage to bias the Gunn-effect device for the best performance. An obvious answer to this problem is to bias the Gunn-effect device at a voltage where maximum output power can be achieved at the highest operating temperature. This conclusion can be made when one considers the sharp power drop with temperature if the Gunn-effect device is biased above this voltage (Fig.47). Not only will the power drop rapidly but due to decreased efficiency the reliability of the Gunn-effect device can be reduced as the device is likely break down thermally and fail to operate.

This means that a relatively low bias voltage of the Gunn-effect device has to be selected (Fig.47). The problem however is that this is in direct conflict with the requirements of a high bias voltage outlined in section 5.5.2.

The choice of the bias voltage of the Gunn-effect device was therefore a trade-off between the output power at high temperatures and a high frequency mode at switch-on at low temperatures. It was decided to bias the Gunn-effect device slightly above (7.5 V) its high temperature maximum power point (6 V) and accept a high frequency mode at switch-on at temperatures lower than -10 °C. In the application in the datalink the latter problem was solved by providing the Gunn-effect device with a supply that on switch-on produces

a voltage spike of up to 8.5 V for 20 msec to fall to 7.5 V, the continuous bias voltage. This method proved successful in the datalink unit and the oscillators switched on at -30 °C without large losses of power output at high temperatures. The power output dropped by 2 dBm over the temperature range. Fig.51 displays the Gunn oscillator after it has been tested at -30 °C.

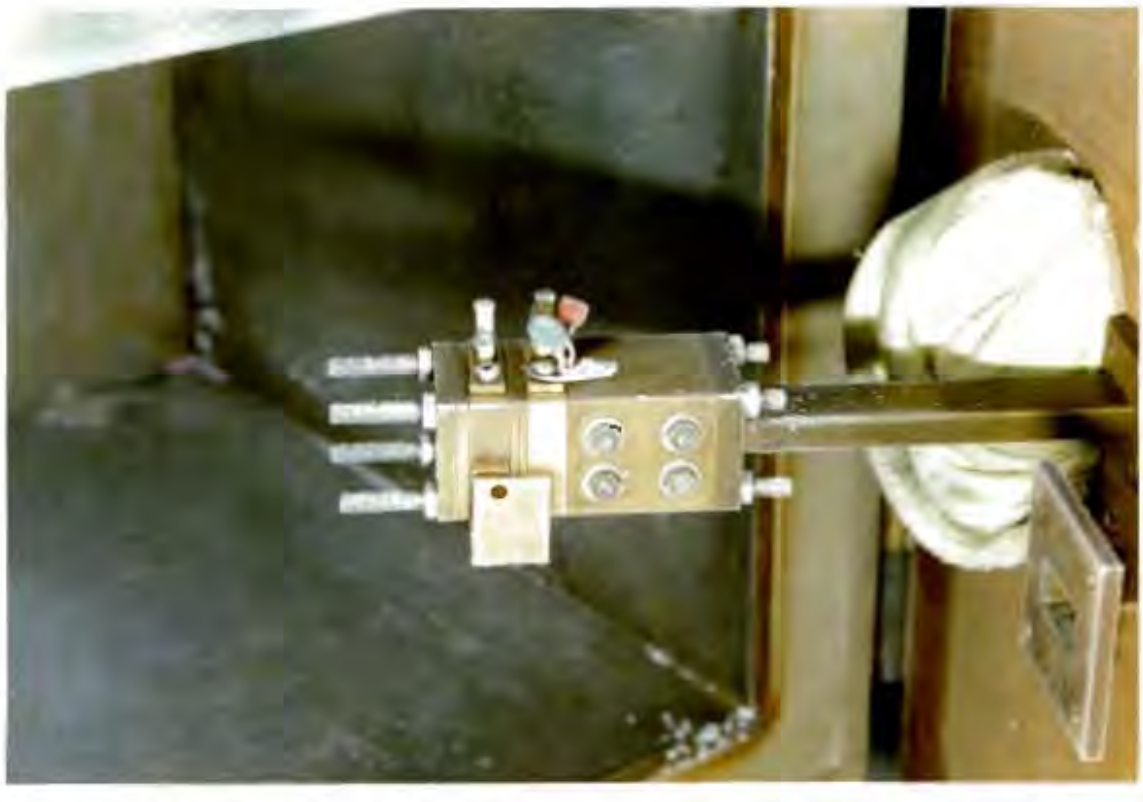

Fig. 51 The Gunn Oscillator after Experiments at -30 °C.

5.7 Temperature Compensation

The oscillators that have been investigated show a temperature drift of up to -3 MHz/°C. The temperature drift is due to the temperature dependence of the Gunn-effect device itself as shown previously and the temperature coefficient of the material of the cavity. This $\delta F/\delta T$ is unacceptably high in particular if it is considered that the oscillators are locked to a temperature compensated crystal and therefore the oscillators have to provide a large tuning range to operate over the temperature range.

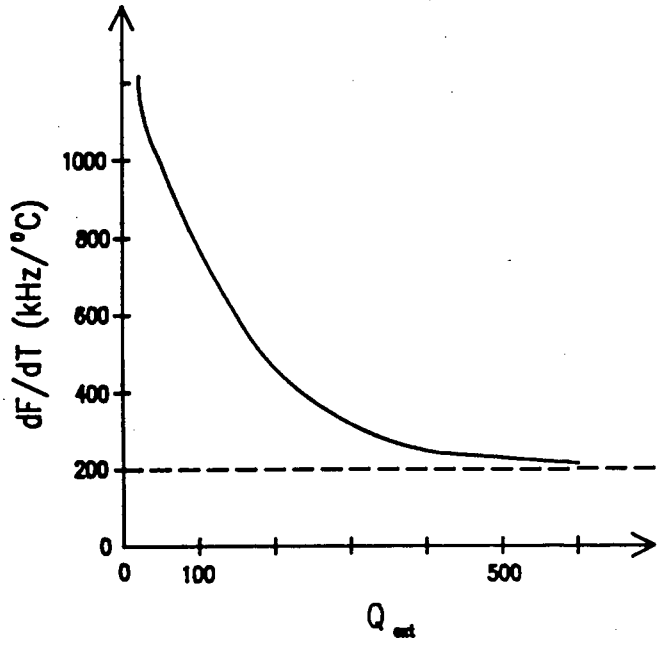

Fig. 52 $\delta F/\delta T$ as a Function of Q-factor.

There are three problems with providing a high tuning range. Firstly, the linearity of the electronic tuning range depends also on how large the tuning range is, secondly the

larger the electronic tuning range the lower the Q-factor of the cavity with the result of a degraded noise performance and stability, and thirdly, the lower the Q-factor is the higher is the temperature drift $\delta F/\delta T$ (Fig.52) [49].

To reduce the electronic tuning range several methods of temperature compensation have been considered. The methods involve either varying the parameters of the diode or by varying some physical parameters of the microwave circuit.

An obvious method would be to vary the bias voltage of the Gunn-effect device. This can be done by using a supply circuit which incorporates a thermistor as temperature sensor. The problem with this method is the highly varying output power of the oscillator over the temperature range (see Fig.46 and Fig.47).

If material with a variable dielectric constant is mounted in the waveguide cavity, acting as a cylindrical waveguide highly stable oscillators can be manufactured [50].

Another method would be to place a bimetallic disc or strip into the waveguide cavity. In this way temperature compensation is achieved by adding a temperature dependent reactance to the microwave circuitry.

If the cavity is designed with a sliding short-circuit for frequency adjustment the sliding short-circuit can be made out of a material that has a high expansion coefficient. In this the sliding short-circuit acts as the frequency

compensator. The problem with this being that the electronic tuning range is affected as well.

Another method [49] is to make the side walls of the cavity of some material that has a high thermal expansion coefficient. In this way the impedance of the waveguide is changed which is given by [51],

$$Z_g = 2\sqrt{(\mu/\epsilon)}\ \frac{L_g b}{L_0 a} \qquad \ldots\ (1)$$

Where L_g is the waveguide wavelength, L_0 the free space wavelength, a the wide waveguide dimension, b the narrow waveguide dimension and μ/ϵ the ratio of permeability and permittivity. This method of compensation has the disadvantage of being bulky as well as mechanically elaborate.

In yet another method [52] the oscillator can be temperature compensated by stabilising it with a high Q cavity. This technique can however only be used when small electronic tuning ranges are required.

The methods described above are either complicated to produce due to the use of special materials or otherwise the methods have got other undesirable effects apart from their frequency compensation.

A method that combined the ease of application and flexibility was chosen. This involved a tuning stub that

protrudes into the waveguide which is mounted to a material that has a high coefficient of thermal expansion. The length L and the coefficient of thermal expansion of the mount determining how much the stub moves per °C. The set-up is shown in Fig.53.

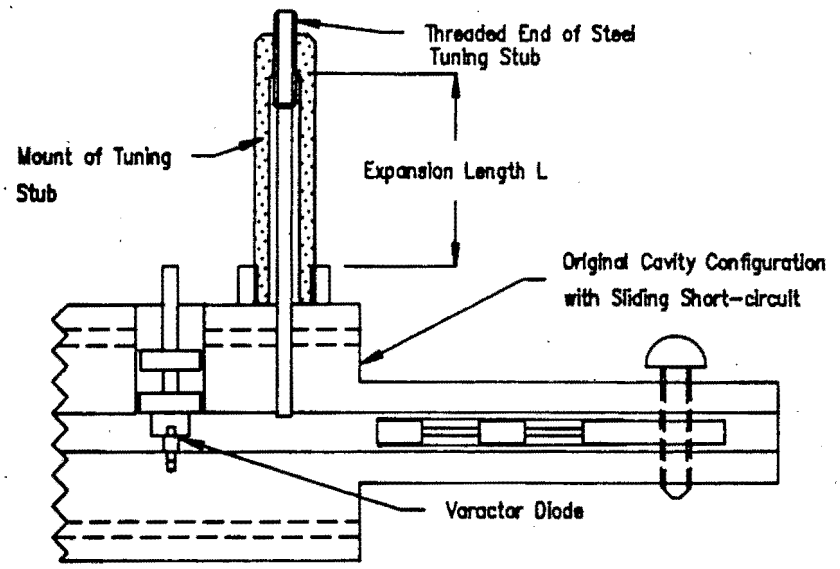

Fig. 53 The Gunn Oscillator with Temperature Compensation Assembly.

To select a suitable material to mount the tuning stub the following table presenting various expansion coefficients of materials is considered.

Material	Coefficient of Thermal Expansion (ppm)
Aluminium	23.4
Brass	18.4
Steel	12.0
Glass, quartz	0.4
Polyethylene	180
Polystyrene	210

Table 6 Thermal Expansion Coefficients of various Materials.

The table shows clearly that materials with high thermal expansion coefficients are plastics. A material called Hytrel 40D, a polyester elastomer, which was freely available as it is used for cable sheathing, was selected. The mechanical properties (see Appendix D pg.151) of the material are that it is very resilient, retains its flexibility at low temperatures and its properties at elevated temperatures. The material melts at 112 °C and has a thermal expansion coefficient of 200 ppm.

5.7.1 The Tuning Rod in the Waveguide

Before it was decided how long the mounting post of the tuning stub should be the effect of the tuning stub on the frequency of the oscillator had to be investigated.

The diameter of the rod was kept small (1.5 mm diameter) to prevent the stub having distributive circuit characteristics

in the waveguide. The material of the stub was chosen to be mild steel as this has a low thermal expansion coefficient and reasonably low loss at microwave frequencies. The stub was inserted in the centre of the broadwall of the waveguide, halfway between the short-circuit backwall and the varactor. The stub was then inserted and recordings of insertion depth and frequency were made.

The graph of insertion depth of the rod versus frequency using the cavity configuration with the Gunn-effect device mounted on a post in the centre of the waveguide is shown in Fig.54.

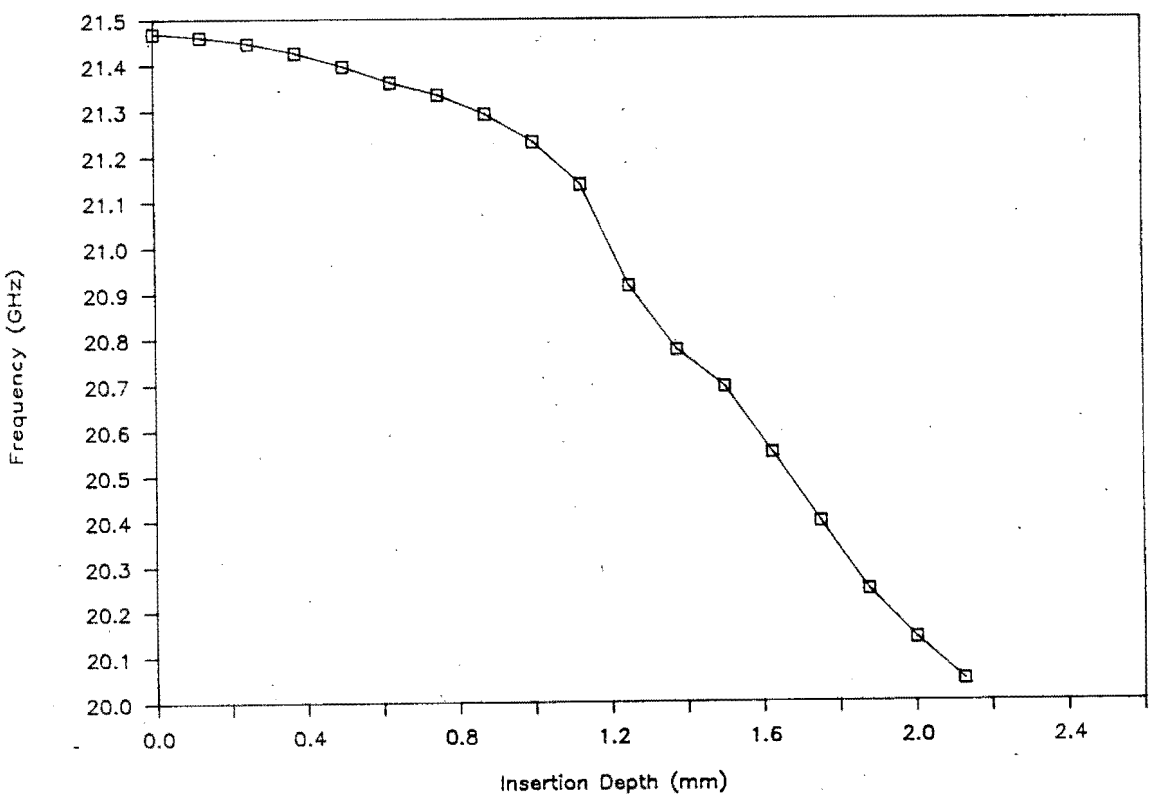

Fig. 54 Frequency versus Insertion Depth of Stub for the Gunn Oscillator.

5.7.2 The Temperature Compensated Oscillator

The graph in Fig.54 shows a varying slope of the frequency versus insertion depth curve. The slope can be calculated and ranges from 68 MHz/mm for shallow insertion depths to 1000 MHz/mm for deep insertion depths (1.3 mm) are measured.

To compute the length required of the mounting material for the tuning stub the following simple relationship can be derived,

$$L = (\delta F/\delta T)/[\propto(\delta F/\delta L)] \qquad .... (2)$$

Where $\delta F/\delta T$ is the temperature drift of the oscillator, $\delta F/\delta L$ is the change of frequency per millimetre at a particular insertion depth of the stub and $\propto$ the coefficient of linear thermal expansion of the material of the mount for the tuning stub.

Using the coefficient of linear thermal expansion for the Hytrel polyester elastomer (200 ppm), a temperature drift of 1.5 MHz/°C and a frequency rate of change of 200 MHz/mm, the length of the mounting material using equation (1) computes to 37.5 mm. The relatively low rate of frequency change was chosen as this means that the stub will not be inserted very much (0.7 mm) into the waveguide to affect other characteristics of the oscillator. The stub was then adjusted to a certain insertion depth, the sliding short-circuit adjusted to compensate for the frequency change caused by the stub and with the varactor voltage constant

measurements of frequency at various temperatures were made. The results are displayed in Fig.55.

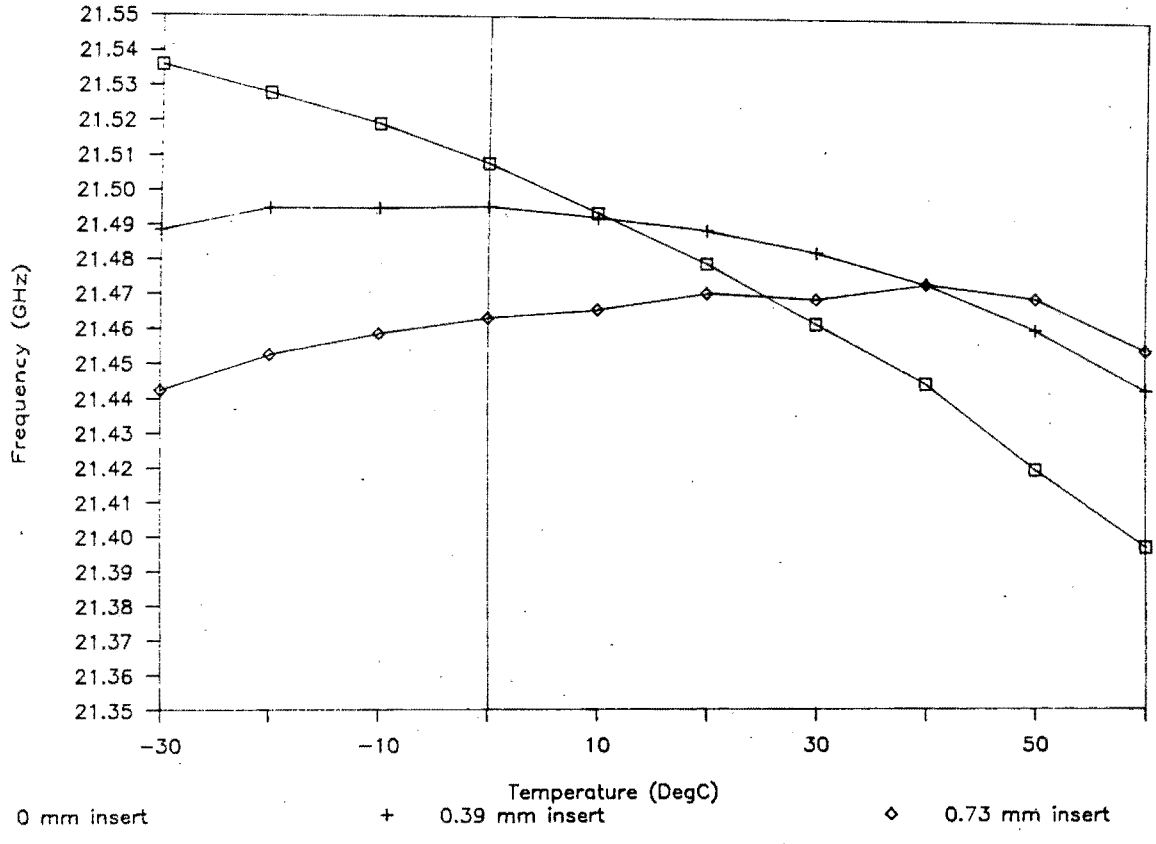

Fig. 55 The Temperature Compensated Oscillator.

From the graph in Fig.55 the following observations can be made. Without the stub inserted the frequency changed by 139 MHz over the temperature range corresponding to a $\delta F/\delta T$ of 1.54 MHZ/°C. With the stub inserted 0.39 mm this drift was reduced to 52.9 MHz over the temperature range ($\delta F/\delta T$ = 0.59 MHz/°C) with the best result achieved at an insertion depth of 0.73 mm where the frequency changed by 30.5 MHz over the temperature range ($\delta F/\delta T$ = 0.34 MHz/°C).

The graph shows that the frequency compensation is not linear. The reason lies with the rapidly changing slope of the frequency versus insertion depth curve (Fig.54). The compensation assembly therefore has different compensation rates at different temperatures.

5.8 Conclusion

The behaviour of the Gunn-effect device and of the oscillator with temperature was investigated. It was found that the bias voltage of the Gunn-effect device is very critical if low changes of microwave output power with temperature are required and effects like mode switching or start-up problems at low temperatures have to be eliminated. A temperature compensation method is investigated and the $\delta F/\delta T$ was reduced from 1.54 MHz/°C to 0.34 MHz/°C.

CHAPTER 6

6. GUNN-EFFECT DEVICE SPREAD

6.1 Introduction

The Gunn oscillators are used in an instrument intended for high volume production (up to 500 per year) and therefore it was necessary to test them for repeatability. In particular the repeatability of tuning range, linearity and output power are important. This chapter investigates the effect of different Gunn-effect devices in the same cavity. An explanation why some devices performed in the specified way described in the previous chapters and other devices had very different characteristics is attempted.

6.2 Oscillator Performance at Room-temperature

6.2.1 Tuning Characteristic and Linearity

These experiments were made in the cavity configuration where the Gunn-effect device is mounted off the floor on a post. The sliding short-circuit backwall was used to compensate for the difference in the devices by adjusting it

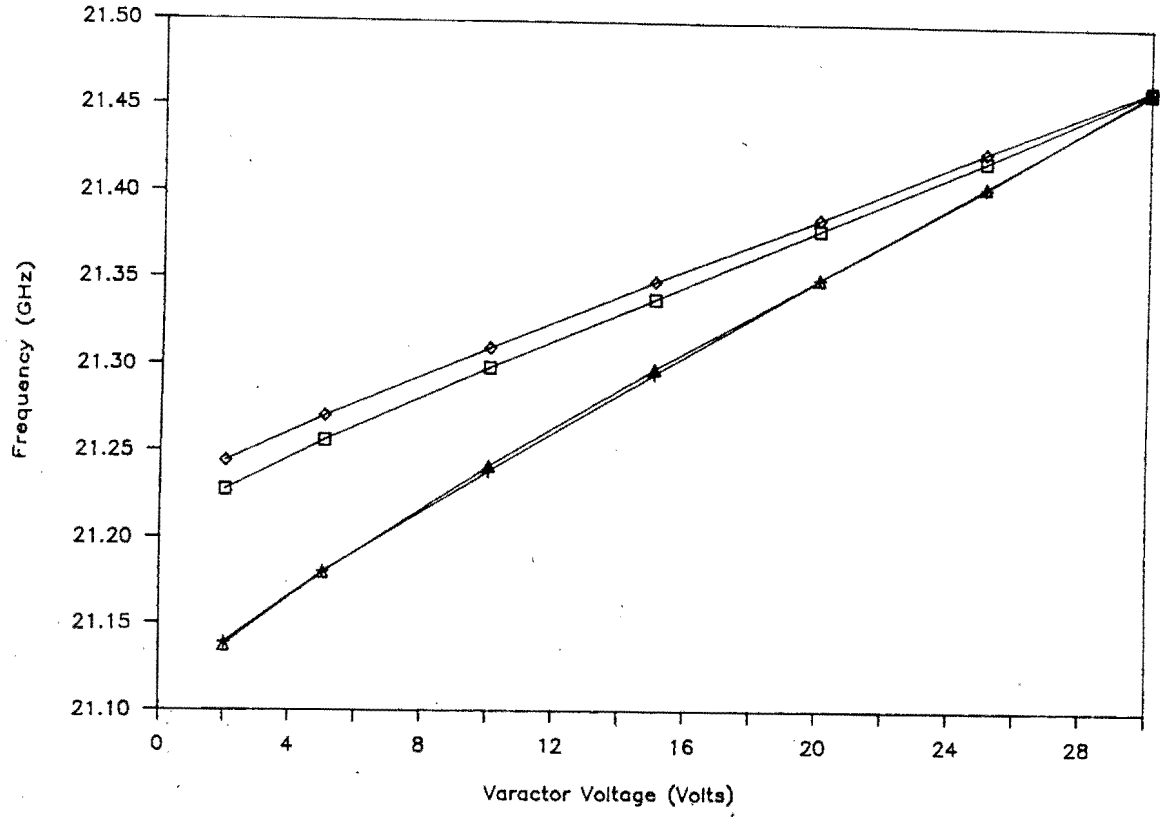

Fig. 56 Electronic Tuning Characteristic for Different Gunn-effect Devices.

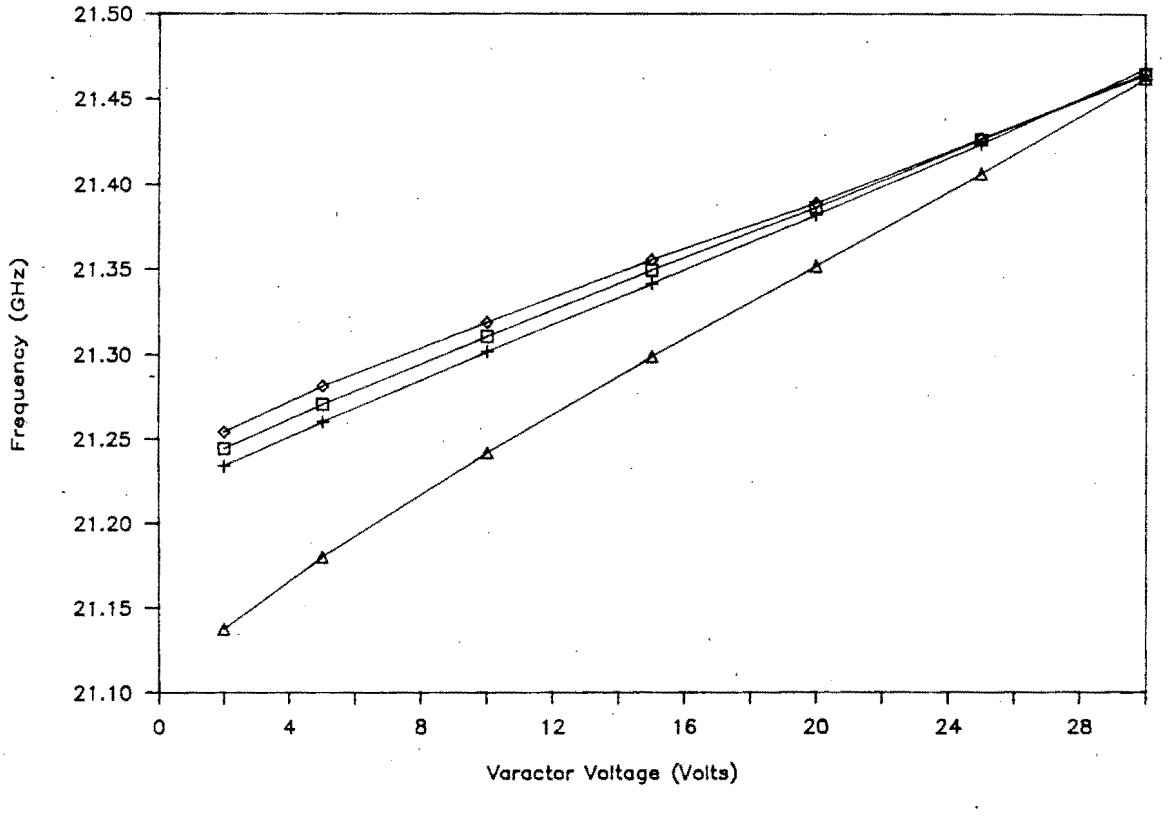

Fig. 57 Electronic Tuning Characteristic for Different Varactor Diodes.

accordingly. The other cavity dimensions and post sizes remained constant. Devices from different batches were used to test the repeatability of the tuning characteristic. The results of placing four different Gunn-effect devices with the same varactor diode into the cavity is shown in Fig. 56. The same experiments have been conducted by exchanging the varactor diode using the same Gunn-effect device. The results are displayed in Fig. 57.

From both graphs it can be seen that the tuning linearity changes to some extent from device to device. But considering the change in tuning range from device to device which implies different impedance relations of the microwave circuit. Thus it can be said that the linear electronic tuning characteristic of the Gunn oscillator is preserved.

6.2.2 Comparison of Devices

To compare the performance of the different devices with respect to output power and tuning range the barcharts in Fig.58 and Fig.59 respectively have been created.

While the output power does not vary significantly as devices are changed, the effect on the tuning range is more prominent. The barchart depicting the tuning range shows that not only the substitution of the varactor changes the tuning range but that the exchanging of the Gunn-effect device has a more significant effect on the tuning range than the varactor.

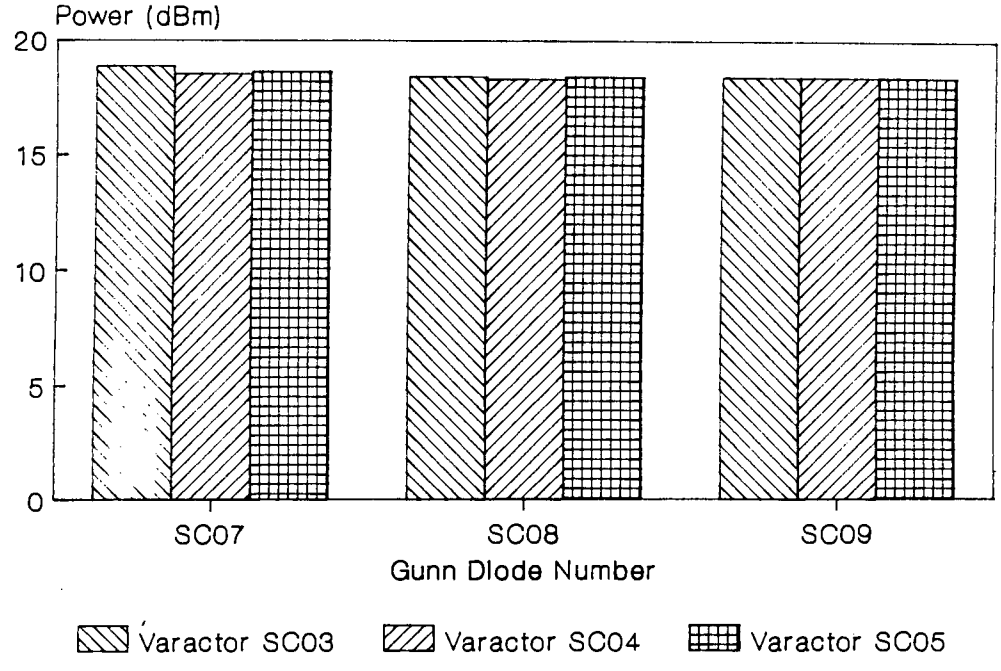

Fig. 58 Histogram of Device Spread with respect to Power.

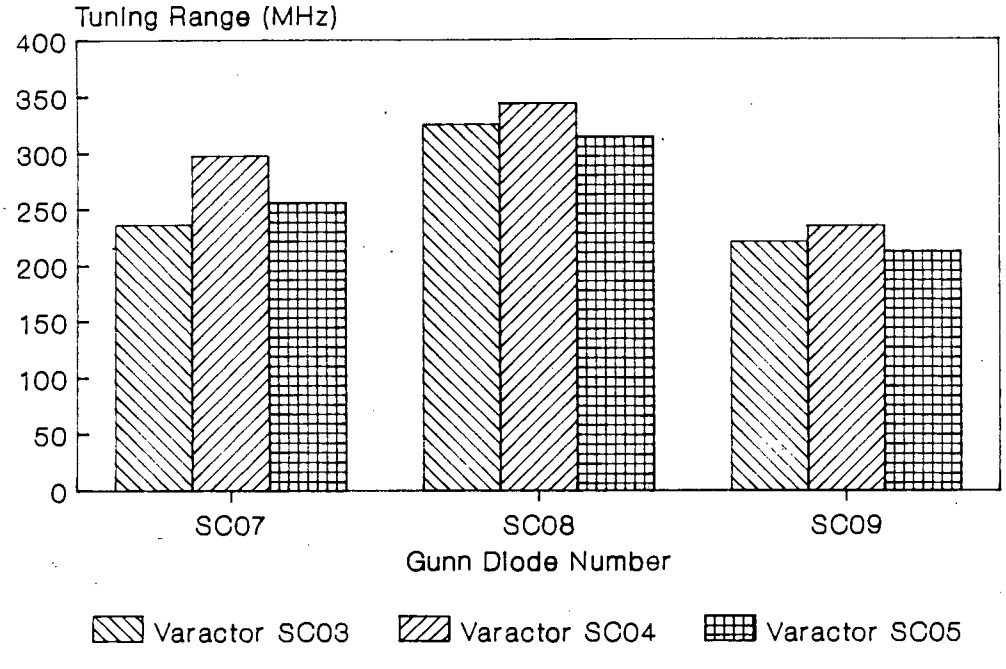

Fig. 59 Histogram of Device Spread with respect to Electronic Tuning Range.

The variation of the electronic tuning range due to the Gunn-effect device can be explained by the varying device capacitance. This capacitance changes the centre frequency of the oscillator which was compensated by the appropriate adjustment of the sliding short-circuit. From the experimental data in chapter 3 it can be seen that the tuning range changes when the short-circuit backwall is adjusted. Therefore the change in electronic tuning range when different Gunn-effect devices are being used.

The slight differences in tuning range due to varying varactor diodes is simply due to their changing voltage/capacitance characteristic from device to device.

6.3 Oscillator Performance at Low Temperatures

It has been found that when the oscillators are temperature tested that some Gunn-effect devices mode switched at low temperatures with corresponding start-up problems and some devices did not exhibit that behaviour. Two Gunn-effect devices that differed in such a way were chosen and examined.

6.3.1 Mode-switching and Gunn-effect Device Spread

For simplicity the two Gunn-effect devices that were examined are named SC 09 and SC 20. The following table shows the voltages at the different temperatures at which the oscillator, with the respective devices, mode switched from the unwanted high frequency mode to the desired mode.

Temperature (°C)	SC 20 Gunn Bias Voltage (Volts)	SC 09 Gunn Bias Voltage (Volts)
-30	8.181	-
-20	8.106	-
-10	7.951	-
0	7.743	8.045
10	7.585	7.854
20	7.405	7.652
30	7.239	7.478
40	7.073	7.395
50	6.957	7.271
60	6.793	7.115

Table 7 Comparison of Bias Voltages of Gunn-effect Device at which Mode Switch to desired Mode occurs.

The above table clearly contrasts the difference between Gunn-effect device SC 20 and SC 09. While device SC 20 could always be biased to switch to the desired mode, device SC 09 remained in the high frequency mode except at temperatures above 0 °C where higher bias voltages in comparison to device SC 20 were required to mode switch the oscillator.

6.3.2 Comparison of Characteristics

The previous section shows a difference of mode switching characteristics at low temperatures for the two Gunn-effect devices. To explain this behaviour the properties of the devices with varying Gunn bias voltage have been recorded. The power output and the oscillator frequency for the variation of Gunn bias voltage are shown in Fig. 60 and Fig. 61 respectively. For comparative purposes the two device characteristics at 30 °C and at -30 °C are shown on the same pair of axis.

From the graphs it is clear that device SC 20 has a wider frequency range as well as a wider power output range than device SC 09. This property is the same at the two temperatures with the only distinction that at -30 °C the difference between the ranges is even more pronounced.

Referring to the discussion of stable oscillation and mode switching in chapter 3 and using the two previous graphs it can be deduced that device SC 20 has a much larger negative conductance variation than device SC 09. This is exhibited in the higher power output range in Fig. 60 and the larger frequency range in Fig. 61 of device SC 20. The negative conductance of the Gunn-effect device has to match the conductance of the microwave circuit for stable oscillation. If in a multi-resonant circuit the variation of the device's negative conductance cannot match the with temperature varying circuit conductance the oscillator will then mode switch to a state of stable oscillation. Gunn-effect device SC 20 is thus a much more broadband device than SC 09.

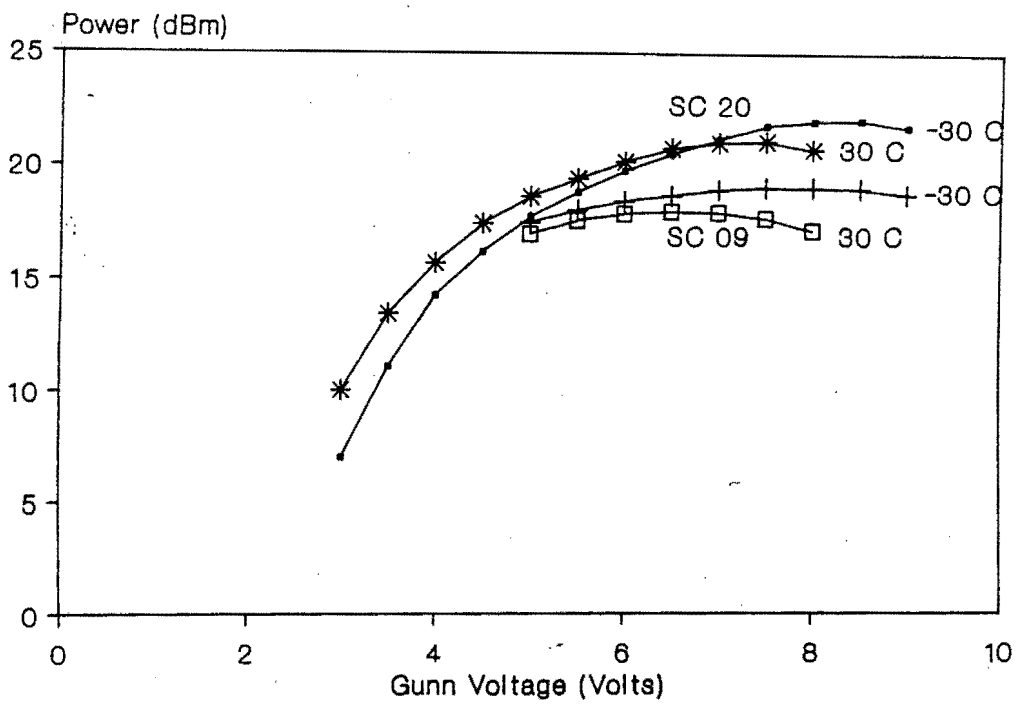

Fig. 60 Power Output versus Bias Voltage for Devices SC 20 and SC 09 at different Temperatures.

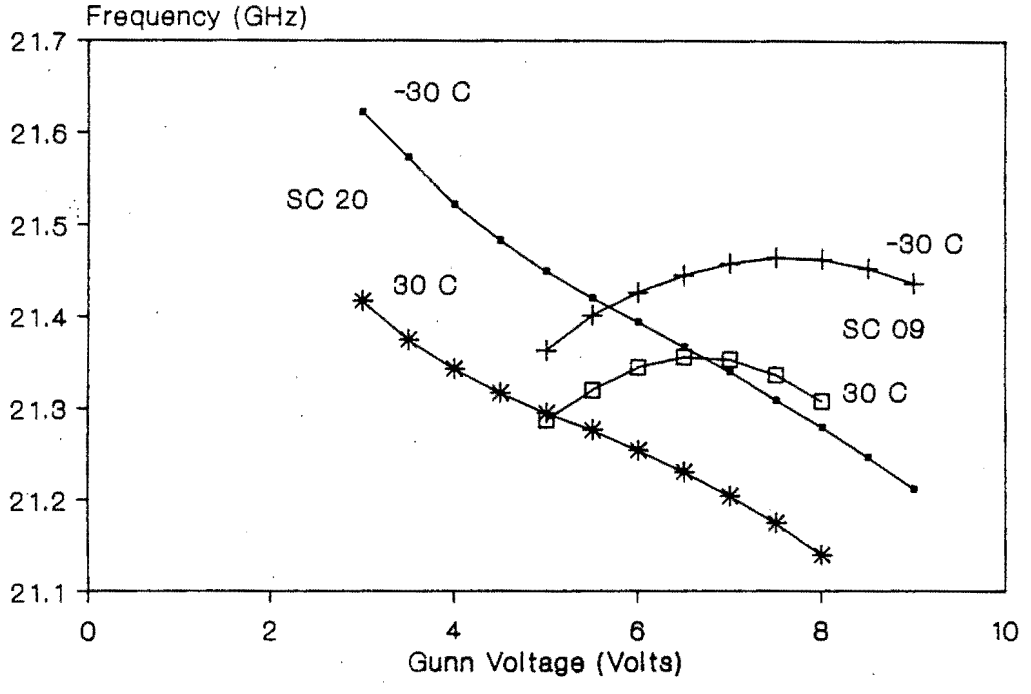

Fig. 61 Frequency Output versus Bias Voltage for Devices SC 20 and SC 09 at different Temperatures.

To correlate the above theory with the findings of table 7 the variation of device conductance with bias voltage has to be kept in mind. The fact that by varying the Gunn bias voltage of device SC 20 it could always be forced to oscillate in the desired mode while for device SC 09 this is only true for temperatures above 0 °C, means that the conductance of device SC 20 could vary enough to match the load conductance of the microwave circuit in the desired frequency mode.

Another aspect of the two Gunn-effect devices was investigated by establishing the maximum output power of the devices at a certain frequency. For these experiments only the Gunn-effect device itself without varactor and its post was mounted in the configuration with the Gunn-effect device in the centre of the waveguide. The cavity had a sliding short-circuit as backwall and to obtain maximum power output from the Gunn-effect device a waveguide segment with 8 matching screws were placed in front of it. The screws are approximately an eighth of a waveguide wavelength apart [31] and of a diameter of 1.5 mm. The procedure was then to adjust all the screws so that none of them protruded into the waveguide. Then the sliding short-circuit backwall was adjusted to the required frequency and then the screws were adjusted to the maximum output power. This arrangement ensured that the Gunn-effect device was very well matched to the cavity in that mode of oscillation. The posts by which the Gunn-effect devices are mounted are of the same

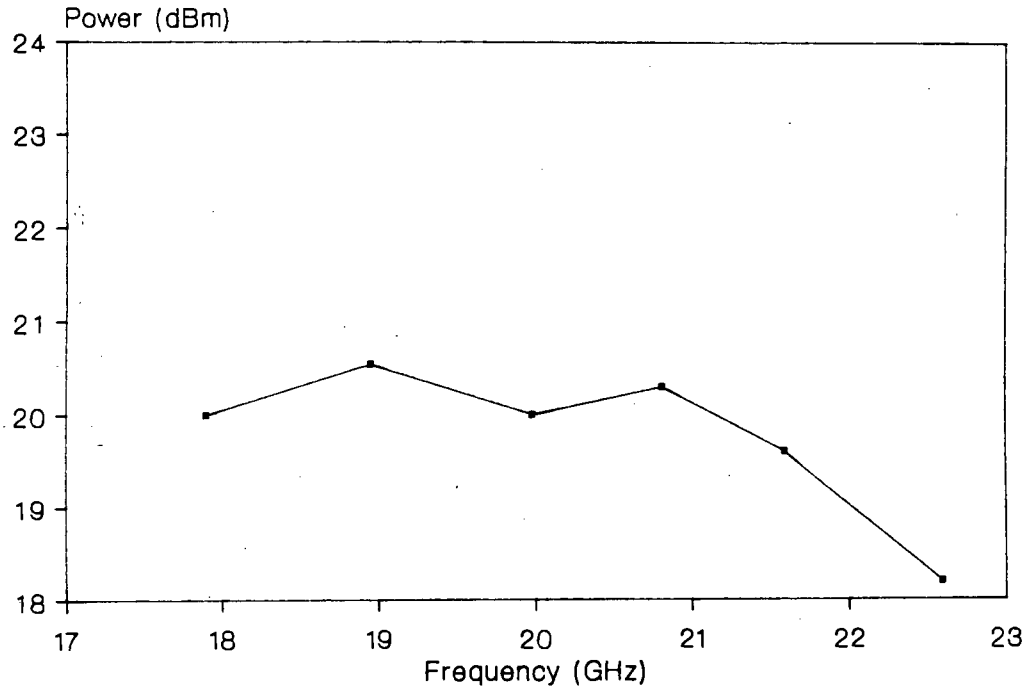

Fig. 62 Variation of Output Power with Frequency in matched Cavity of Device SC20.

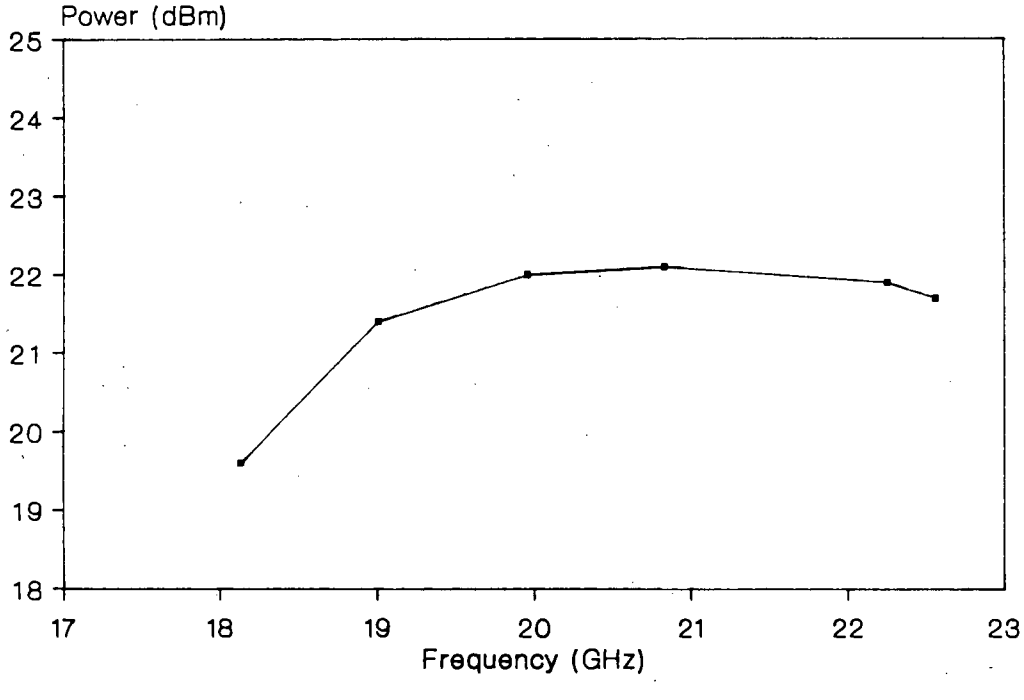

Fig. 63 Variation of Output Power with Frequency in matched Cavity of Device SC09.

diameter. The results of this investigation are displayed in Fig. 62 and Fig. 63 for device SC 20 and SC 09 respectively.

The first difference that can be seen is that device SC 09 has a lower output power (1.5 dB) than device SC 20. More important however is the variation of power with frequency. The frequency of operation over which the Gunn oscillators are required to operate is from 21.2 GHz to 23.6 GHz. While Gunn-effect device SC 20 has high output power at 21.2 GHz that continue to be high to frequencies just short of 23 GHz, Gunn-effect device SC 09 has low power output at 21.2 GHz dropping rapidly toward 23 GHz. This can be seen as another reason of the unsatisfactory performance of device SC 09 with respect to mode switching. The mode switching experiments and device characteristics were measured in a cavity without matching screws at a frequency of approximately 21.5 GHz. This is a frequency at which device SC 09 is operating only marginally within the devices operating frequency range in that mode.

6.4 Conclusion

The chapter investigated the effect of device spread on various characteristics of the Gunn oscillator. The most important characteristic, the linearity of the oscillator has been found to be highly repeatable. Mode switching problems at low temperatures occur with some devices and an investigation revealed that the devices that mode switched did not give maximum power output at 23 GHz and had a limited negative conductance variation. To ensure good

repeatability of oscillators in production the manufacturer of the Gunn-effect devices (Microwave Associates) will be asked to test and select devices with maximum output power at 23 GHz and high negative conductance variation.

CHAPTER 7

7. NOISE PERFORMANCE OF THE GUNN OSCILLATOR

7.1 Introduction

The overall performance of the radio unit with respect to bit error rates, receiver sensitivity and noise figure depends very much on the noise performance of the crystal locked Gunn oscillator which is being used as local oscillator and transmit source. This chapter investigates possible sources of noise of the oscillator and how noise performance was optimised.

7.2 Sources of Noise in Gunn Oscillators

There are three different sources of noise in Gunn oscillators:

1) Flicker noise, a frequency modulation noise, which is produced by the current noise of the bias [53] of the Gunn-effect device. The origin of the current noise is due to erratic domain triggering caused by local electric field variations. This produces time fluctuations as the electric field reaches the threshold for domain formation [54]. The noise bandwidth is from zero to 10 kHz, the noise power

varying by 1/f. This type of noise is also referred to as pink noise.

2) Generation/recombination noise which is a function of trapping centres and impurities of the semiconductor material. This noise is significant at frequencies between 1 kHz and 10 MHz and also follows approximately the 1/f law. This type of noise can be distinguished from flicker noise as it varies with temperature [55].

3) Thermal noise or otherwise known as shot noise is mainly contributing at frequencies above 1 MHz.

The noise sources described in 1) and 2) do not only produce FM noise but also AM noise. The reason for this is that they are noise currents and depending on the bias resistance this produces a noise voltage. Chapter 2, 5 and 6 describe the frequency and output power variation with the Gunn-effect device's bias voltage. It is clear from those discussions that noise on the bias voltage will produce FM and AM noise. The amount of FM and AM noise depends very much on the bias voltage as well as the device characteristics. Ideally the bias voltage should be adjusted to a point where frequency and power variation with bias voltage are at a minimum, ie. the bias-frequency and power pushing characteristic is minimised.

7.3 Methods of Reduction of Excess Noise.

The noise generated by the Gunn-effect device in any of the ways discussed in the previous section cause random phase fluctuations with respect to the device controlling waveforms associated with the RF energy stored in the cavity. These fluctuations in turn cause random fluctuations of the cavity control waveform as some energy is delivered to it by the device. The phase deviations are small if the energy stored in the cavity is much greater than the energy delivered to the cavity.

The loaded Q-factor Q_L of the cavity can be written as [56]:

$$Q_L = \frac{2\pi \text{ (energy stored in cavity)}}{\text{(total energy dissipation per cycle)}}$$

The loaded Q-factor therefore has to be as large as possible for low noise operation by increasing the energy stored in the cavity. A method to increase the stored energy of the cavity is to increase the length of the cavity. The distance between the active device and the short-circuit backwall can be increased in multiples of half waveguide wavelengths. This has been shown to increase the Q-factor of the cavity as well as improving the noise performance of the oscillator [57]. The problem with this technique being that high Q cavities have poor electronic tunability and mode switch more easily.

The Gunn oscillators that have been designed have Q-factors that are as high as possible. The reason for this was not only to improve the noise performance of the cavity but also to reduce the $\delta F/\delta T$ of the oscillator. On the other hand the oscillator was required to have an electronic tuning range of approximately 300 MHz which requires a lower Q-factor. The Q-factor was therefore a trade-off between electronic tuning range, noise performance and temperature drift.

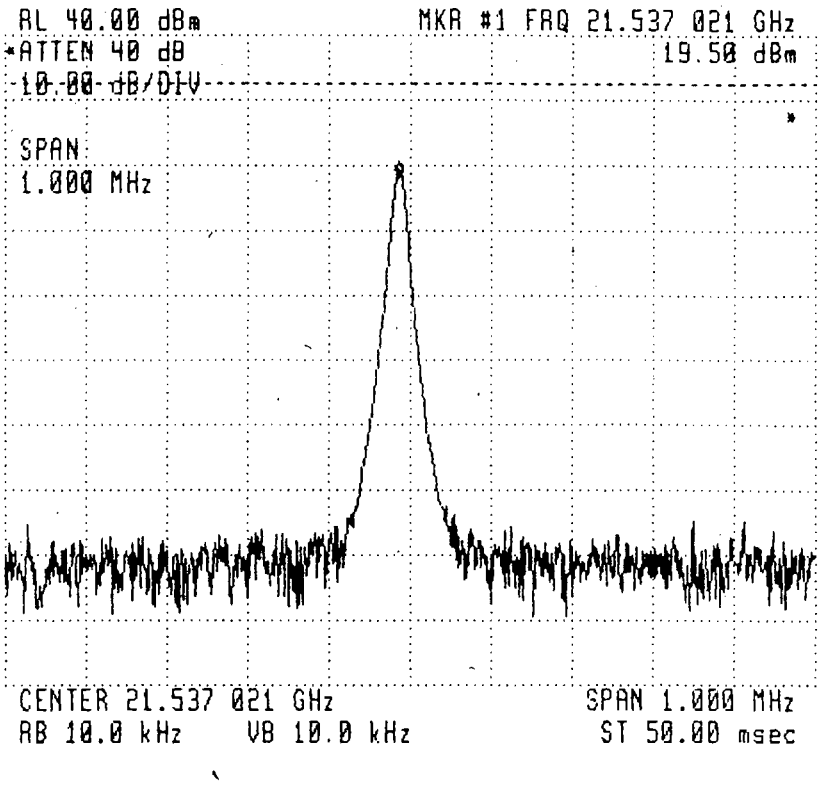

Fig. 64 The Spectrum of the Gunn Oscillator.

The other method of reducing oscillator noise is to adjust the Gunn-effect device bias voltage to the point where the variation of power and frequency with bias voltage is at a minimum as outlined in the previous section. The problem

with this technique being that mode switch problems might occur at low temperature as the bias voltage is not large enough (Chapter 5 and 6).

To reduce the noise of the oscillator as much as possible the impedance of the bias supply have been reduced to a practical minimum and decoupled with a capacitance of 35 μF and 0.47 μF. The spectrum of the oscillator is shown in Fig.64.

8. CONCLUSION

The dissertation describes the design process of 23 GHz varactor controlled Gunn oscillators which are to be used as crystal locked local oscillator and transmit source of a digital datalink. An accurate design procedure for these oscillators is given by deriving the characteristics of Gunn oscillators. The use of advanced modulation methods requires linear voltage/frequency characteristics of the Gunn oscillator. A method of linearisation is described and linear voltage/frequency characteristics with a worst case slope change of 1:1.15 have been achieved. The operating temperature from -30 °C to 55 °C causes the Gunn oscillator to drift excessively and a method of temperature compensation reduced the drift from -2 MHz/°C to 0.3 MHz/°C. The oscillators were tested using several devices and the repeatability of the most important characteristics, linearity, output power and tuning range was confirmed. Methods of how to overcome mode switching also at low temperatures and to improve the noise performance of the oscillator are also described.

The datalink has been developed and an ADM (advanced development model) model was tested extensively. The unit performed without problems over ranges of 24 km during rainy conditions and operated satisfactorily over the temperature range. A detailed description of the system operation and its performance has been published by the author [58].

Appendix A

Specifications of Gunn-effect Device

HIGH FREQUENCY CW GUNN DIODES—18 TO 94 GHz (CATHODE HEAT SINK EXCEPT WHERE NOTED)

This series of high frequency Gunn diodes features low noise (both AM and FM), good efficiency and one-step conversion from dc to microwave energy using a single, low voltage power supply.

These devices are ideally suited for use as paramp pump sources and as transmitters in point to point telecommunication links. The noise performance of these diodes is better than that of comparable reflex klystrons, thus making them attractive for use as local oscillators for noise measurements of mixer diodes.

MODEL NUMBER[1,2,3]	STD. CASE STYLE[4]	FREQ. RANGE[5] (GHz)	MIN. OUTPUT PWR.[5] (mW)	OPERATING VOLT, V_{OP}[6] (VOLTS) MIN.	OPERATING VOLT, V_{OP}[6] (VOLTS) MAX.	MAX. OPER. CURRENT, I_{OP}[6] (mA)
MA-49190-118[7]	118	18-26.5	10	4.0	7.0	250
MA-49179-118	118	18-26.5	50	5.0	8.0	600
MA-49179-138	138	18-26.5	50	5.0	8.0	600
MA-49180-118	118	18-26.5	100	5.0	8.0	1000
MA-49180-138	138	18-26.5	100	5.0	8.0	1000
MA-49178-118	118	18-26.5	250	5.0	8.0	1600
MA-49191-138[7]	138	26.5-40	10	3.0	6.0	250
MA-49172-138	138	26.5-40	50	3.5	6.0	800
MA-49173-138	138	26.5-40	100	3.5	6.0	1200
MA-49877-138	138	26.5-40	100	3.5	6.0	1400
MA-49837-138	138	26.5-35	250	4.0	8.0	1600
MA-49192-138[7]	138	40-60	10	2.0	4.0	300
MA-49181-138	138	40-50	50	2.5	4.5	1200
MA-49193-138	138	40-50	75	2.5	4.5	1400
MA-49838-138	138	40-50	100	2.5	4.5	1600
MA-48182-138	138	50-60	50	2.5	4.5	1200
MA-49839-138	138	50-60	100	2.5	4.5	1600
MA-49840-138[7]	138	94	10	2.5	4.5	1400

Specifications of Varactor Diode

CERAMIC PACKAGED SILICON ABRUPT JUNCTION MICROWAVE TUNING VARACTORS

The MA-45200 series of silicon abrupt junction microwave tuning varactors has been designed to obtain the highest Q possible. Each device in this series has a high density silicon dioxide passivation which results in exceptionally low leakage currents and low post tuning drift.

This series is ideally suited for frequency tuning applications through K-Band. These devices are designed for use in solid state electronic tuning of transistor, Gunn and IMPATT oscillators. They may also be used in tunable filters, phase shifters, up and down converters and low order multipliers.

MODEL NUMBER[1]	MIN. BREAK-DOWN VOLT., V_B[2] (VOLTS)	TOTAL CAP., C_T[3] (pF)	MIN. CAP. RATIO[4] $C_{T_0}/C_{T_{V_B}}$	MINIMUM Q[5]	SUGGESTED FREQ. RANGE (GHz)
MA-45225	30	0.5	2.7	5500	10—12
MA-45226	30	0.6	2.9	5500	9—11
MA-45227	30	0.8	2.9	5000	8—10
MA-45228	30	1.0	3.0	4800	7—9
MA-45229	30	1.2	3.2	4800	6—8
MA-45230	30	1.5	3.3	4500	6—8
MA-45231	30	1.8	3.5	4000	5—7
MA-45232	30	2.2	3.6	4000	5—7
MA-45233	30	2.7	3.7	4000	4—6
MA-45234	30	3.3	3.7	3500	4—6
MA-45235	30	3.9	3.8	3500	3—5
MA-45236	30	4.7	3.8	3000	3—5
MA-45237	30	5.6	3.9	3000	2—4
MA-45238	30	6.8	3.9	3000	2—4
MA-45245	45	0.5	3.3	4000	9—11
MA-45246	45	0.6	3.7	4000	8—10
MA-45247	45	0.8	3.9	3800	5—7
MA-45248	45	1.0	4.0	3500	5—7
MA-45249	45	1.2	4.2	3500	4—6
MA-45250	45	1.5	4.4	3300	4—6
MA-45251	45	1.8	4.6	3000	3—5
MA-45252	45	2.2	4.8	2700	3—5
MA-45253	45	2.7	5.0	2700	2—3
MA-45254	45	3.3	5.2	2400	2—3
MA-45255	45	3.9	5.3	2200	1.5—2.5

Appendix B

Cross-Coupler S-Parameters

1) Transmission Loss

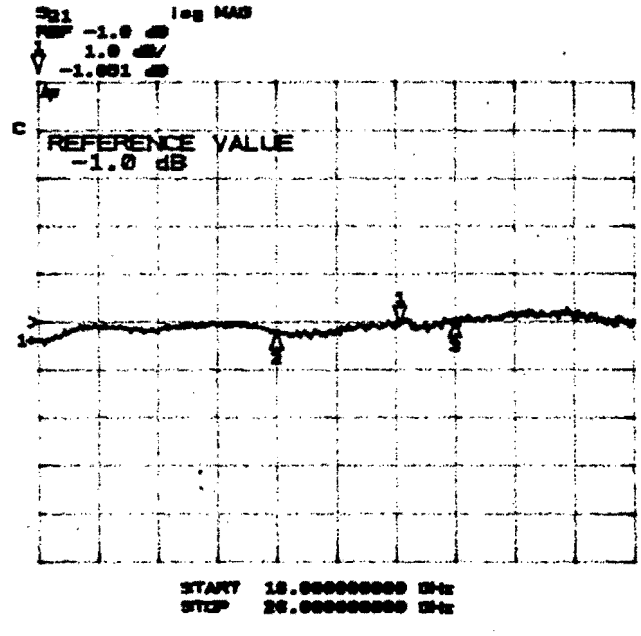

2) Return Loss

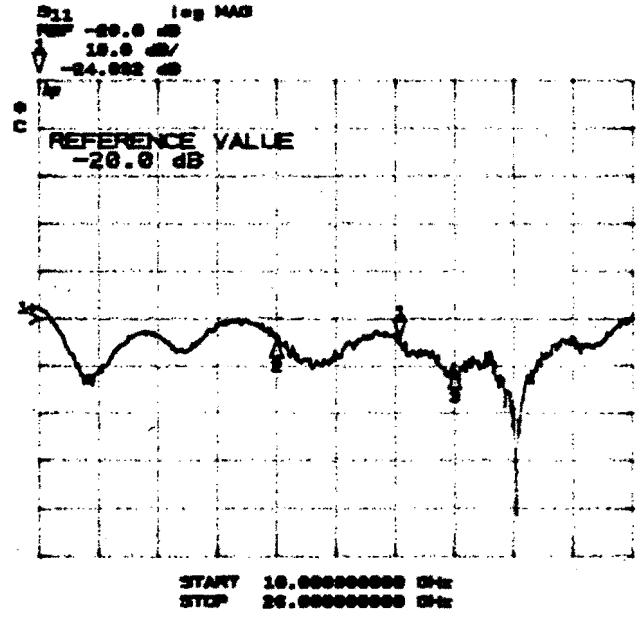

3) Coupling

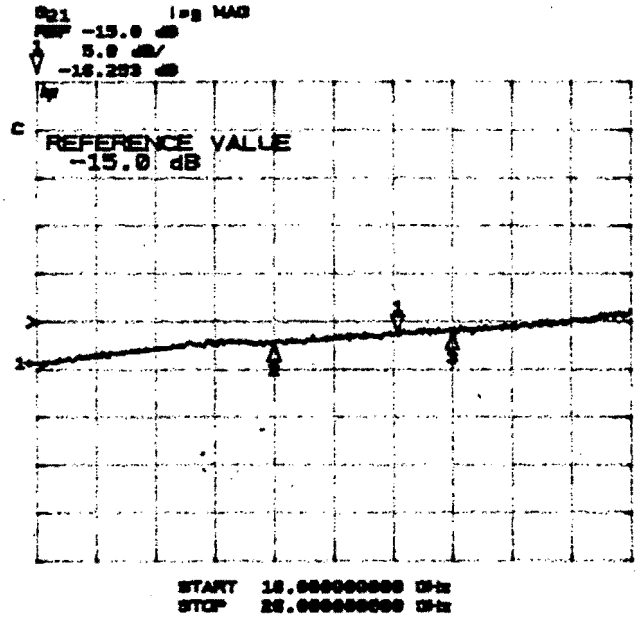

4) Isolation

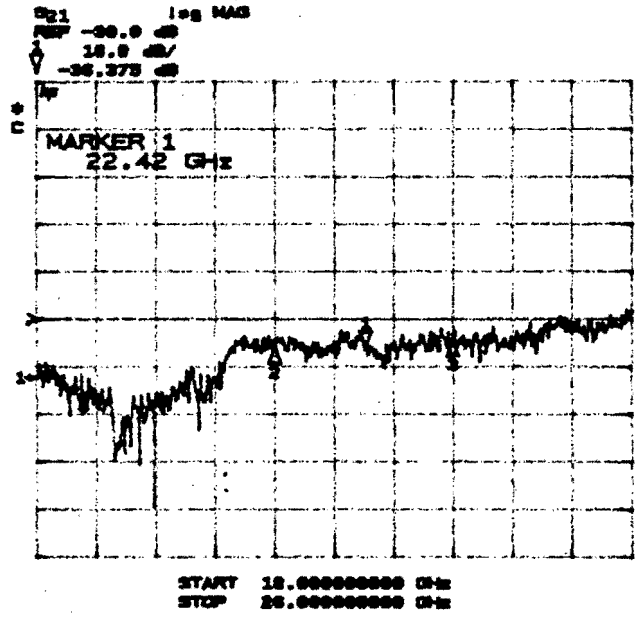

Attenuator S-Parameters

1) Transmission Loss

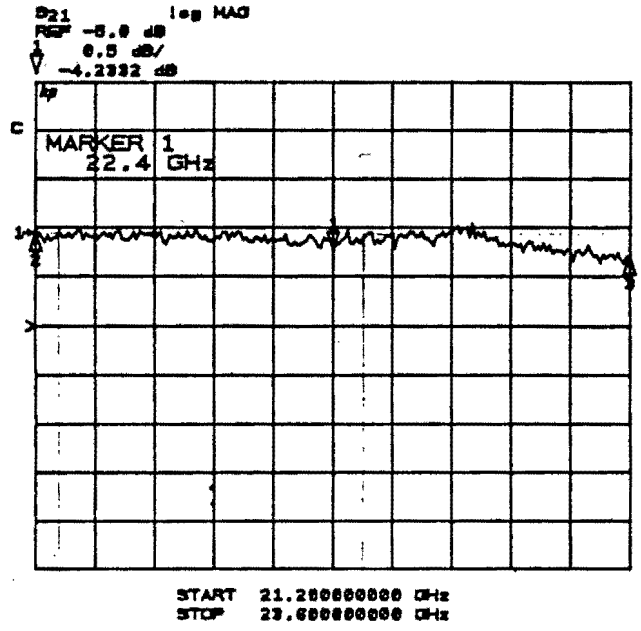

2) Return Loss

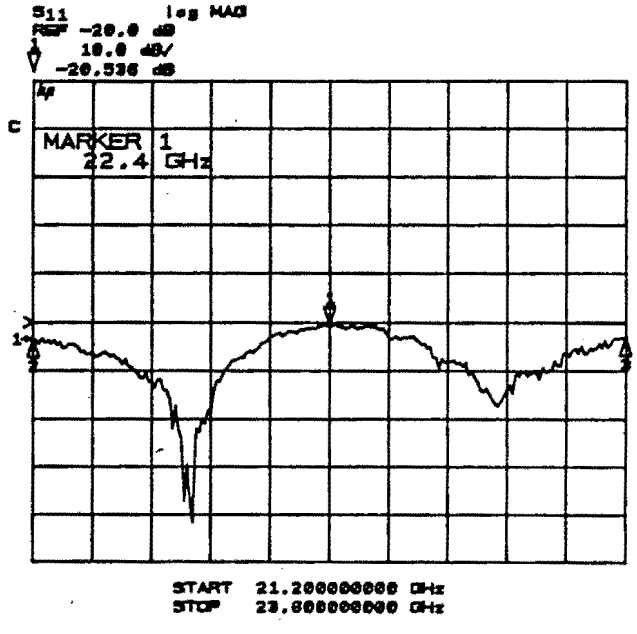

Termination S-Parameters

1) Return Loss

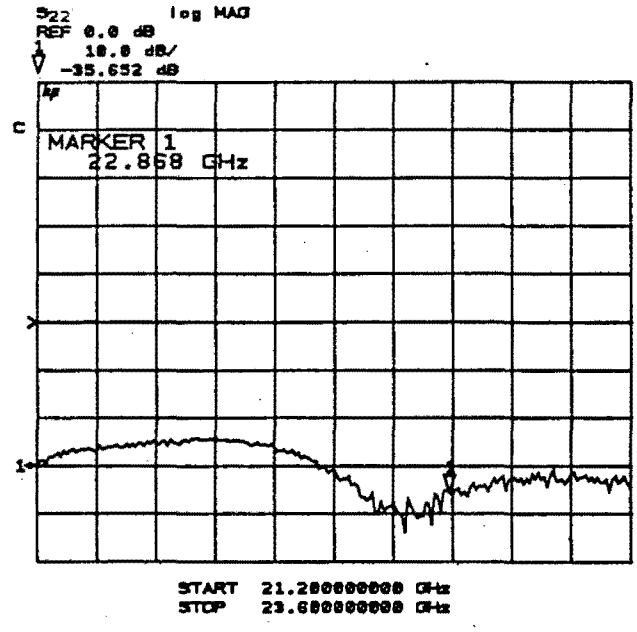

Appendix C

Test Report for Lotus 123 Spreadsheet

Test results for 23 GHz Gunn oscillator

Test number _____
Date of test _____
Time of test _____

Name of person performing test
Lutz Kratzenstein

Ambient Temperature (DegC) _____
Gunn voltage.(Volts)..... _____
Spacing Gunn/varactor (mm) _____
Spacing varactor/wall (mm) _____
Spacers Gunn/varactor _____
Spacers varactor/wall _____
Gunn post diameter (mm) _____
Varactor post diameter (mm) _____
Second LO output (GHz) _____

Test Aim:

Test Setup Comments:

Comments:

Item	Varactor Voltage (Volts)	Counter Freq. (GHz)	Actual Freq. (GHz)	Power (dBm)	Gunn Current (Amps)	Temp. (DegC)
1						
2						
3						
4						
5						
6						
7						
8						
9						
10						

Appendix D

Mechanical Properties of Hytrel 40D

Table I

Typical Mechanical Properties

Property†	Units	ASTM Method	HYTREL Polyester Elastomer Hardness (Durometer) Grades 40D	55D	63D
Tensile Strength	psi [MPa]	D-638	3 700 [25.5]	5 500 [37.9]	5 700 [39.3]
Ultimate Elongation	%	D-638	450	450	350
25% Modulus or Yield Point	psi [MPa]	D-638	1 100 (M25) [7.6]	2 000 (M25) [13.8]	2 500 (Yield) [17.2]
Stress at 25% Compression	psi [MPa]	D-575A	2 000 [13.8]	4 300 [29.6]	5 100 [35.2]
Flexural Modulus	psi [MPa]	D-790	7 000 [48.3]	30 000 [207]	50 000 [345]
Resilience, Bashore	%	–	62	53	43
Compression Set Resistance, 22 hours at 158°F [70°C]					
25% Deflection	%	D-395B	60[a]	56[a]	Not applicable
Constant Load (1350 psi) [9.3 MPa]	%	D-395A	27	4	2
Tear Strength					
Die B	lb/in [kN/m]	D-624	631 [110]	935 [164]	1 055 [185]
Die C	lb/in [kN/m]	D-624	700 [122]	900 [158]	850 [149]
Resistance to Flex Cut Growth					
Ross (Pierced)	cycles to failure	D-1052	$>3x10^5$	$>3x10^5$	$2.8x10^5$
DeMattia (Pierced)	cycles to failure	D-813	$>2x10^5$	$>7x10^4$	Not applicable
Notched Impact, Izod					
at 75°F [24°C]	ft-lb/in [J/cm]	D-256A	>20 (No [10.6] break)	>20 (No [10.6] break)	>20 (No [10.6] break)
at −40°F [−40°C]	ft-lb/in [J/cm]	D-256A	>20 (No [10.6] break)	>20 (No [10.6] break)	0.5 [0.3]
Taber Abrasion					
CS-17 Wheel, 1000 g load	mg/1000 cycles	D-1044	3	5	8
Softening Point, Vicat	°F [°C]	D-1525	234 [112]	356 [180]	363 [184]
Heat Distortion Temperature					
66 psi [0.5 MPa]	°F [°C]	D-648	No data	315 [157]	No data
264 psi [1.8 MPa]	°F [°C]	D-648	No data	110 [43]	No data
Brittleness Temperature	°F [°C]	D-746	<-94 [<-70]	<-94 [<-70]	<-94 [<-70]
Coefficient of Linear Expansion	in/in/°C [$°C^{-1}$]	D-696	$20x10^{-5}$ [$20x10^{-5}$]	$18x10^{-5}$ [$18x10^{-5}$]	$17x10^{-5}$ [$17x10^{-5}$]
Water Absorption, 24 hours	%	D-570	0.6	0.5	0.3
Specific Gravity	–	D-720	1.17	1.20	1.22

References

1. FEHER, K.: '*Digital Communications: Microwave Applications*', Prentice-Hall Inc., Chapter 1, 3 & 6, New Jersey, 1981.

2. GUNN, J.B.: '*Microwave Oscillations of Current in III-IV Semiconductors*', Solid State Commun., vol.1, pp.88-91, September 1963.

3. RIDLEY, B.K., and WATKINS, T.B.: '*The Possibility of Negative Resistance Effects in Semiconductors*', Proc. Physic. Soc., vol. 78 Part 1, pp.293-304, July 1961.

4. HILSUM, C.: '*Transferred Electron Amplifiers and Oscillators*', Proc. Inst. Radio Engineers, 50, pp.185-189, February 1962.

5. SHURMER, H.V.: '*Microwave Semiconductor Devices*', Pitman Publishing, Great Britain, p.164, 1971.

6. GUNN, J.B.: '*Instabilities of Current and of Potential Distribution in GaAs and InP*', I.B.M. Research Paper, R.C. 1216, June 1964.

7. SHOJI, M.: '*Two-Dimensional Gunn-Domain Dynamics*', IEEE Trans. Electron Devices, vol. ED-16, pp.748-758, September 1969.

8. COPELAND, J.A: '*Characterisation of bulk negative resistance diode behaviour*', IEEE Trans. on Electron Devices, ED-14, No.9, September 1967.

9. ROBSON, P.N., and MAHROUS, S.M.: '*Some Aspects of Gunn Effect Oscillators*', Radio and Elec. Engineer, vol.30, pp.345-352, December 1965.

10. KINO, G.S., and KURU, I.: '*High-Efficiency Operation of a Gunn Oscillator in the Domain Mode*', IEEE Trans. Electron Devices, vol. ED-16, pp.735-748, September 1969.

11. CARROLL, J.E., and GIBLIN, R.A.: '*A Low-Frequency Analog for a Gunn-Effect Oscillator*', IEEE Trans. Electron Devices, vol. ED-14, pp.640-656, October 1967.

12. ORTON, J.W.: '*Material for the Gunn-Effect*', Mills&Boon Ltd., pg.39, London 1971.

13. MORTENSON, K.E.: '*Variable Capacitance Diodes*', Artech House Inc., Massachusetts, pp.1-4, 1974.

14. WILSON, K.: '*Gunn Effect Devices and their Applications*', Mullard Tech. Com., No.100, pp.286-293, July 1969.

15. ZIEGER, D.: '*Frequency Modulation of a Gunn-Effect Oscillator by Magnetic Tuning*', Electronics Letters, vol.3, pp.324-325, July 1967.

16. OMORI, M.: '*Octave Electronic Tuning of a C.W. Gunn Diode using a YIG Sphere*', Proc. IEEE, vol. 57, p.97, January 1969.

17. EASSON, R.M.: '*Design and Performance of YIG tuned Gunn Oscillators*', Microwave Journal, vol.14, No.2, pp.53-68, February 1971.

18. PAIK, S.F.: '*Q Degradation in varactor-tuned oscillators*', IEEE Trans. Microwave Theory Tech., vol. MTT-22, pp.578-579, May 1974.

19. CAWSEY, D.: '*Wide range tuning of solid-state microwave oscillators*', IEEE J. Solid-State Circuits, vol. SC-5, pp.82-84, April 1970.

20. CAWSEY, D.: '*Varactor-tuned Gunn-effect oscillators*', Electronics Letters, vol.6, p.246, April 1970.

21. AITCHISON, C.S., and NEWTON, B.H.: '*Varactor-Tuned X Band Gunn Oscillator using Lumped Thin-Film Circuits*', Electronics Letters, vol.7, pp.93-94, February 1971.

22. DOWNING, B.J., Phd Thesis Sheffield, 1973, Chapter 1.

23. LEE, B.K., and HODGART, M.S.: '*Microwave Gunn oscillator tuned electronically over 1 GHz*', Electronics Letters, vol. 4, pp.240-242, June 1968.

24. SMITH, R.B., and CRANE, P.W.: '*Varactor-tuned Gunn-effect oscillator*', Electronics Letters, vol.6, p.139&140, March 1970.

25. DOWNING, B.J., and MYERS, F.A.: '*Broadband (1.95 Ghz) Varactor-tuned X-Band Gunn Oscillator*', Electronics Letters, vol. 7, pp.407-409, July 1971.

26. DOWNING, B.J., and MYERS, F.A.: '*Q Band (38 GHz) varactor tuned Gunn oscillators*', Electronics Letters, vol. 9, p.244&245, May 1973.

27. JOSHI, J.S.: '*Wide-band varactor-tuned X-Band Gunn oscillators in full-height waveguide cavity*', IEEE Trans. Microwave Theory Tech., vol. MTT-21, pp.137-139, March 1973.

28. TEMPLIN, A.S., and GUNSHOR, R.L.: '*Analytic model for varactor-tuned waveguide Gunn oscillators*', IEEE Trans. Microwave Theory Tech., vol.MTT-22, pp.554-556, May 1974.

29. JOSHI, J.S., and CORNICK, J.A.F.: '*Some general observations on the tuning characteristics of "Electromechanically" tuned Gunn oscillators*', IEEE Trans. Microwave Theory Tech., vol. MTT-21, pp.582-586, September 1973.

30. TAYLOR, B.C., FRAY, S.J., and GIBBS, S.E.: '*Frequency saturation effects in transferred electron oscillators*', IEEE Trans. Microwave Theory Tech., vol. MTT-18, pp.799-807, November 1970.

31. EVANS, D.S., and JESSOP, G.R.: '*VHF-UHF Manual*', Radio Society of Great Britain, London, 1979, pp. 8.13-8.20.

32. THEODORE, S.S Ed.: '*Microwave Engineer's Handbook*', Vol.2, Artech House Inc., Massachusetts, 1971, p.9.

33. EISENHART, R.L., and KHAN, P.J.: '*Some Tuning Characteristics and Oscillation Conditions of a Waveguide-Mounted Transferred-Electron Diode Oscillator*', IEEE Trans. Electron Devices, vol. ED-19, pp.1050-1055, September 1972.

34. TSAI, W.C., ROSENBAUM, F.J., and MacKENZIE, L.A.: '*Circuit Analysis of Waveguide-Cavity Gunn-Effect Oscillator*', IEEE Trans. Microwave Theory Tech., vol. MTT-18, pp.808-817, November 1970.

35. JETHWA, C.P., and GUNSHOR, R.L.: '*An Analytical Equivalent Circuit Representation for Waveguide-Mounted Gunn Oscillators*', IEEE Trans. Microwave Theory Tech., vol. MTT-20, pp.565-572, September 1972.

36. KUROKAWA, K.: '*Some Basic Characteristics of Broadband Negative Resistance Oscillator Circuits*', Bell Syst. Tech. J., vol. 48, pp.1937-1955, July 1969.

37. KENYON, N.D.: '*A Lumped-circuit Study of Basic Oscillator Behaviour*', Bell Syst. Tech. J., vol. 49, pp.255-272, February 1970.

38. WATERMEYER, I.R., M.Sc. Thesis, Cape Town, 1987, Chapter1 & Appendix A.

39. ALDERA, M.A., and BRAUN, R.M.: '*An Analytical Investigation into the Error Performance of MSK with incorrect Modulation Index*', Unpublished Work, Cape Town, Febuary 1988.

40. CORBEY, C.D., DAVIES, R., and GOUGH, R.A.: '*Wide-band varactor-tuned coaxial oscillators*', IEEE Trans. Microwave Theory Tech., vol. MTT-24, pp.31-39, January 1976.

41. AITCHISON, C.S.: '*Method of improving tuning range obtained from a varactor-tuned Gunn oscillator*', Electronics Letters, vol.10, p.94&95, April 1974.

42. AITCHISON, C.S.: '*Gunn oscillator electronic tuning range and reactance compensation: An experimental result at X-Band*', Electronics Letters, vol. 10, p.488&489, November 1974.

43. GUPTA, K.C., GARG, R., and CHADHA, R.: '*Computer aided Design of Microwave Circuits*', pp.139-148, pp.265-267, and pp.285-289, Artech House Inc., Massachusetts 1981.

44. BOTT, I.B., and HOLLIDAY, H.R.: '*The performance of X-Band Gunn oscillators over the temperature range 30 DegC to 120 DegC*', IEEE Trans. Electron Devices, vol. ED-14, pp.522-525, September 1967.

45. BOTT, I.B., and FAWCETT W.: '*Theoretical study of the effect of temperature on X Band Gunn oscillators*', Electronics Letters, vol.4, p.207-209, May 1968.

46. DAVIES, R., GURNEY, M.S.C., and MIRCEA, A.: '*Frequency/Temperature characteristics of Gunn devices*', Electronics Letters, vol.8, p.349-351, July 1972.

47. BIRD, J., BOLTON, R.M.G., and EDRIDGE, A.L.: '*Gunn diodes with improved frequency-stability/temperature variations*', Electronics Letters, vol. 7, pp.299-301, June 1971.

48. HOWELL, C.M.: '*Gunn Diode Oscillators, Part 1 & 2*', Microwaves & RF, vol. 26, pp.125-133 and pp.195-205, April 1987 and May 1987.

49. STEVENS, R., and MYERS, F.A.: '*Temperature compensation of Gunn oscillators*', Electronics Letters, vol.10, p.463&464, October 1974.

50. SECHI, E.N, and ZIEGER, D.: '*Stable frequency-temperature characteristics for TEO's*', Microwave Journal, pp.33-45, July 1974.

51. WHITE, J.F.: '*Simplified theory for post coupling Gunn diodes to waveguide*', IEEE Trans. Microwave Theory Tech., vol. MTT-20, pp.372-378, June 1972.

52. KNÖCHEL, R., and SCHÜNEMANN, K.: '*Temperature compensation of cavity stabilised Gunn oscillators*', Electronics Letters, vol.13, pp.723-724, November 1977.

53. FAULKNER, E.A., and MEADE, M.L.: '*Flicker Noise in Gunn Diodes*', Electronics Letters, vol. 4, pp.226-227, May 1968.

54. HOBSON, G.S.: '*Source of FM Noise in Cavity-Controlled Gunn-Effect Oscillators*', Electronics Letters, vol. 3, pp.63-64, February 1967.

55. GNERLICH, H.R., and ONDIRA, J.: '*A New Look at Noise in Transferred Electron Oscillators*', IEEE Trans. Microwave Theory and Tech., vol. MTT-25, pp.977-981, December 1977.

56. BULMAN, P.J., HOBSON, G.S., and TAYLOR, B.C.: '*Transferred Electron Devices*',pp.231-244, Academic Press, London 1972.

57. COURT, W.P.N., HERMAN, P., HILSUM, C., HOLLIDAY, H.R., and WARNER, F.L.: '*Reduction of Frequency Modulation Noise from Gunn Oscillators*', Electronics Letters, vol. 3, pp.567-569, December 1967.

58. KRATZENSTEIN, L. et al.: '*23 GHz Digital Microwave Transceiver*', The SAIEE 2nd Joint Symposium on Antennas & Propagation and Microwave Theory & Tech., pp.15.1-15.15, August 1988.